INTERNATIONAL ATOMIC ENERGY AGENCY
UNITED NATIONS EDUCATIONAL, SCIENTIFIC AND CULTURAL ORGANIZATION
INTERNATIONAL CENTRE FOR THEORETICAL PHYSICS
I.C.T.P., P.O. BOX 586, 34100 TRIESTE, ITALY, CABLE: CENTRATOM TRIESTE

H4.SMR/473-12

**COLLEGE ON NEUROPHYSICS**

**"Neural correlates of behaviour, development, plasticity and memory"**

**1-19 October 1990**

# *PLASTICITY IN OLFACTION I*

**Obaid Siddiqui**

**Tata Institute of Fundamental Research**
**Bombay, INDIA**

O SIDDIQI



# PLASTICITY IN OLFACTION I

## 1. Remarks:

Plasticity has now become a respectable subject. (Molecular + cellular mechanisms beginning to be evident)

Plastic animals Vs stereotyped animals somewhat misleading distinction.

Levels of plasticity:

a. Peripheral: Receptors (molecular) Transduction biochem. — Trans 1.

b. Neural connections: Bulb Cortex

c. Functional level: Learning Memory.

Lecture I will be about the first level — mainly on Drosophila

Lecture II will cover b. and c. we will talk more about vertebrates and olfaction in computers. — Trans 2

Olfactory system is primitive ie. more prominent in lower vertebrates. It is also simple; some recognition occurs at the receptor itself. — Trans 3

At the same time olfaction has strong connections to memory and emotions

Ref: Wyrocki, National Geographic 2 1986 - September

It is a synthetic sense ie. maps complex stimulus input as a unitary perception (Salmon, Police dog). Hence a specially attractive area from the point of view of coding and representation.

## 2. Olfactory Pathway

Ref: Engen; Hall book of Senses Vol IV. Olf.

Main pathway Receptor → Bulb ⇌ Cortex

Concerned with categorization and classification, is short and simple (eg. compared with visual pathway). But it has extensive inputs and output connections to many centres.

Anatomy of connections well studied (eg. olfactory bulb). Excitatory and inhibitory synapses form characteristics "feed back" and "feed forward" loops. We will return to anatomy later.

The pathway in Drosophila: is similar but somewhat simpler.

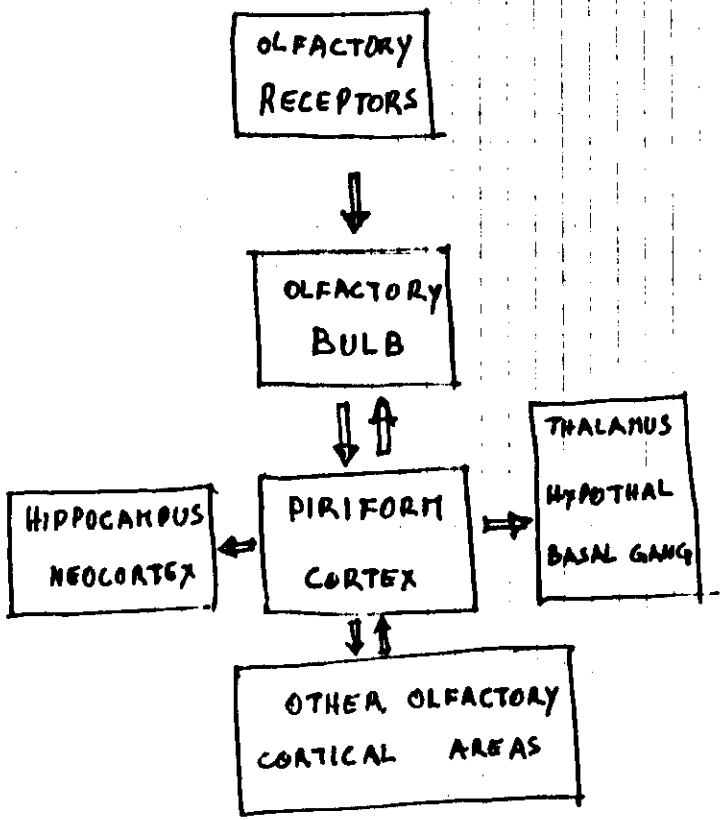


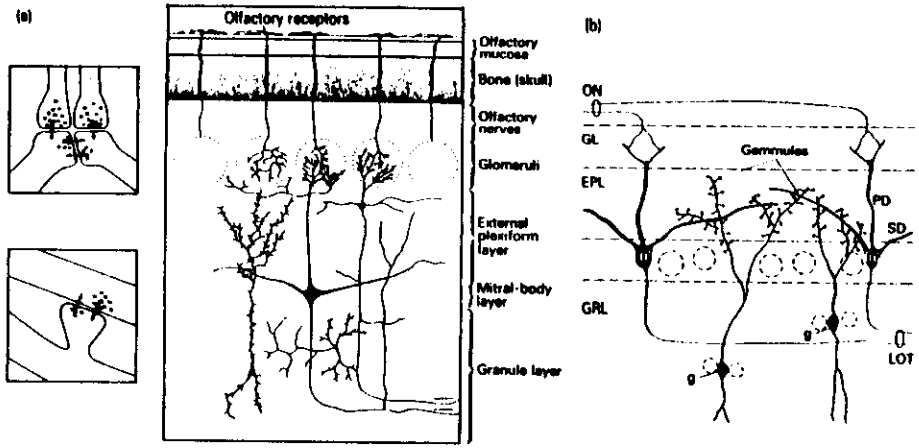


**Figure 2.** (a) Human olfactory bulb (Ref. 23). The olfactory bulb is a relay station linking the sensory receptors in the nose to the brain, and contains numerous microcircuits that transmit and process olfactory information. (b) Feedback connections in olfactory bulb (Ref. 22): GL, glomerular layer; EPL, external plexiform layer; GRL, granular layer; ON, olfactory nerve; LOT, lateral olfactory tract; g, granule cell; m, mitral cell; PD, primary mitral dendrite; SD, secondary mitral dendrite.

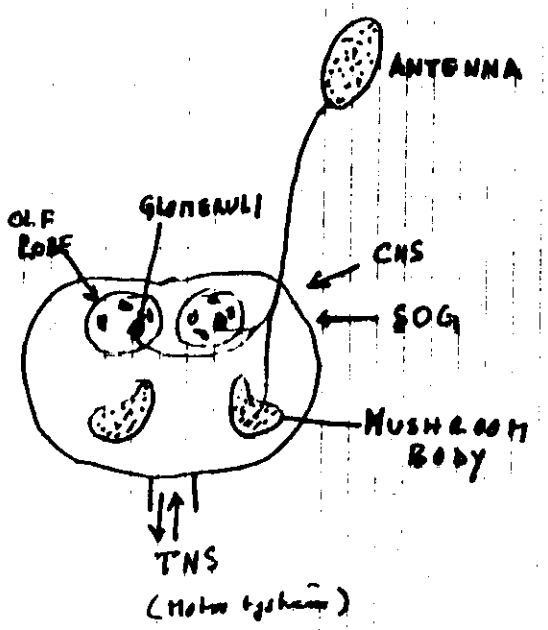


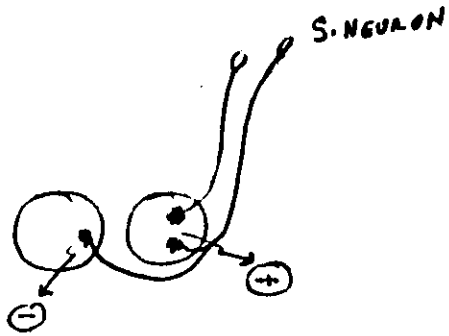


## 3. Molecular nature of olfactory receptors.

Slide 1 — Drosophila antenna

Slide 2 — ~ 500 sensilla 3 types

Slide 3 — Five sens neurons

Slide 4 — Small number of stereospecific receptors.

= receptors distributed on neurons in overlapping subsets.

The sensilla have a characteristic spatial organization; genetically regulated

Receptors highly sensitive, believed to be glycoproteins; not much known about them.

(Reference Siddiqi, In Chemical Senses Vol 3. Edited by Morad D...

Slide 5a

Slide 5b — Genetic analysis of receptors; The N.Y.

Slide 6 — olf genes of Drosophila, C-DNA in Drosophila sequence of olfE; Homology to Vertebrate receptors

### Vertebrate olfactory receptors

Although there has been much speculation in the past about their nature, I believe that vertebrate olfactory receptors are similar, although their number may be somewhat larger (~ 2

Anosmia work on human olfactory receptors.

Decimel scale — Ref. See Wysocki 1986 - Nat. Geog. (September)

Variability. ($T_1$)

Anosmias ($T_2$)

ans. 4 and 5

## 4. Plasticity of receptor organization:

Graziadei's pioneering work. Olfactory neurons turn over. Their brain connections reform; the receptors change (young & old neurons).

Q4: P. Graziadei & M. Graziadei — Brain Res. 262, 303; J. comp. Neurol. 217, 17

Drosophila gustatory receptors turn-over with a half-life of ~ 2 hrs.

Is the receptor set on sensory neurons modulated? Does this play a part in selective sensitization and desensitization? (Wysocki experiments on sweat anosmia). This is an area that needs careful study.

T1

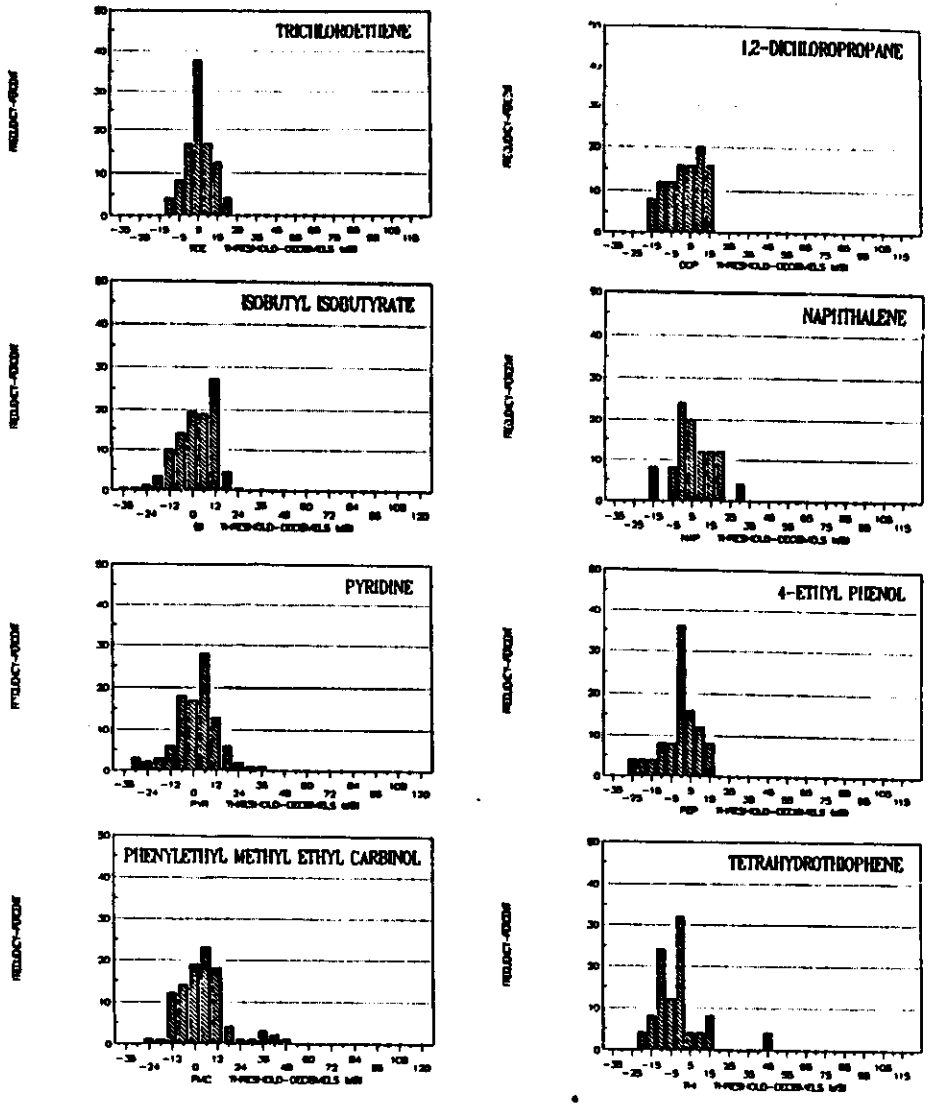


Distributions of olfactory detection thresholds for eight odorants that show little or no signs of hyposmia. These are re-calculated for samples of 100 subjects. Odor thresholds expressed on the "decismel scale"

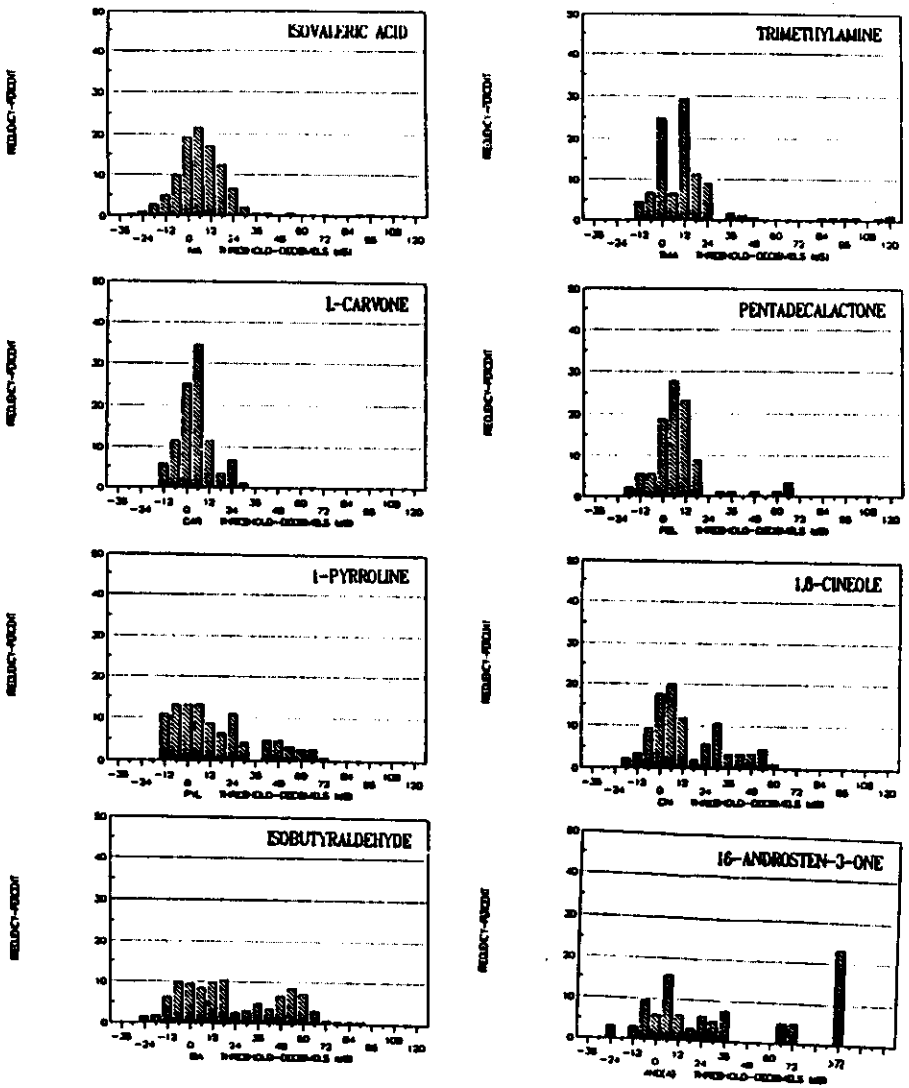


Olfactory thresholds for eight "primary odorants" that exhibit, from top to bottom, increasing proportions of specific anosmics in the population samples. Original data were in binary steps, recalculated as decismels.

## 5. Transduction Biochemistry

Trans 6a

Second messenger cascade is involved in olfactory transduction. It provides a way of:

- Amplification
- Gain control
- Connects stimulus to cellular metabolism.

Evidence for odorant stimulated phosphorylation and protein modification in Vertebrates an invertebrates is extensive. (Channels before)

Recently $IP_3$ has been identified as an early second-messenger in insects.

There are many unsettled questions. How many G proteins? How specific? Is the transduction pathway (or some part) shared between different modalities?

Slide 7

This problem lends itself to genetic dissection. (Drosophila mutants).

Trans 6b

## 6. Bacteria chemotaxis

One of the best examples of the molecular biology of behavioural plasticity.

exemplified by the work of Adler, Koshland, Berg, Mel Simon and many others on bacterial chemotaxis

Second Messenger Cascade

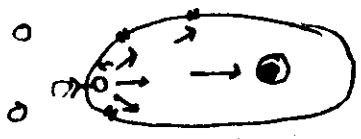

Amplification
Gain Control
Gene switching

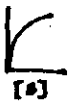


Trans.

Chemotaxis in E. coli

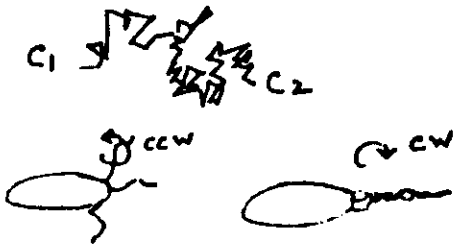


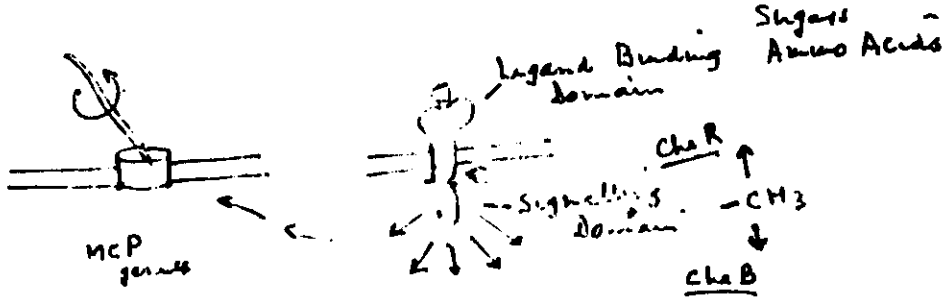


## 7. Olfactory learning in Drosophila

The work of Chip Quinn and others on learning mutants (dunce, Tabaqui, Cabbage).

Short term learning
Consolidation

Biochemical defects in learning mutants lie in defects in protein modification. (Kandel's work on Aplysia)

Defects in
- Phosphodiesterase
- Adenyl cyclase
- Kinase

(NMDA receptors + Hebbian learning)

# 7

# Olfaction in *Drosophila*

**Obaid Siddiqi**

*Molecular Biology Unit Tata Institute of Fundamental Research*
*Bombay, India*

## I. INTRODUCTION

Some years ago Veronica Rodriques and I described a set of X-linked olfactory (*olf*) genes in *Drosophila melanogaster* whose mutations cause specific anosmias (Rodrigues and Siddiqi, 1978). It was known that *Drosophila* has a well-developed olfactory sense and a rich repertoire of chemosensory behavior (Barrows, 1907; Thorpe, 1939; Begg and Hogben, 1946). We wished to take advantage of the highly developed genetics and molecular biology of Drosophila to gain some insight into odor perception. In particular, it seemed to us that the study of electrophysiologic and biochemical defects in anosmic mutants was likely to throw light on the vexing problem of olfactory receptors and on the mechanism of odor discrimination.

To detect lesions in olfactory mutants it was necessary to obtain a sufficiently detailed account of the wild type. Toward this end, our group has studied the Canton special strain from which most of the mutants are derived. I first describe the salient features of olfaction in normal flies before discussing mutants. In several respects *Drosophila* combines richness of chemosensory behavior with an underlying simplicity of structure and physiology that makes it eminently suitable as a model animal for the study of olfactory perception.



## II. OLFACTORY BEHAVIOR OF *DROSOPHILA*

The reactions of *Drosophila* to volatiles are not indiscriminate. At the beginning of our studies, we examined the olfactory responses of *Drosophila* to a set of about 50 odorants that were known to be either potent attractants or repellents to other insects or constituents of *Drosophila* food sources. The fly responds selectively to a small subset of these (Figure 1) (Rodrigues, 1980; Siddiqi, 1983). Chemicals of the same group often elicit very unequal responses. Ethyl acetate, isoamyl acetate, and butanol are strong attractants, but citronellyl acetate and geraniol are relatively ineffective. Benzaldehyde is a strong repellent but other aldehydes are only weakly so (Figure 2).

We then investigated the chemical specificity of the presumptive receptors by studying mutual interactions between odors. If the response to an odor is measured with increasing concentrations of a second odor in the background, the background is expected to inhibit the response when the two chemicals compete for a common receptor. If the two odors are detected by independent receptors, there should be no interference. Such odor "masking" or "jamming" experiments were carried out using larval behavior (Figure 3) or the adult electroantennogram (Figure 4). Strong interferences were encountered only when the odors belonged to the same chemical group. We inferred that *Drosophila* employs a small number of odor receptors corresponding to the functional groups of the volatiles in which the fly is most interested, namely acetates, alcohols, ketones, aldehydes, and certain fatty acids. For some groups, such as acetates and alcohols, there seem to be more than one receptor (Siddiqi, 1983; Borst, 1983) so that the functional group is not the only factor determining receptor specificity. Nevertheless, the range of specificity of the olfactory receptors is broad and accommodates considerable variation in size and shape. We have chosen a set of six chemicals representing the chief receptor classes to study the olfactory behavior of *Drosophila*. This canonical set of six odors does not exhaust the olfactory world of the fly. There clearly remain other molecules, for instance the sex pheromones, which are important to *Drosophila*. The role of olfaction in courtship has been extensively studied by Hall, Tompkins, and Jallon (Jallon, 1984; Tompkins, 1984; Gailey et al., 1986). The odors we investigated provide an overview of the fly's olfactory system and the strategy for detecting odors that it employs.

The larvae of *Drosophila* do not show any repulsion at lower concentrations of odors. They are attracted by all volatiles, including such noxious substances as pyridine. In the case of some chemicals, on reaching the source the larvae do not run into the source but form a ring around it. The diameter of the ring is directly proportional to the concentration at the source (Rodrigues, 1980). It is not known how the larvae orients toward the odor. At elevated concentrations it makes a beeline toward the source, but with decreasing strength of the cue its track assumes the character of biased wandering

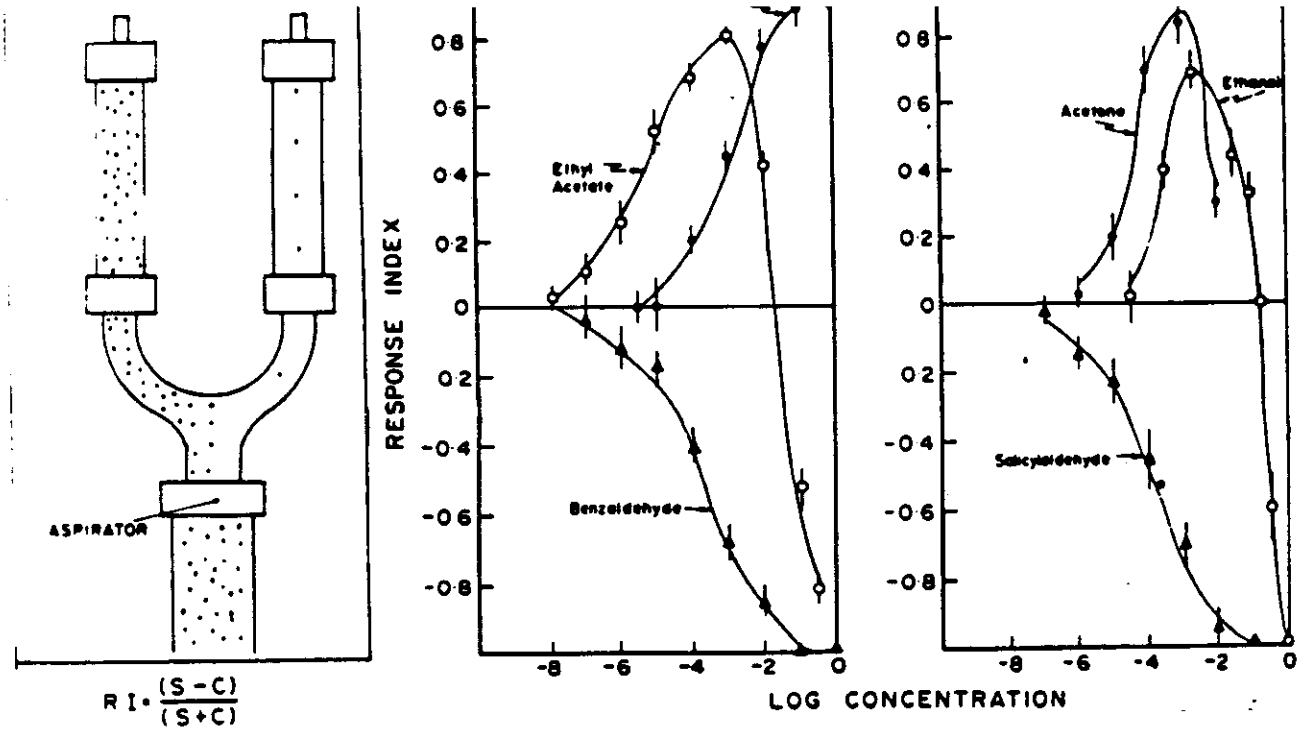


**FIGURE 1** Olfactory responses of *Drosophila*. The response of adult flies is measured in a Y olfactometer (left). One arm of the olfactometer is connected to the odor source (S) and the other to control air (C). The response index RI is computed from the number of flies in the collecting arms (RI = (S − C)/(S + C). The curves show the responses of normal Canton special strain to a few chemicals. Note the reversal of attraction above 1000-fold dilution. (From Rodrigues, 1980).



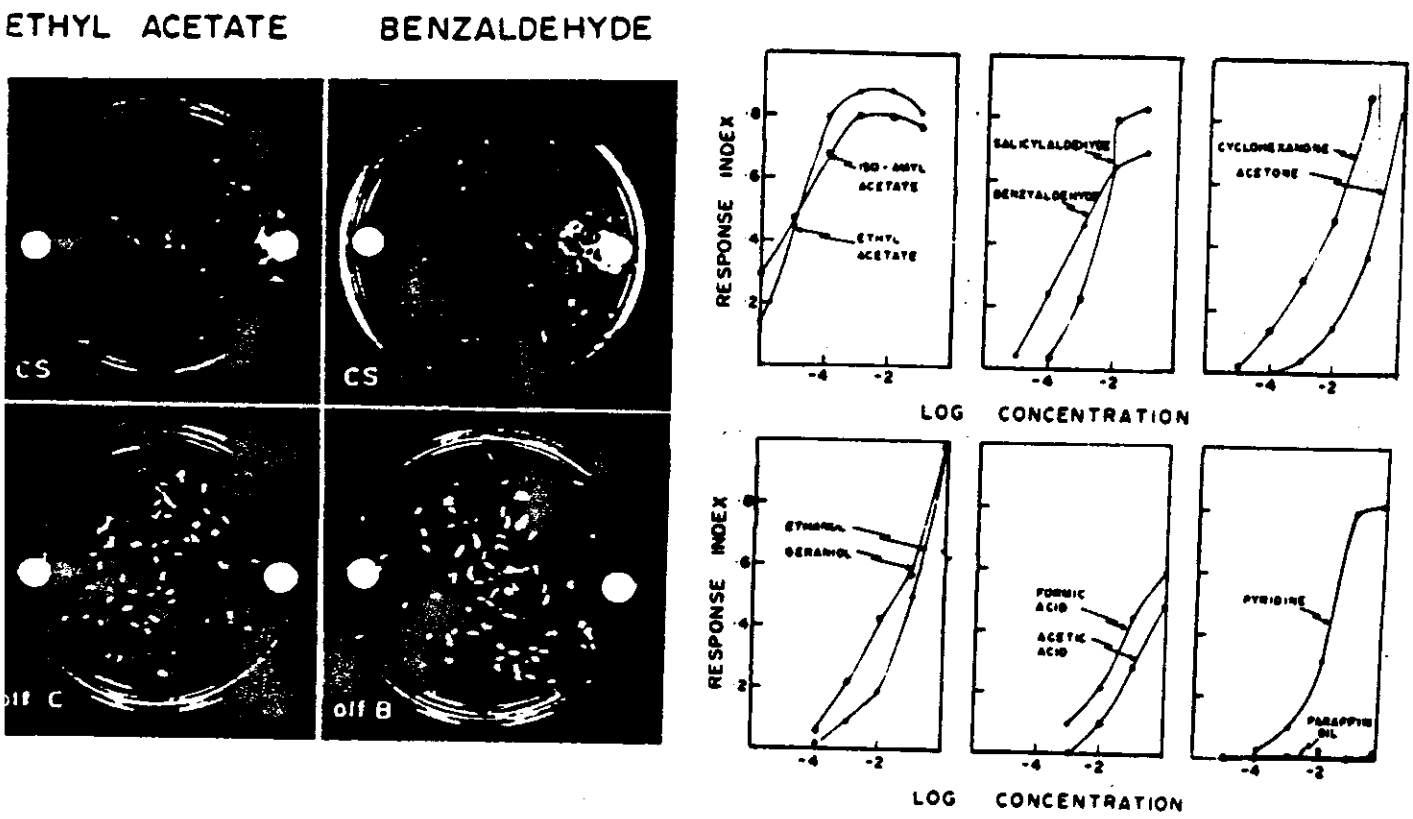


**RE 2** Larval response. The photograph on the left shows the response of wild-type and mutant strains to ethyl acetate and benzal-e. The response curves on the right show attraction to all tested odors. (From Rodrigues, 1980.)

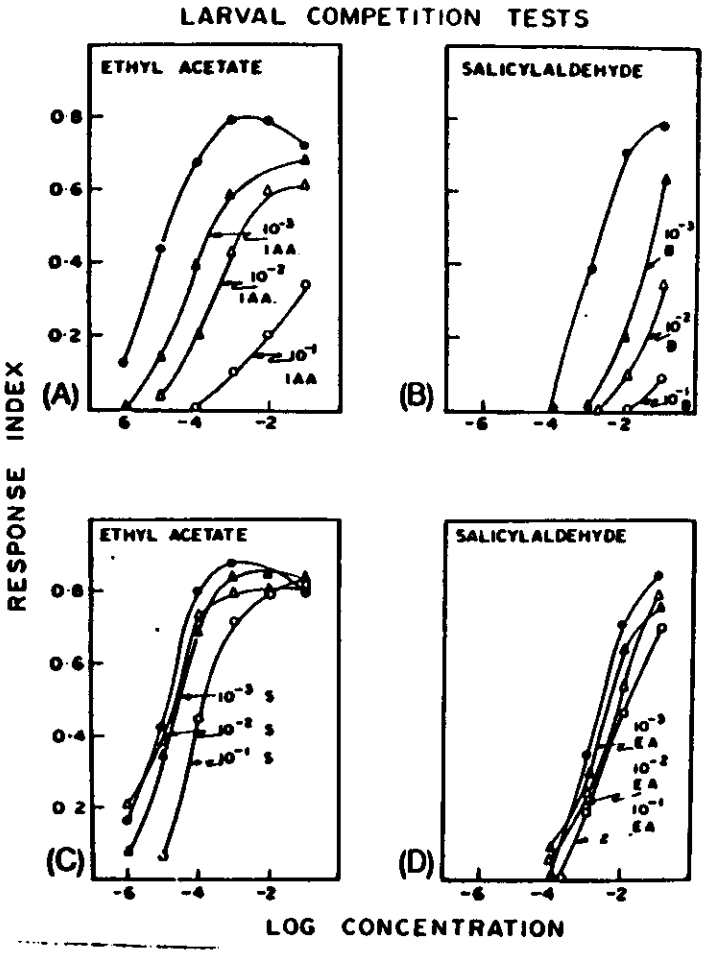


**FIGURE 3** Effect of background odor on larval taxis. The response curves for ethyl acetate and salicylaldehyde against increasing concentrations of the background odors: (A) isoamyl acetate (IAA); (B), benzaldehyde (B); (C) salicylaldehyde (S); (D) ethyl acetate (EA). (From Rodrigues, 1980.)

The adult fly discriminates between attractants and repellents. Benzaldehyde, the strongest among repellents, is avoided at extremely low concentrations. Many of the attractants elicit a mixed response. At higher concentration the response changes from attractant to repulsion. Even the most potent attractants, such as ethyl acetate and isoamyl acetate, turn into repellents at concentrations higher than a 1000-fold dilution at source. In this sense it is



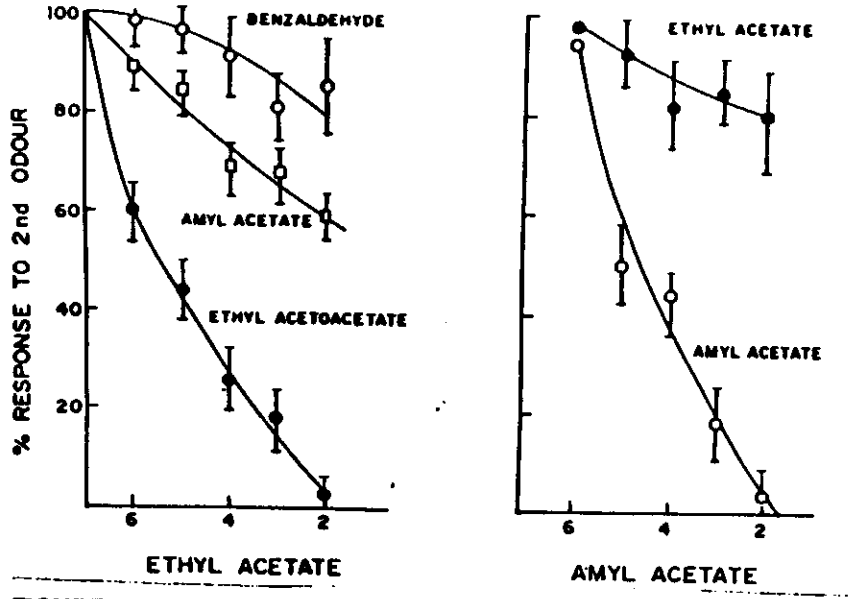


**FIGURE 4** Inhibitory effect of background on the amplitude of electroantennogram (EAG). Abccissa, negative logarithm of dilution of the background stimulus. Ordinate, response to the test stimulus. (From Siddiqi, 1983.)

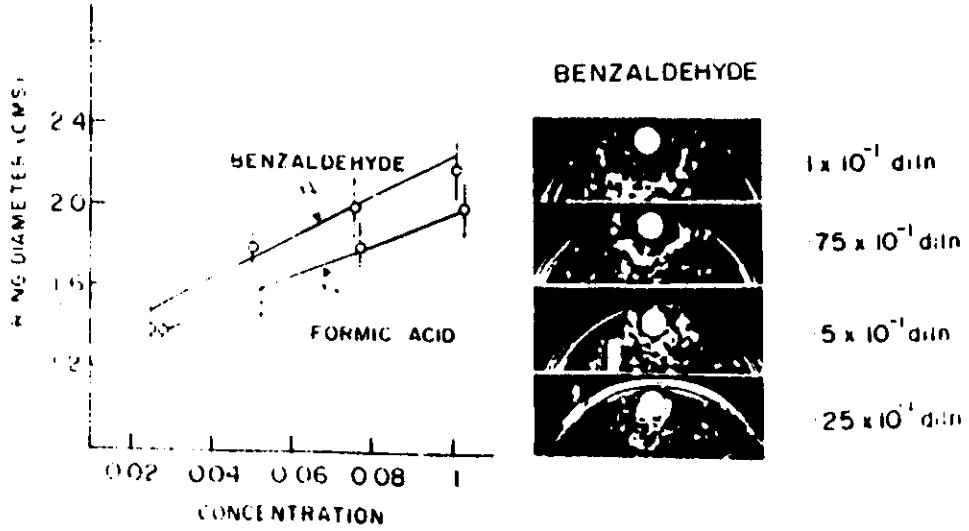


**FIGURE 5** Larval avoidance reaction at close quarters. Repulsion to high source concentrations could be due to contact with diffusing chemical. (From Rodrigues,

newhat misleading to describe the chemicals as attractants or repellents thout specifying the concentration. The volatiles used in olfactometric exriments are lipophilic, and one must bear in mind the possibility that the ponse at nonphysiologic concentrations may involve mechanisms different m those that underlie normal responses at lower concentrations. This is rticularly important in choosing methods for screening of mutants.

The sensitivity to a particular odorant is measured by the threshold for response and the maximal response that can be obtained. The exact meaements of these indices depend upon the design of the olfactometer and "state" or "disposition" of the fly. Y mazes, which introduce odors in airstream, give low detection thresholds compared to mazes without airflow. e optimal conditions for measuring attraction and repulsion are not the ne. Repulsion is best measured in rapid tests when alarmed flies are forced nake a quick binary choice. On the other hand, attraction is stronger when flies are allowed to explore the maze relatively at ease.

Borst and Heisenberg (1982) have shown that a concentration of attract odor on one antenna 1.67 times the concentration on the other antenna kes a positive turning response. It is doubtful whether, in nature, the two ennae encounter a concentration difference as large as this. The exact chanism of this osmotropotaxis thus remains to be understood.

## SENSORY PHYSIOLOGY

e third antennal segment of *Drosophila* carries the three types of sensory rs usually found in insects. The sensilla basiconica and sensilla coeloconica pond to odors. The sensilla trichoidea are probably also olfactory, but ir function remains to be determined.

The structure of the olfactory sensilla and their distribution on the funicr surface have been described by Singh and his associates, who have also orted a group of olfactory hairs on the maxillary palp (Venkatesh and gh, 1983; Singh and Nayak, 1985). The larva possesses well-developed actory organs (Singh and Singh, 1984), but their physiology has not been died.

Anil Gupta and I have examined the electrophysiologic responses of sena basiconica, the principle sensors of general odors in adult flies. The sinunit responses of over a hundred neurons in a sample of more than half *basiconica* on the funiculus is summarized in Figure 7. The hairs can be sified into recognizable response types. Neglecting types V and VII, which represented by a small number of units, at least six major types of response terns are distinguishable. Type I hairs respond to all six test odors. Type espond to the four attractants. Type I and type II hairs are highly sensi, three or four orders of magnitude more sensitive than the other hairs. y also exhibit a high rate of background firing. It is possible that these



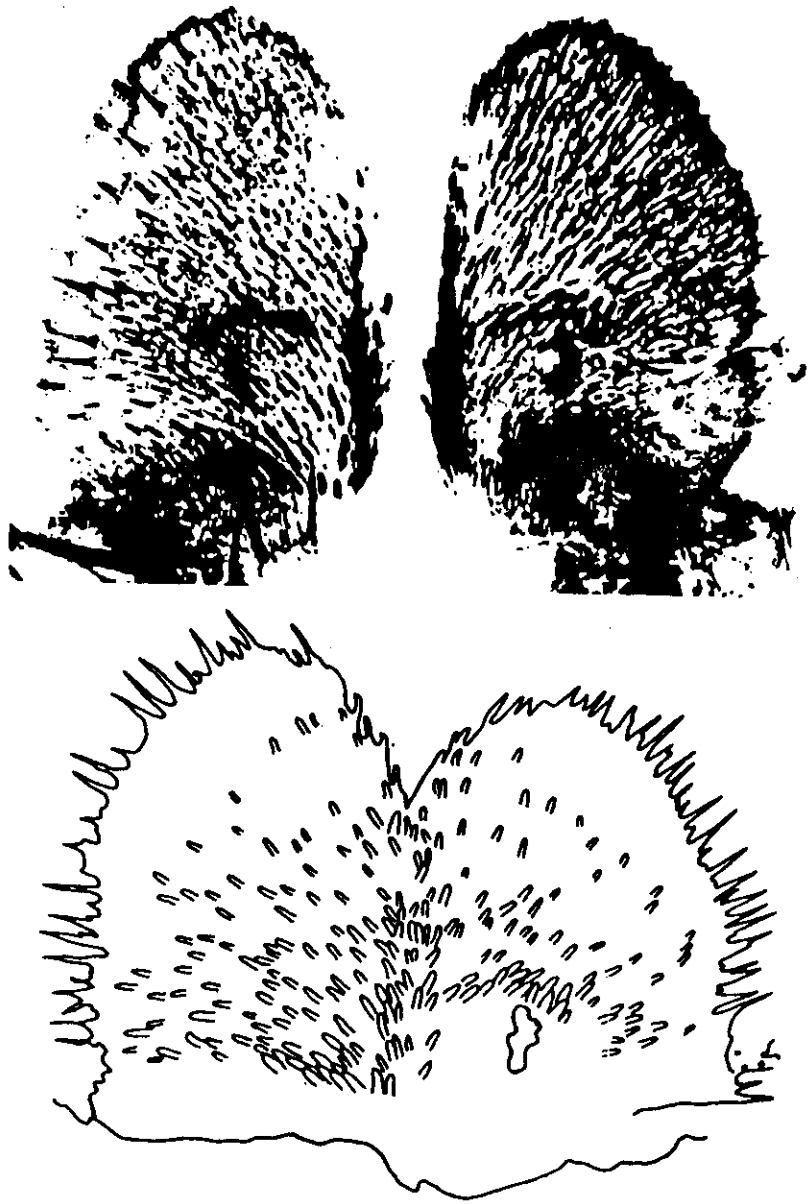

**FIGURE 6** Sensory hairs on the funiculus. Top: *Sensilla basiconica* on the three faces of the antenna. The hairs have been impregnated with silver. Bottom: Map of the antennal surface showing the pattern of distribution in *basiconica*.

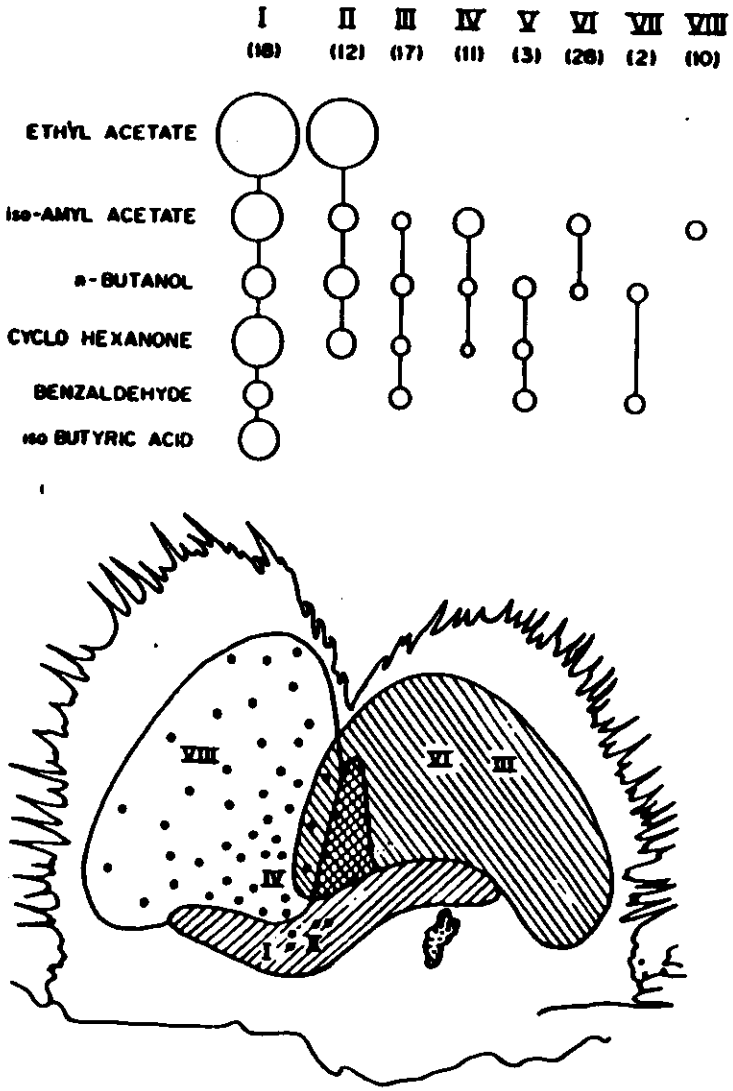


**FIGURE 7** Response spectra of sensilla basiconica: Top: Responses of 101 single units. Diameter of circle denotes sensitivity on a logarithmic scale. Bottom: Map showing topographic distribution of six different response types.



hairs constitute a high-sensitivity-low-acuity system of detection and the other hairs mediate the recognition of odors at higher concentrations. The remaining hair types III, IV, VI, and VIII respond selectively to other subsets of odors: four, three, two, or one. The responses are not distributed in random combinations. There is an orderly organization of receptor specificity, and only a small subset of all possible combinations of sensitivity is actually present.

The orderliness of the receptor system is also seen in the spatial distribution of the response types (Figure 7). Each hair type occupies a continuous patch on the antennal surface. These patches overlap, giving rise to areas that contain different combinations of sensillary types. The pattern of distribution of basiconica is fairly invariant. One can recognize hairs of known response characteristics from their positions and record from a given type of hair repeatedly. This makes the *Drosophila* antenna particularly suitable for electrophysiologic investigations on mutants. Another convenient feature of the olfactory neurons of *Drosophila* is the absence of peripheral inhibition. The neurons, as a rule, respond to odors with an increased firing. The classification of response spectra is therefore comparatively easy.

## IV. CENTRAL PROJECTIONS OF ODORS

The neurons of the antennal sensilla project to the antennal lobes; some 1100 axons converge to 22 glomeruli of each lobe (Pinto et al., 1988). The connections of the antennal neurons to the glomeruli are very simple. Each neuron is connected to a specific glomerulus. Some project only ipsilaterally, but others send a branch along the antennal commissure to the same glomerulus on the contralateral side (Stocker et al., 1983). The antennal glomeruli can be recognized by their position, shape, and size. The three types of olfactory sensilla are connected to different subsets of glomeruli (Figure 8).

Rodrigues, in collaboration with Buchner, used the deoxyglucose (DOG) uptake method to map the activity pattern in the antennal lobe generated by elementary odors. (Rodrigues 1988; Rodrigues and Buchner, 1984; Rodrigues and Bulthoff, 1985). They have shown that odor quality is represented by a discrete spatial pattern of excitation in the antennal lobe (Figure 9). Four of the six test odors project to different but overlapping subsets of a set of 12 glomeruli (Figure 10).

An unexpected finding of the DOG experiments is the striking difference in the pattern of activity generated by the repellent benzaldehyde compared to other odorants. Other odors cause mainly ipsilateral excitation, but unilateral stimulation with benzaldehyde excites the lobes on both sides. This observation provides a neurologic correlate of the finding by Borst and Heisenberg (1982) that benxaldehyde fails to evoke an orientation response. At present the DOG results are of a somewhat qualitative nature. The technique needs

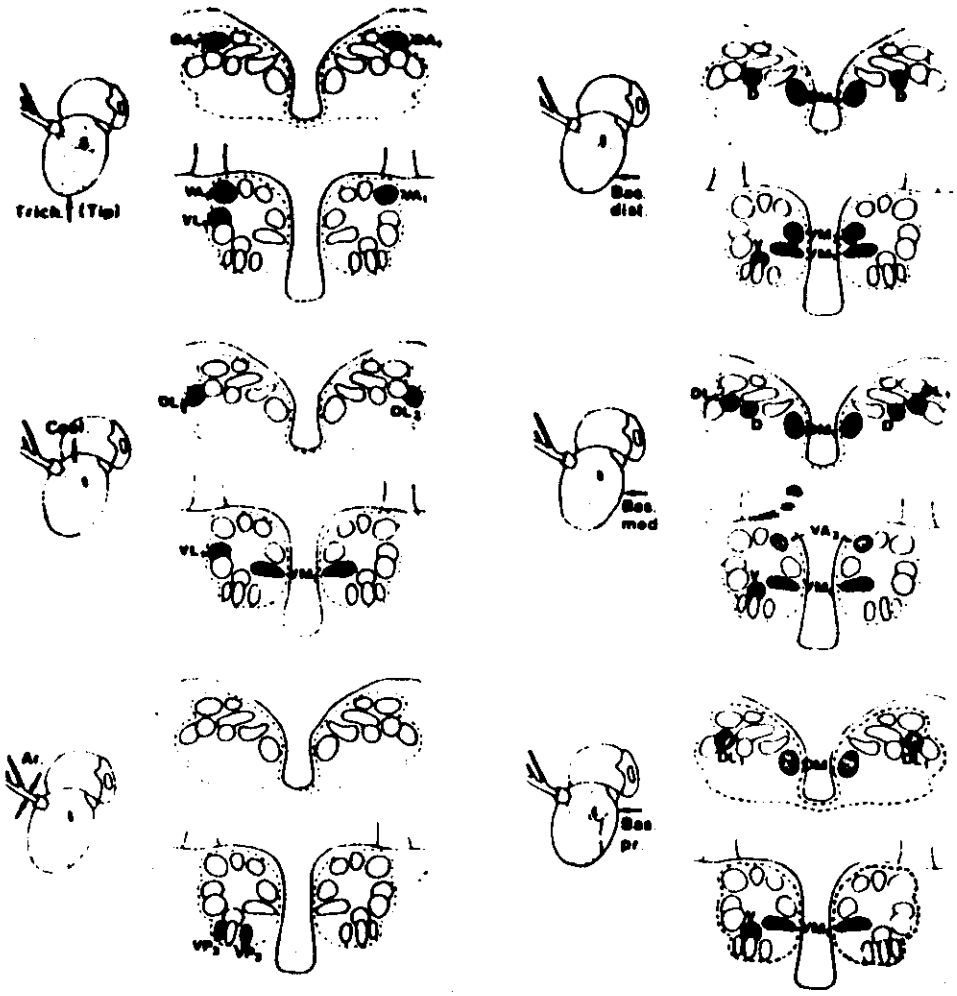

**FIGURE 8** Projection of different sensilla to antennal glomeruli. The site of cobalt injection is indicated by arrows. A total of 19 glomeruli are shown in two sections. The upper section shows 8 dorsal glomeruli; the lower section shows 11 ventral glomeruli. Altogether, 22 glomeruli can be identified. (From Stocker et al., 1983; Pinto et al., 1985.)

9



**FIGURE 9** Deoxyglucose labeling of glomeruli. Top: Ipsilateral excitation by acetate. The contralateral branch of the axon is labeled, but not the glomerulus. Bottom: Bilateral excitation by benzaldehyde. Notice labeling on both sides. The left antenna was removed. The output axons are also labeled.

to be improved and made quantitative before a confident assessment of the invariance of activity patterns can be made.

Our knowledge of the circuitry of antennal lobes and the attendant processing of sensory signals is still very inadequate. Golgi preparations reveal a variety of interneurons (unpublished work by Fischbach, Borst, and Singh). These must integrate the incoming signals, but in the absence of detailed information about the network of relay neurons, not much can be said regarding the output signals that go to the mushroom body and dorsal protocerebrum.

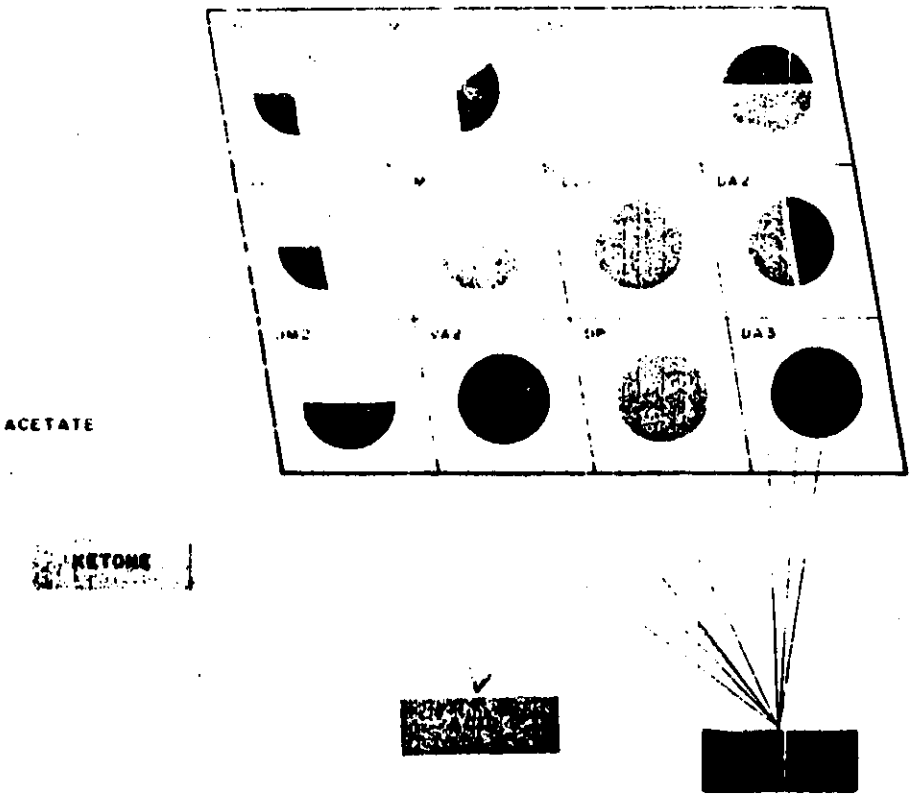


**FIGURE 10** The pattern of projection of odors on a subset of 12 glomeruli (data from V. Rodrigues). Symbols D, V, A, and P refer to dorsal, ventral, anterior, and posterior locations.

The input into glomeruli is convergent, but the output from the lobes diverges to a few thousand Kenyon cells in the mushroom body. A major step forward in understanding odor perception will come from understanding the nature of mapping between the glomeruli and the Kenyon cells. In principle it should be possible to extend functional mapping beyond the antennal glomeruli.

## V. OLFACTORY NEUROGENETICS

Mutations can alter the olfactory behavior of the fly in a variety of ways. Peripheral lesions may affect specific receptors, cellular signaling pathways, or electrical excitability of the membrane. In each case the mutation is expected



to change the firing response of the neuron. Mutations affecting the central connections of the olfactory pathway are likely to change the osmotactic responses of the fly without changing the electrical output of the sensory neurons. One can use a number of diagnostic tests that should serve to distinguish peripheral from central defects.

In 1978 we described a set of four *olfactory* genes on the X chromosome of *Drosophila* (Rodrigues and Siddiqi, 1978). More mutants were subsequently isolated by Padhye and Ayyub. The *olf* mutants in our laboratory were induced by ethylmethanesulfonate and screened by testing mutagenized lines in the olfactory Y maze. John Carlson and his group at Yale have developed other methods of screening for olfatory mutants.

The six X-linked genes we studied are shown in Figure 11. Four of these, *olfA*, *olfB*, *olfE*, and *olfF*, reduce the response to aldehydes; *olfC* mutants are defective in the response to acetate esters. The gene *olfD* blocks responses to all odors that have been tested. Experiments in Carlson's laboratory show that *olfD* mutants are allelic to *smell blind*, a gene previously isolated by Aceves-Pina and Quinn (1979).

All the *olfactory* mutants examined so far are partial; absolute odor blocks have not been found. Some of the genes increase the threshold concentration

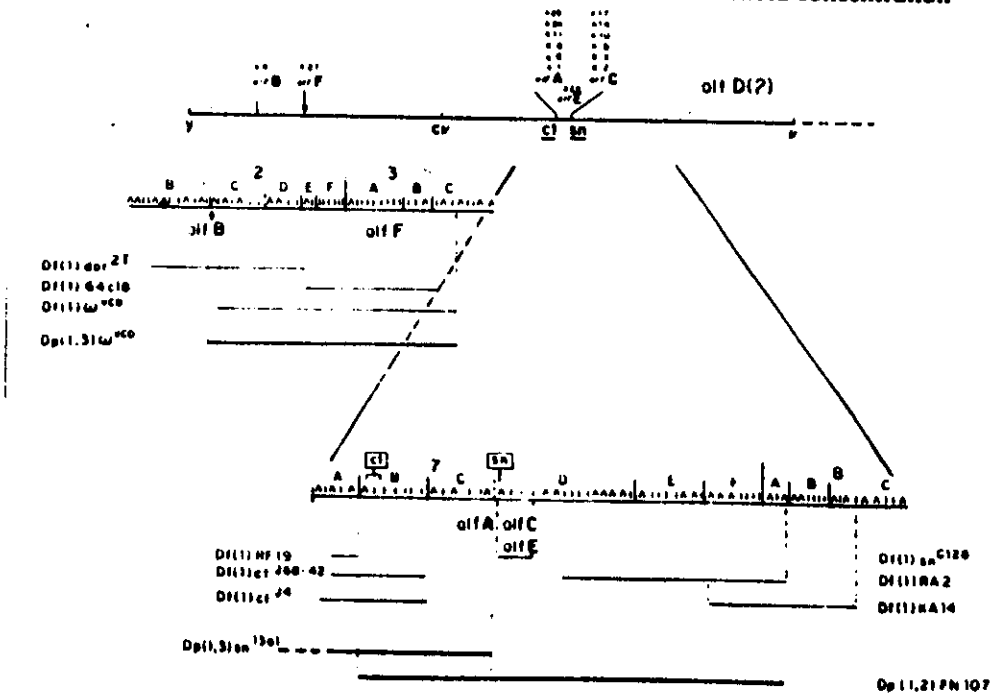


**FIGURE 11** Cytogenetic localization of olfactory genes on the X chromosome.

of the response without reducing the maximal response; others cause a reduction in the maximal response (Figure 12). Mutations at all six loci affect the adults as well as the larvae, although the effect on the larval response is somewhat weaker.

The genes *olfA*, *olfC*, and *olfE* are closely linked to the genes *cut* and *singed* and have been investigated in some detail. Hasan and Ayyub have found

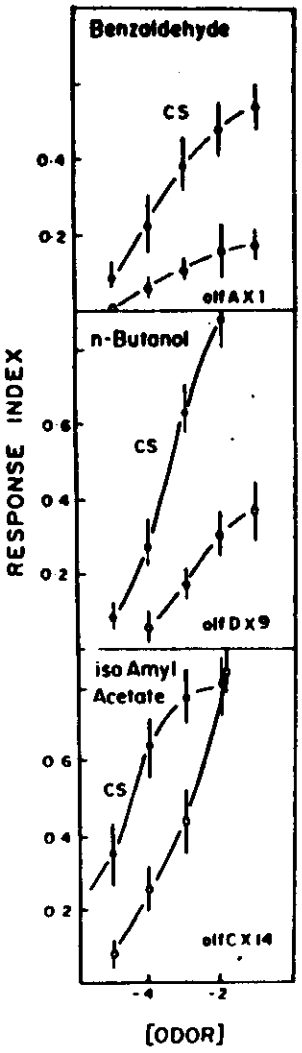


**FIGURE 12** The larval responses of *olfactory* mutants to odors. (Siddiqi, 1987.)



that a fraction of P-induced mutations in the *singed* locus cause olfactory blocks. Several of these *sn olf* isolates fail to complement *olfA* and *olfE* alleles. The P element in these strains is inserted in the *singed* locus in only one of the two possible orientations. Hasan and Ayyub (1988) ascribe this to a polar effect of insertions on the neighboring *olf* loci. A chromosome walk to map the *olf* genes in this region has been carried out.

So far little is known about the primary functions of the *olf* genes. The most striking feature of the phenotype of these genes is the chemical specificity of the odor block. The six alleles of the *olfC* locus, for instance, belong to two sub groups. X2, X3, and X10 are defective in response to ethyl acetate as well as isoamyl acetate; X5, X14, and X17 are blocked to isoamyl acetate alone. This suggests that these mutations affect some step in reception. Venard and Pichon (1984) have reported that some of the *olfC* alleles have a defective electroantennogram (EAG) response to acetates. We are currently examining the single-unit responses of *olfactory* mutants.

It has been found that the *olfD* mutants are also defective in taste response (Mary Lilly, unpublished). Some of the new mutants isolated in Carlson's laboratory also show alterations in visual physiology. These results imply that there are common steps in the pathways of chemosensory and visual reception.

## VI. SUMMARY

The most attractive feature of the olfactory pathway of *Drosophila* is its relative simplicity. Odorants are detected by an apparently small number of specific receptor sites. The presumptive receptors correspond to the functional groups in the volatiles of interest to the fly. The receptor sites are distributed on the sensory neurons in an overlapping fashion so that odors excite specific subsets of neuron types, each with a characteristic spectrum of sensitivity. The excitation patterns of the sensory neurons maps on the glomeruli in the antennal lobes, where each odor is represented by a pattern of glomerular activity. The simplicity of glomerular organization in *Drosophila* makes this pattern recognizable.

A number of *olfactory* genes have been identified. Some of these give rise to odor-specific anosmias; others produce multiple blocks or smell blindness. The primary lesions in the *olfactory* mutants remain to be identified, but some of the *olf* mutations affect electrophysiologic responses, suggesting a defect in reception. There are mutations that simultaneously affect the sensory responses to olfactory, gustatory, and visual stimuli, showing that some of the steps in cellular signaling are common to the three modalities.

## REFERENCES


Aceves-Pina, E. O., and Quinn, W. G. (1979). Learning in normal and mutant *Drosophila* larvae. *Science* 206:93-95.

Barrows, W. (1907). The reactions of the pomace fly *Drosophila ampelophila* to odorous substances. *J. Exp. Zool.* 4:515-537.

Begg, M., and Hogben, L. (1946). Chemoreceptivity of *Drosophila melanogaster*. *Proc. R. Soc. (Lond.) [Biol.]* 133:1-19.

Borst, A. (1983). Computation of olfactory signals in *Drosophila melanogaster*. *J. Comp. Physiol.* 152:373-383.

Borst, A., and Heisenberg, M. (1982). Osmotropotaxis in *Drosophila melanogaster*. *J. Comp. Physiol.* 132:235-242.

Gailey, D. A., Lacaillade, R. C., and Hall, J. C. (1986). Chemosensory elements of courtship in normal and mutant, olfaction-deficient *Drosophila melanogaster*. *Behav. Genet.* 16:375-405.

Hasan, G., and Ayyub, C. (1988). Olfactory behaviour of P element-induced *singed* mutants of *Drosophila melanogaster*. (in preparation).

Jallon, J. M. (1984). A few chemical words exchanged by *Drosophila* during courtship and mating. *Behav. Genet.* 14:483-520.

Pinto, L., Stocker, R. F., and Rodrigues, V. (1988). Anatomical and neurochemical classification of the antennal glomeruli in *Drosophila melanogaster*. *Int. J. Embryol. Exp. Morphol.* ~~(in the press).~~ 17: 335-344

Rodrigues, V. (1980). Olfactory behaviour of *Drosophila melanogaster*. In *Development and Neurobiology of* Drosophila, O. Siddiqi, P. Babu, L. Hall, and J. Hall (Eds.). Plenum, New York, pp. 361-371.

Rodrigues, V. (1988). Spatial coding of *olfactory* information in the antennal lobe of *Drosophila melanogaster*. *Brain Res.* 453:299-307.

Rodrigues, V., and Buchner, E. (1984). [$^3$H]2-deoxyglucose mapping of odour-induced activity in the antennal lobes of *Drosophila melanogaster*. *Brain Res.* 324:374-378.

Rodrigues, V., and Bulthoff, I. (1985). Freeze substitution of *Drosophila* heads for subsequent [$^3$H]2-deoxyglucose autoradiography. *J. Neurosci. Methods* 13:183-190.

Rodrigues, V., and Siddiqi, O. (1978). Genetic analysis of chemosensory pathway. *Proc. Indian Acad. Sci. [B]* 87:147-160.

Siddiqi, O. (1983). Olfactory neurogenetics of *Drosophila*. In *Genetics: New Frontiers*, Vol. III (Proceedings XV Int. Congress of Genetics, December 1983), V. L. Chopra, R. P. Sharma, B. C. Joshi, and H. C. Bansal (Eds.). Oxford I.B.L., New Delhi, pp. 243-261.

Siddiqi, O. (1987). Neurogenetics of olfaction in *Drosophila malanogaster*. *Trends Genet.* 3:137-142.

Singh, R. N., and Nayak, S. (1985). Fine structure and primary sensory projections of sensilla on the maxillary palp of *Drosophila melanogaster*. *Int. J. Insect Morphol. Embryol.* 14:291-306.

Singh, R. N., and Singh, K. (1984). Fine structure of the sensory organs of *Drosophila melanogaster* larva. *Int. J. Insect Morphol. Embryol.* 13:255-273.





Stocker, R. F., Singh, R. N., Schorderet, M., and Siddiqi, O. (1983). Projection patterns of different types of antennal sensilla in the antennal glomeruli of *Drosophila melanogaster*. *Cell Tissue Res.* 232:237-248.

Thorpe, W. H. (1939). Further studies on pre-imaginal olfactory conditioning in insects. *Proc. R. Soc. Lond. [Biol.]* 127:424-433.

Tompkins, L. (1984). Genetic analysis of sex appeal in *Drosophila*. *Behav. Genet.* 14:411-440.

Venard, R., and Pichon, Y. (1984). Electrophysiological analysis of peripheral response to odours in wild type and smell-deficient *olfC* mutants of *Drosophila melanogaster*. *J. Insect Physiol.* 30:1-5.

Venkatesh, S., and Singh, R. N. (1983). Sensilla on the third antennal segment of *Drosophila melanogaster*. *Int. J. Insect Morphol. Embryol.* 13:51-63.

*cknowledgements*
*Thanks to Brian oycott, David Edgar, Paul Letourneau and Diana Moss for their elpful comments on this article.*

presumably accompanied by the assembly of cortical structures, including actin filaments. Extension allows portions of the growth cone to penetrate for short distances into fluid-filled spaces and is not obviously dependent on local contacts with the substratum. Retraction is due to regional contractions in the actin-rich cortex of the growth cone, which tend to make filopodia and lamellipodia retreat into the cell. Whether this force in fact succeeds in causing filopodia and lamellipodia to retract depends on the strength of their adhesion to the substratum. On a highly adhesive surface, retraction will be prevented; on a moderately adhesive surface, some cell extensions will retract and others not. In the latter situation, the degree to which retraction takes place may form the basis of a mechanism of growth cone guidance.

Whatever the nature of the surface over which the growth cone is migrating and however adhesive it is, the assembly of membrane and cytoskeletal components into axonal structures will be promoted and controlled by the actin-based movements just described.

## Selected references

1 Marsh, L. and Letourneau, P. C. (1984) *J. Cell Biol.* 99, 2041–2047
2 Yamada, K. M., Spooner, B. S. and Wessells, N. K. (1971) *J. Cell Biol.* 49, 614–635
3 Kumagai, H., Imazawa, M. and Miyamoto, K. (1986) *Brain Res.* 392, 270–274
4 Menko, A. S., Toyama, Y. and Holtzer, H. (1983) *Mol. Cell. Biol.* 3, 113–125
5 Goldberg, D. J. and Burmeister, D. W. (1986) *J. Cell Biol.* 103, 1921–1931
6 Letourneau, P. C. (1979) *Exp. Cell Res.* 124, 127–138
7 Bray, D. and Chapman, K. (1985) *J. Neurosci.* 5, 3204–3213
8 Snaw, G. and Bray, D. (1977) *Exp. Cell Res.* 104, 55–62
9 Nakai, J. (1960) *Z. Zellforsch. Mikrosk. Anat.* 51, 108–122
10 Wessells, N. K., Letourneau, P. C., Nuttall, R. P., Luduena-Anderson, M. and Geiduschek, J. M. (1980) *J. Neurocytol.* 9, 647–655
11 Bray, D. and Bunge, M. B. (1973) in *Locomotion of Tissue Cells (CIBA Symposium 14)*, pp. 195–207, Elsevier
12 Dunn, G. A. (1980) in *Cell Adhesion and Motility (British Society for Cell Biology Symposium 3)* (Curtis, A. S. G. and Pitts, J. D., eds), pp. 409–423, Cambridge University Press
13 Heath, J. P. (1983) *J. Cell Sci.* 60, 331–354
14 Bentley, D. and Toroian-Raymond, A. (1986) *Nature* 323, 712–715
15 Letourneau, P. C. (1975) *Dev. Biol.* 44, 91–101
16 Kapfhammer, J. P., Grunewald, B. E. and Raper, J. A. (1986) *J. Neurosci.* 6, 2527–2534
17 Berlot, J. and Goodman, C. S. (1984) *Sciences* 223, 493–495
18 Bastiani, M. J., Doe, C. Q., Helfand, S. L. and Goodman, C. S. (1985) *Trends Neurosci.* 8, 257–266
19 Wessells, N. K. and Nuttall, R. P. (1978) *Exp. Cell Res.* 114, 111–112
20 Bray, D. (1982) in *Cell Behaviour* (Bellairs, R., Curtis, A. and Dunn, G., eds), pp. 299–317, Cambridge University Press
21 Letourneau, P. C. (1984) in *Molecular Bases of Neuronal Development* (Edelman, G. M., Gall, W. E. and Cowan, W. N., eds), pp. 269–293, John Wiley & Sons
22 Tamkun, J. W., De Simone, D. W., Fonda, D., Patel, R. S., Buck, C., Horwitz, A. F. and Hynes, R. O. (1986) *Cell* 46, 271–282
23 Horwitz, A., Duggan, K., Greggs, R., Decker, C. and Buck, C. (1985) *J. Cell Biol.* 101, 2134–2144
24 Bozyczko, D. and Horwitz, A. F. (1986) *J. Neurosci.* 6, 1241–1251
25 Tomaselli, K. J., Reichardt, L. F. and Bixby, J. L. (1986) *J. Cell Biol.* 103, 2659–2672
26 Haydon, P. G., Cohan, C. S., McCobb, D. P., Miller, H. R. and Kater, S. B. (1985) *J. Neurosci. Res.* 13, 135–147
27 Cohan, C. S. and Kater, S. B. (1986) *Science* 1638–1640
28 Harris, A. K., Wild, P. and Stopak, D. (1980) *Science* 208, 177–179

# Plasticity of olfactory output circuits related to early olfactory learning

Michael Leon

*ichael Leon is at the Department of Psychobiology, University of alifornia, Irvine, CA 92717, USA.*

*Olfactory preference learning begins* in utero *and continues neonatally, allowing young rats to become attracted to the odors of their mother. Such learning is critical for nursing and the maintenance of periodic contact with the mother. The developing olfactory system is responsive to a variety of maternal, as well as non-maternal odors, and olfactory preferences to these odors persist into adulthood. If olfactory learning occurs via one naris before the commissural connections develop, these memories are retained on that side of the brain. Once the connections have developed, the untrained side of the brain can access olfactory memories on the contralateral side. Odor preferences formed early in life provoke an enhanced response in the olfactory bulb, measured by increased 2-deoxyglucose uptake in specific areas of the glomerular layer. The region of the glomerular layer producing this enhanced activity is enlarged and the output signal from neurons in that part of the bulb is altered by early learning. This type of learning shares mechanisms both with other forms of developmental plasticity and with adult olfactory learning.*

The question of how normal variation in sensory experience produces individual differences in brain and behavior has remained largely unanswered. The usual laboratory approach to this question has been to impose abnormal stimulation on the developing organism by sensory deprivation rather than by normally differing aspects of the environment. While the deprivation paradigm provides an understanding of normal development through observation of induced abnormalities, there is no reason to believe that there is only a single course of normal development. Recent investigations into the neurobiology of olfactory preference learning in early life have revealed a remarkable plasticity in the developing brain that could underlie life-long individual differences in behavior. Since early olfactory learning occurs in many species, ranging from invertebrates to humans[1], these findings could have broad implications for understanding neurobehavioral plasticity during development.

Olfactory learning begins surprisingly early in rats. Fetal rats can be trained to avoid odors by pairing an odor injected into the uterus with aversive stimulation (lithium chloride toxicosis). These rats have an aversion to such odors when tested postnatally[2]. Such training alters olfactory preferences into adulthood.

Prenatal learning is essential for postnatal survival. Young rats normally become attracted to the chemicals present in their mother's uterine fluids[3], which mother rats deposit on their nipples. The pups are thereby able

 0378 - 5912/87/$02.00

to use uterine chemical cues to locate and attach to their mother's nipple for the first time[3]. Indeed, the fact that such a critical behavior should depend on learning suggests that the mechanism underlying early olfactory learning must be very reliable.

Rat pups will also learn to attach to their mother's nipples in the presence of a non-maternal odor. Fetuses exposed to citral both *in utero* and postnatally will attach to washed nipples scented with citral. They will even attach to a citral-scented nipple in preference to a naturally scented one[34].

While the first nipple attachment is facilitated by uterine odors that have been deposited on the nipple, suckling alters the olfactory characteristics of nipples. Subsequent attachments are directed by odors derived from the saliva that pups left on the nipples during their previous suckling episodes. Pups deprived of their sense of smell or given washed nipples do not attach[3]. When washed nipples are painted with material swabbed from pup mouths, the pups are again able to attach to the nipples[3].

Postnatal olfactory experience produces a preference only if it is accompanied by the kind of tactile stimulation that mimics maternal contact[4]. This ability to mimic a normal learning situation provides a powerful tool for studying the neurobiology of learning.

As Norway rats grow and become mobile, they continue to reunite periodically with their mother to nurse. At that time, another maternal attractant, produced by enteric microorganisms, is used to facilitate these reunions[1]. The microorganisms produce different odors with different maternal diets, naturally exposing litters to different dominant maternal odors[1]. Rat pups subsequently approach the specific maternal odor that they experienced early in life. They can also develop attractions to non-maternal odors experienced postnatally[1].

## Neural responses to learned odors

### *Accessory bulb*

The vomeronasal organ, which sends its sensory information to the accessory bulb, is specialized to respond to chemical cues in fluids. The fetus is surrounded by uterine fluids and the accessory system may be involved in prenatal chemosensory learning. The accessory olfactory system of fetal rats appears to be chronically activated, as reflected by the uptake of the labelled glucose analogue 2-deoxyglucose (2-DG)[4]. This high activity in the accessory bulb may be due to a chronic activation of the system by uterine odorants sensed by the vomeronasal organ. 2-DG activity is not seen in the rat accessory bulb after birth.

### *Modified glomerular complex*

After birth, nipple odor (which is now modified by pup saliva) provokes an increased uptake of 2-DG in a modified glomerular complex located in the dorsomedial aspect of the main olfactory bulb near the accessory bulb[4]. This complex is composed of several glomeruli that may function as a unit to process nipple odor. Some other areas of the glomerular layer show increased 2-DG uptake in response to nipple odor, but

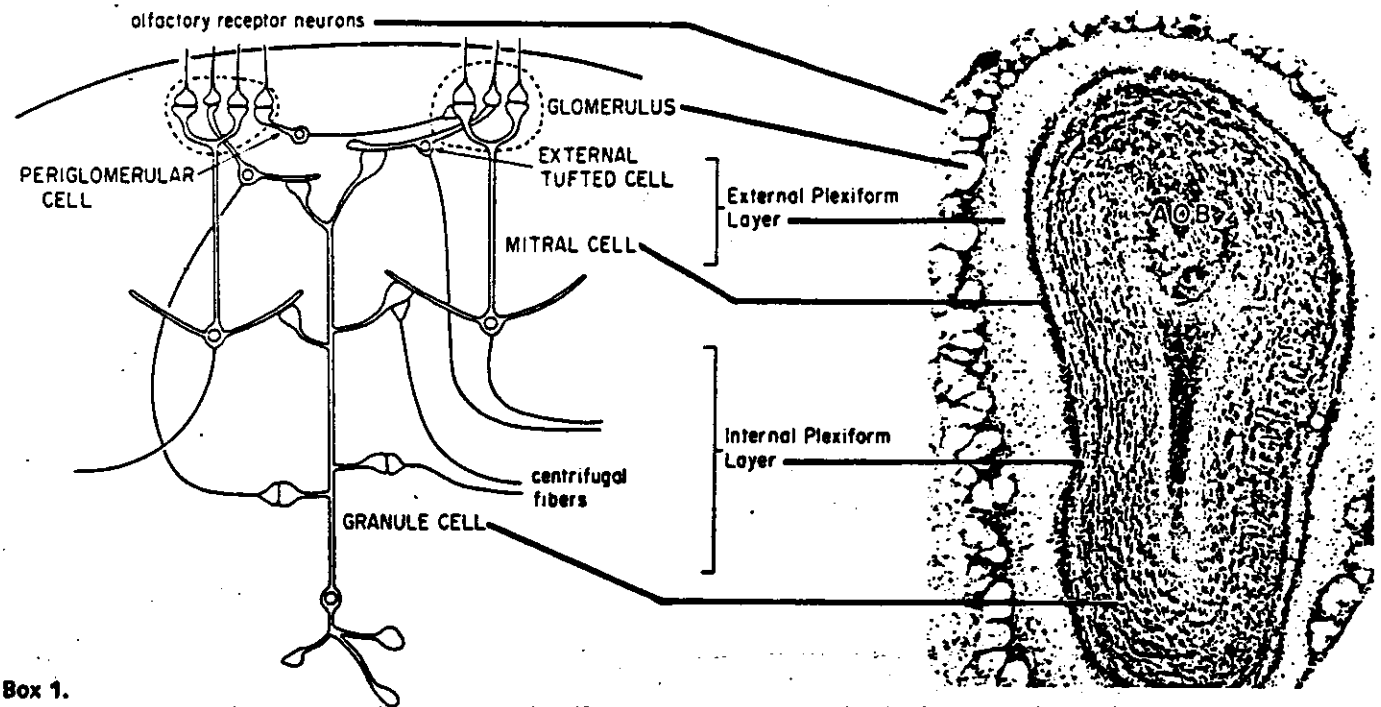


**Box 1.**

*The main olfactory bulb reacts to stimuli activating the olfactory receptor neurons that are located in the nasal turbinates. The olfactory receptor neurons receive chemical cues in the olfactory mucosa, situated in the nasal turbinates. The chemical signal is transduced to a neural signal and enters the olfactory bulb via the axons of the receptor neurons. These axons synapse with mitral, tufted and periglomerular cells in large synaptic structures called glomeruli. Mitral cells are the dominant output neurons of the bulb. Tufted cells are composed of subpopulations that project both from and within the bulb. Periglomerular cells appear to mediate interglomerular inhibition. The granule cells are inhibitory interneurons. The external plexiform layer (EPL) is between the glomerular and mitral cell layers and contains the secondary dendrites of mitral and tufted cells, as well as some tufted cell bodies. The internal plexiform layer (IPL) contains granule cell dendrites and mitral and tufted cell axons.*

*The accessory olfactory bulb (AOB) is located in the dorsomedial aspect of the main olfactory bulb, although it is entirely separate from the main bulb. The AOB receives projections from receptor neurons in the vomeronasal organ, which is located in the palate. The laminae of the accessory bulb are less distinct than in the main bulb and there are no tufted cells in this structure. Otherwise, the cell types and circuitry of the accessory bulb are similar to the main olfactory bulb.* (Modified from Ref. 5.)

the uptake in the modified glomerular complex is much greater and more focused than in other glomerular-layer regions. These data raise the possibility that the modified glomerular complex is involved in the learning of a preference for nipple odors during the postpartum period. The modified glomerular complex is well developed at birth, while the rest of the glomeruli in the main bulb are diffusely organized until the end of the first week postpartum. While lesion of this area does not affect nipple attachment[6], the modified glomerular complex may be involved in nipple-odor learning, but not memory. Alternatively, its function may be assumed by other glomerular areas following extirpation.

Similarly, the attraction of young rabbits to maternal nipple odors normally develops *in utero*, and the young also have the ability to develop an attraction to a non-maternal odor postnatally[7]. While a learned attractive odor activates the modified glomerular complex of young rabbits, among other areas, any lesion less than a complete extirpation of both bulbs does not block responsiveness to the maternal nipple odor[8].

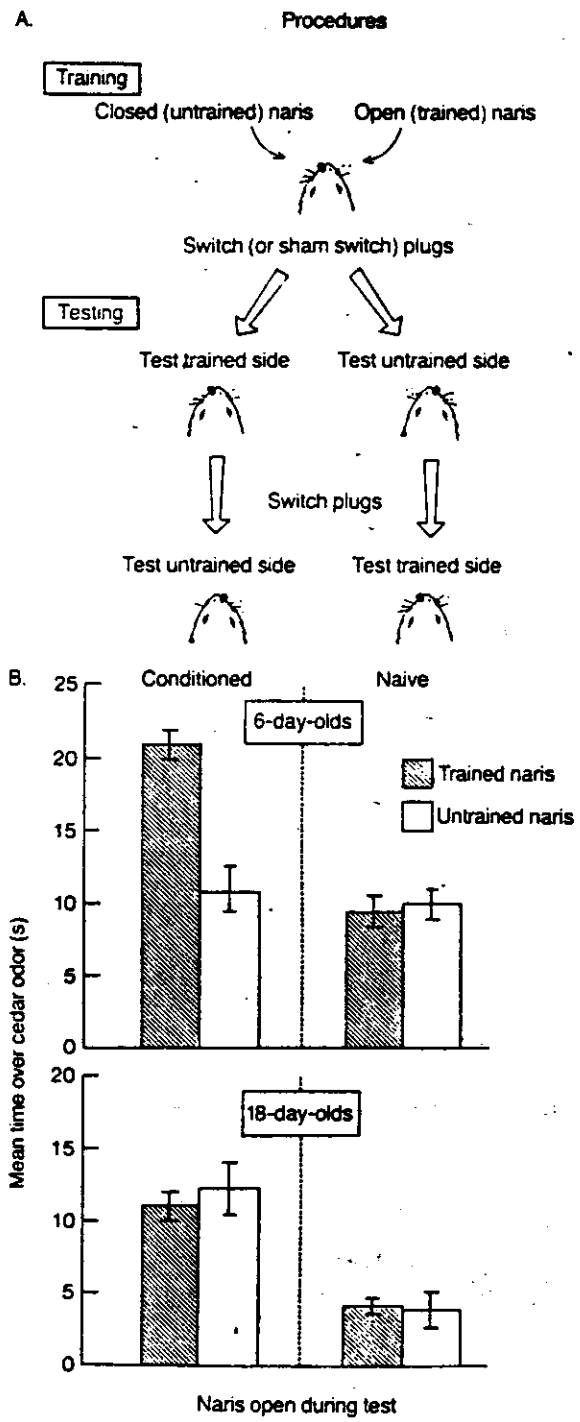


**Fig. 1.** (A) *Paradigm for unilateral early olfactory preference training.* (B) *Time over cedar odor for learning and control pups with their naris open during preference trials (trained or untrained) for 6-day-old (top) and 18-day-old pups (bottom).* (Taken, with permission, from Ref. 10.)

### *Commissural connections*

An exciting recent finding is that memories for odors learned unilaterally early in life can be localized in one side of the brain (Fig. 1)[9,10]. Unilateral learning is accomplished by occlusion of a single naris with a temporary plug. A behavioral preference can be observed in these rat pups when the same naris is open during both olfactory preference training and testing, but such a preference is absent when tested through the naris that has been occluded during training. By 18 days, when the commissural connections have developed[11], the untrained side can access the memory on the trained side. If these connections are cut, the pups cannot remember a memory learned on the contralateral side of the brain. Therefore, there is a natural split brain for olfactory memories early in life. As the crossed olfactory pathways develop and reach the contralateral olfactory cortex, previously formed olfactory memories can be accessed.

### *Enhanced glomerular response*

When adult or neonatal rats are exposed to different odors, their olfactory bulbs reliably show spatially distinct, odor-specific 2-DG uptake patterns within the glomerular layer[4,12]. While there is no change in the spatial pattern of 2-DG uptake after early olfactory learning, there is an increased 2-DG uptake in those areas of the glomerular layer that are normally activated by the learned odor[13]. The increased uptake is not due to increased respiration[13].

Only pups that were simultaneously stroked with a brush to mimic maternal contact and exposed to peppermint odor had both a peppermint preference and an enhanced neural response to the odor[14]. These data suggest that associative processes, rather than simply sensory experience, is involved in the formation of both odor preferences and the enhanced glomerular response.

The enhanced glomerular response is specific to the learned odor[15], and while it endures into adulthood[16], similar olfactory experience given to adults does not increase their glomerular response[17]. Indeed, the ability to develop the enhanced glomerular response appears to be restricted to the first week postpartum[17].

## Structural plasticity

The peppermint-learning pups have a striking change in the structure of the glomerular layers in the region associated with the increased 2-DG activity compared to those same regions in control pups (Fig. 2)[18]. Regions of increased 2-DG uptake have enlarged glomerular clusters, often protruding from the glomerular layer into the external plexiform layer. Clusters are occasionally observed in other, particularly medial, parts of the bulb that are not associated with the focal areas of 2-DG uptake. This situation could reflect the fact that pups may become attracted to other odors early in life. However, where there is an area of enhanced 2-DG uptake, there is an enlarged glomerular cluster.

While neither the number of glomeruli associated with each 2-DG focus nor the size of the 2-DG foci differ between groups, there is an increase in the size

of the glomerular region underlying the enhanced 2-DG uptake. This increase is apparently due to an increase in both the size of the glomerular neuropil and associated cell bodies[18]. Ultrastructural changes in these glomeruli following early learning have not yet been documented.

### Neurophysiological plasticity

To determine whether the signal emanating from the bulb is altered by early learning, the response of output neurons was recorded from the subpopulation of mitral cells (the major output neurons of the bulb) associated with the responsive glomerular areas[19,20]. The output cells of peppermint-learning pups have significantly fewer excitatory and significantly more suppressive responses to peppermint than the output cells of controls. No differences in response pattern of these cells is evoked by orange odor, an odor that activates a different part of the bulb. Peppermint odor learning neither decreases the number of cells that are responsive (either suppressive or excitatory), nor changes the magnitude of the response to either peppermint or orange odor. The altered response pattern in peppermint-learning pups to peppermint odor is restricted to those areas of the bulb associated with peppermint-activated glomerular areas[20].

The increase in 2-DG uptake in the glomerular region that contains mitral cell dendrites is interesting in light of the fact that their cell bodies have suppressed activity. It seems likely, then, that the increased glomerular layer activity is not due to mitral cell activity, but to the activity of another class of neurons. Indeed, it has been suggested that 2-DG activity in the glomerular layer of the bulb is produced by juxtaglomerular tufted cells[21]. An increase in the activity of tufted cells could suppress local mitral cell activity by activating granule cells in the ipsilateral internal plexiform layer[22]. These inhibitory interneurons would then suppress local mitral cell activity.

If this hypothesis has some validity, one might expect increased activity of granule cells in the internal plexiform and/or granule cell layers, deep to the enlarged glomerular clusters of odor-learning pups. To address this possibility we stained olfactory bulbs for glycogen phosphorylase, another activity-dependent enzyme, to increase the spatial resolution of activity measurement in the bulb. Only in peppermint-learning pups is there a restricted line of increased activity in the internal plexiform layer, deep to the modified glomerular clusters in response to peppermint odor (Fig. 3)[23]. The increase in activity is likely to be due to tufted cell activation of granule cells, which would suppress the response of local mitral cells.

How could increased tufted cell activity develop in odor-learning pups? Activation of tufted cells by early olfactory learning might prevent their death, or increase the size of their dendritic arbors. The increased number and/or size of tufted cells would produce the observed enlargement of the glomerular region. The increased response by these tufted cells to the learned odor may increase the activation of granule cells in the internal plexiform layer, thereby inhibiting neighboring mitral cells.

### Relation to development

Similarities between this work and other research raise the fascinating possibility that there may be

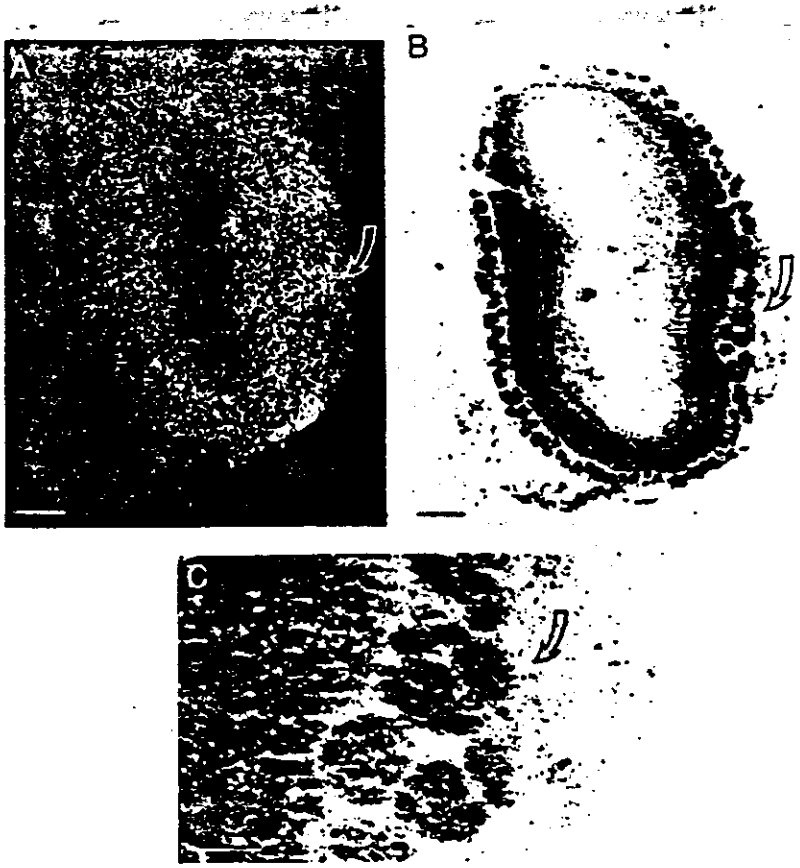


**Fig. 2.** (A) *Sample autoradiograph and* (B) *adjacent section stained for succinic dehydrogenase (SDH) from a pup that has acquired a preference for peppermint odor. Arrow in (A) points to a focus of 2-DG uptake, arrow in (B) points to corresponding glomerular cluster, determined by the alignment of adjacent sections. The enlarged glomerular cluster can be seen at higher magnification in* (C). *Scale bar in (A) and (B) is 400 μm; in (C), 100 μm.* (Taken, with permission, from Ref. 18.)

mechanisms of neural organization during development that are shared throughout the brain. Specifically, there are parallels emerging between the development of olfactory learning and the establishment of ocular dominance within the visual system in cats. Visual stimulation, which is necessary to maintain binocularity of striate cortex neurons, is unable to influence cortical organization if the NMDA-type glutamate receptors are blocked[24]. Such treatment also blocks the neurobehavioral consequences of early olfactory learning[25]. Ocular dominance plasticity can be maintained only if visual stimulation is accompanied by arousing stimulation from the thalamus or reticular formation[26]. These data are reminiscent of the finding that arousing tactile stimulation is needed for early olfactory learning[14]. Finally, visual, olfactory and somatosensory developmental plasticity appear to involve noradrenergic stimulation[27–29].

### Olfactory learning in adults

The activation of the noradrenergic pathway to the olfactory bulb also appears to modulate adult olfactory learning. At least 40% of noradrenergic neurons emanating from the locus coeruleus project to the olfactory bulb and these fibers synapse onto granule cells[30]. Noradrenergic modulation of several types of olfactory learning has been reported. For example, female mice learn the odor of their sexual partner, and abort their pregnancy if the odor of a strange male is subsequently sensed by her accessory olfactory

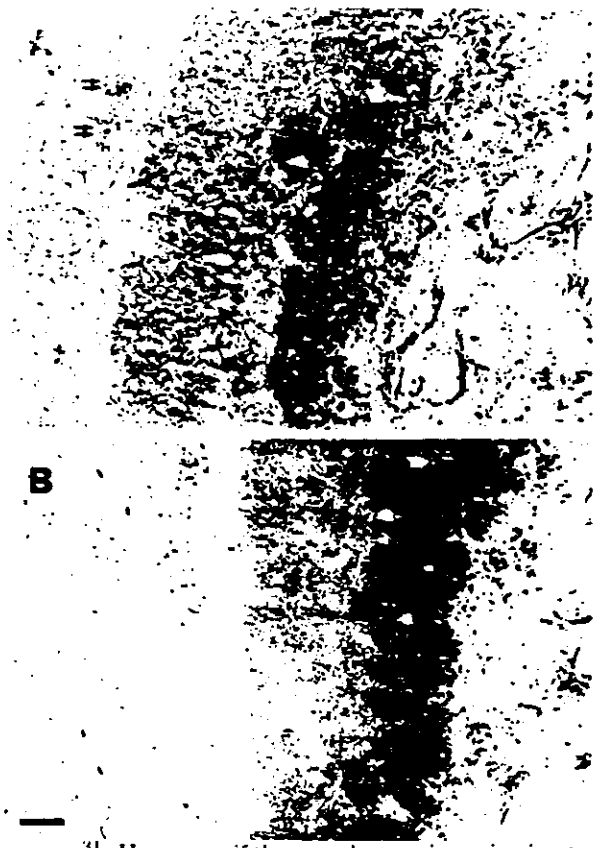


Fig. 3. Olfactory bulbs of pups that have been given preference training for peppermint odor just after being exposed to peppermint odor. The tissue has been stained for glycogen phosphorylase-activity. Small arrows (A) point to patches of staining in the internal plexiform layer, deep to the enlarged glomerular clusters. (B) Comparable areas in untrained pups exposed to peppermint odor. Scale bar is 0 μm. (Taken, with permission, from Ref. 23.)

system[31]. However, if the noradrenergic projection to the accessory olfactory system is depleted, she does not remember the odor of her sexual partner and aborts in his presence[32]. Similarly, ewes require noradrenergic activation of their olfactory system to be able to remember the olfactory identify of their offspring[33]. Ewes identify their lambs by a signature odor and normally reject other young. Depletion of the noradrenergic projection to their olfactory system induces the ewes to accept other lambs. Depletion of norepinephrine does not alter the ability of either female mice or ewes to discriminate other odors, suggesting that the effect on olfactory memories is not due to a general disability or an inability to sense odors.

The characteristic EEG spatial pattern in the olfactory bulb evoked by an odor is modified by olfactory learning[34]. This modification can be prevented during training by blockade of the β-adrenergic receptors with the drug propranolol[35]. Conversely, microinjections of norepinephrine in association with the odor, but in the absence of the reinforcing stimulation, can induce the modification of the bulbar EEG. These data suggest that noradrenergic stimulation may mediate the effects of reinforcement on learning[36]. Such an action of norepinephrine may well be shared by neonate and adult.

## Concluding remarks

Just as the use of invertebrate nervous systems has facilitated our understanding the changes that occur in relatively simple neural circuits during learning, developing mammals may provide accessible systems for the study of the complexities of brain modifications during learning. The strategy of using the olfactory system may also have some important advantages for the study the neurobiology of learning and memory[37]. An understanding of how higher mammalian brain structures are involved in cognition requires a detailed knowledge of the neurobiology of the sensory system through which learning occurs. Olfactory information is processed through a well-defined, simple pathway for which detailed anatomical and physiological information is known. In addition, unlike other sensory systems, the olfactory system has direct access to higher neural centers. Specifically, the olfactory receptors are but a single neuron from the olfactory cortex, which projects to the hippocampus and frontal cortex. Since these brain areas are involved in higher-order cognitive functions, mammalian olfactory system organization may be particularly useful for the study of the neurobiology of cognitive function.

*knowledgements*
*I thank R. Coopersmith, Guthrie, J. Lincoln, R. M. Sullivan, D. Wilson and C. C. Woo for their ontributions to this earch program and P. Yahr for her comments on the manuscript.*

## Selected references

1 Leon, M. (1983) in *Pheromones and Mammalian Communication* (Vandenbergh, J., ed.), pp. 38–77, Academic Press
2 Stickrod, G., Kimble, D. P. and Smotherman, W. P. (1982) *Physiol. Behav.* 28, 5–7
3 Blass, E. M. and Teicher, M. H. (1980) *Science* 210, 15–22
4 Pederson, P. E., Greer, C. and Shepherd, G. M. (1986) in *Handbook of Behavioral Neurobiology* (Vol. 8) (Blass, E. M., ed.), pp. 163–204, Plenum Press
5 Shepherd, G. M. (1972) *Physiol. Rev.* 52, 864–917
6 Risser, J. M. and Slotnick, B. M. (1985) *Chem. Senses* 10, 410
7 Hudson, R. (1985) *Dev. Psychobiol.* 18, 575–585
8 Hudson, R. and Distel, H. *Brain Res.* (in press)
9 Kucharski, D., Johanson, I. and Hall, W. G. (1986) *Behav. Neurol. Biol.* 46, 472–490
10 Kucharski, D. and Hall, W. G. *Behav. Neurosci.* (in press)
11 Schwob, J. E. and Price, J. L. (1984) *J. Comp. Neurol.* 223, 1260–1266
12 Sharp, F. R., Kauer, J. S. and Shepherd, G. M. (1975) *Brain Res.* 98, 596–600
13 Coopersmith, R. and Leon, M. (1984) *Science* 225, 849–851
14 Sullivan, R. M. and Leon, M. (1986) *Dev. Brain Res.* 27, 400–403
15 Coopersmith R., Henderson, S. R. and Leon, M. (1986) *Dev. Brain Res.* 27, 191–197
16 Coopersmith, R. and Leon, M. (1986) *Brain Res.* 371, 400–403
17 Woo, C. C. and Leon, M. (1986) *Soc. Neurosci. Abstr.* 12, 123
18 Woo, C. C., Coopersmith, R. and Leon, M. *J. Comp. Neurol.* (in press)
19 Wilson, D. A., Sullivan, R. M. and Leon, M. *J. Neurosci.* (in press)
20 Wilson, D. A. and Leon, M. (1986) *Soc. Neurosci. Abstr.* 12, 123
21 Macrides, F., Schoenfeld, T. A., Marchand, J. E. and Clancy, A. N. (1985) *Chem. Senses* 10, 175–202
22 Orona, E., Rainer, E. C. and Scott, J. W. (1984) *J. Comp. Neurol.* 226, 346–356
23 Coopersmith, R. and Leon, M. (1987) *J. Comp. Neurol.* 261, 148–154
24 Singer, W., Kleinschmidt, A. and Bear, M. F. (1986) *Soc. Neurosci. Abstr.* 12, 786
25 Lincoln, J., Coopersmith, R., Harris, E. W., Monaghan, D. T., Cotman, C. W. and Leon, M. (1986) *Soc. Neurosci. Abstr.* 12, 124
26 Singer, W. and Rauschecker, J. (1982) *Exp. Brain Res.* 134, 568–572
27 Kasamatsu, T. and Pettigrew, J. D. (1979) *J. Comp. Neurol.* 185, 139–162
28 Sullivan, R. M. and Leon, M. (1986) *Soc. Neurosci. Abstr.* 12, 124
29 Loeb, E. P., Chang, F-L. F. and Greenough, W. T. (1987) *Brain Res.* 403, 113–120
30 Shipley, M. T., Halloran, F. J. and De La Torre, J. (1985) *Brain Res.* 329, 294–299
31 Keverne, B. E. B. and De La Riva, C. (1982) *Nature* 7, 907–913
32 Rosser, A. E. and Keverne, E. B. (1985) *Neuroscience* 15, 1141–1148
33 Pissonier, D., Thierry, J. C., Fabre-Nys, C., Poindron, P. and Keverne, E. B. (1985) *Physiol. Behav.* 361–363
34 Freeman, W. J. and Skarda, C. A. (1985) *Brain Res. Rev.* 10, 147–176
35 Gray, C. M., Freeman, W. J. and Skinner, J. E. (1986) *Behav. Neurosci.* 100, 585–596
36 Aston-Jones, G. (1985) *Physiol. Psychol.* 13, 118–126
37 Staubli, U., Fraser, D., Faraday, R. and Lynch, G. *Behav. Neurosci.* (in press)

# Olfactory cortex: model circuit for study of associative memory?

Lewis B. Haberly and James M. Bower

Lewis B. Haberly is at the Department of Anatomy, University of Wisconsin, 1300 University Avenue, Madison, WI 53706, USA and James M. Bower is at the Division of Biology 216–76, California Institute of Technology, Pasadena, CA 91125, USA.

*The piriform (olfactory) cortex is a phylogenetically old type of cerebral cortex with parallels in its organization to the architecture of certain 'neural network' models for distributed pattern recognition and association. These features, in combination with unique structural characteristics that facilitate experimental study, make the piriform cortex a potentially good model for analysis of associative (content-addressable) memory processes.*

One of the fundamental questions in neurobiology is how the CNS is able to store, retrieve and associate complex patterns of neuronal activity. Over the past several years significant progress in addressing this question has been made on two fronts. First, with the aid of increasingly powerful experimental tools, neurobiologists have derived considerable structural, physiological and biochemical information that may assist in understanding higher order functions. Of particular significance are new insights concerning long-lasting, activity-dependent changes in synaptic efficacies[1]. Second, the question of how brain-like networks behave dynamically and, in particular, how they might store and retrieve information has become a focus of many mathematicians and physical scientists interested in building devices with pattern recognition abilities. The ideas being generated by these theoretical efforts are having a significant influence on the work of an increasing number of neurobiologists.

In this article we attempt to relate the parallel endeavors of biologists and theorists in the context of the mammalian olfactory cortex, which we believe to be a particularly good model system for study of the neural substrate for learned pattern recognition and association. First, however, we will provide an overview of models with brain-like abilities that have been developed by mathematicians and physical scientists. We will then introduce the circuitry of the olfactory cortex and point out parallels in architecture with the theoretical constructs. Finally, we will describe the initial attempts to model the olfactory cortex within the framework of these constructs.

## Neural networks and associative memory

In recent years there has been a rediscovery and rapid development of models and artificial devices for recognition and association of complex patterns that rely on large numbers of relatively simple processing elements that are highly interconnected and operate in parallel. Because of certain similarities between these models and general features of the CNS, they have come to be known as 'neural networks'. The basic design of such neural network models contrasts sharply with conventional digital computers where a highly complex 'central processing unit' carries out computations in a step-by-step serial fashion. For both non-technical and rigorous descriptions of the many forms of artificial neural networks, as well as accounts of the history of their development, the reader is referred to the recent volumes by Anderson and Rosenfeld[2] and Rumelhart and McClelland[3].

One of the principal reasons for interest in neural network models is the fact that many perform associative functions as a direct consequence of their architecture (and are therefore sometimes termed 'associative memory' models). These associative functions include the ability to reconstruct original learned patterns from inputs that are fragmented or distorted versions of these patterns, the related ability for novel input patterns to elicit outputs of related patterns that were previously stored in memory, and the ability to link two or more unrelated patterns, especially when they occur at the same time, so that subsequent input of one elicits the others from memory.

Key features of artificial neural networks that are related to their ability to perform such associative functions are the direct distribution of inputs across the processing array and memory storage via alterations in the strengths of connections between the processing elements (hence the term 'connectionist' models). Memories are coded in a 'distributed' fashion with individual connections participating in the storage of many different patterns. Another key feature of some neural networks is the ability to self-organize by altering strengths of connections based exclusively on local conditions such as the degree of synchrony of inputs converging on to individual processing elements. This allows these networks to develop their own internal representations for stored data. Neural network models of this form can be said to be 'content-addressable' since retrieval occurs when inputs directly elicit output from the array of interconnected processing elements. This form of retrieval contrasts with that of digital computers where information is accessed by a code that is unrelated to content (termed 'location-addressable' memory).

There are intriguing similarities in architecture, operation and other features of certain artificial neural networks and the cerebral cortex. In addition to the brain-like self-organizing associative abilities described above, these models display a relative immunity to the effects of damage to individual processing elements that is characteristic of association areas of the cerebral cortex. Requirements for processing elements are also within the capabilities of cortical



 0166-2236/89/$02.00

neurons: because processing occurs in parallel, complex pattern analysis can be carried out rapidly with elements that operate on the time scale of neurons (orders of magnitude slower than logical 'gate' operations in digital computers). Whereas many early associative memory models employed linear summation rules, increasingly, more complex neuron-like input–output operations are being incorporated*. Furthermore, algorithms for modification of the strengths of connections between processing elements in many associative memory models are reminiscent of the properties of cortical synapses where efficacies can be altered by coincident activation of inputs as described below.

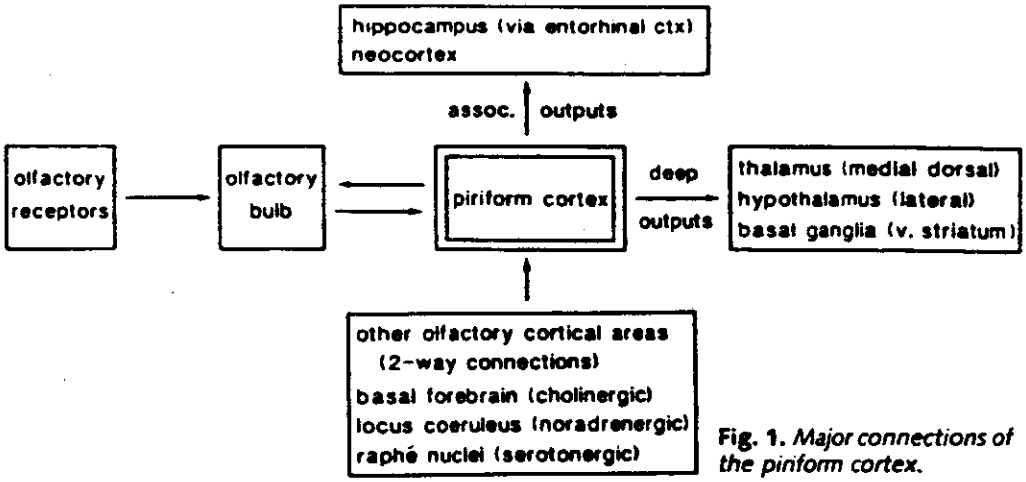


**Fig. 1.** *Major connections of the piriform cortex.*

## Why olfactory cortex?

While computer simulations have established the feasibility of many associative, content-addressable memory models for complex pattern recognition and other tasks, it has not been determined whether any real neuronal circuit functions in a similar fashion. For several reasons the olfactory cortex would appear to be an ideal system for addressing this question[4]. First, as described below, the circuitry in the olfactory cortex matches characteristics of recent associative memory models in important respects. Second, as also described below, there is a convergence of information from different sensory modalities and other brain systems on to different parts of the olfactory cortex. This convergence imparts the potential for complex associative functions. Third, its circuitry is amenable to experimental analysis: the olfactory cortex is only one synapse removed from the peripheral receptors and has a laminar segregation of different neuronal elements including fiber systems, cells of different types and different dendritic segments of pyramidal cells. Fourth, the olfactory cortex has close connections with monoaminergic, cholinergic and hippocampal systems that are believed to play important roles in learning and memory (Fig. 1). Finally, olfactory information at the level of the cortex appears to be in the form of a highly distributed ensemble code (Ref. 53 and Fig. 2C).

## Neuronal circuitry in piriform cortex

Several morphologically distinct parts of the cerebral cortex receive a direct input from the olfactory bulb [the receiving structure for axons from olfactory receptor cells (Fig. 1)] and are therefore termed olfactory cortex. While the present account will be confined to the piriform cortex, which is the largest of the olfactory cortical areas, it should be noted that there are similarities between the piriform cortex and the other types of olfactory cortex so that conclusions for the piriform cortex may apply to other areas[4]. The olfactory bulb is also outside the scope of the present article, but it must be recognized that models for the olfactory cortex will ultimately have to incorporate this structure, especially in view of the presence of two-way connections between the bulb and cortex[5,6]. Several mathematical models for the olfactory bulb have been developed[7–10].

The structure and physiology of the piriform cortex and other olfactory cortical areas have been described in some detail in recent reviews[4,11,12]. Features of the neuronal circuitry in the piriform cortex with relevance to the development of associative memory models are described below.

*Lamination.* The piriform cortex is usually described in terms of three layers (Fig. 3): layer I is a so-called plexiform layer that contains few neuronal cell bodies and is dominated by ascending dendrites from deeper layers and fiber systems. Layer I has been subdivided into a superficial sublamina, layer Ia, where afferent fibers from the olfactory bulb terminate and a deep sublamina, layer Ib, where association fibers terminate[13]. Layer II is a compact zone of neuronal cell bodies. Layer III contains neuronal cell bodies at a lower density than layer II and a large number of dendritic and axonal elements.

*Cells.* Pyramidal cells, which are the principal integrative elements in the piriform cortex, have much in common with their counterparts in the neocortex and hippocampal cortex[14–16] (Fig. 4). As in these other types of cerebral cortex, dendrites consist of an apical tree directed toward the brain surface and a basal tree that radiates from cell bodies. Pyramidal cells are found in both layers II and III (SP and DP, respectively, in Fig. 3). Primary axons give rise to a profusion of fine unmyelinated collaterals that synapse near parent cell bodies as well as at long distances. Afferent fibers from the olfactory bulb and association fibers from other pyramidal cells make excitatory synapses primarily on spines that isolate them from dendritic shafts[17]. Synapses from these two fiber systems are completely excluded from cell bodies. Indirect evidence indicates that inhibitory synapses are distributed over cell bodies, axon initial segments, and the entire extents of apical and basal dendritic trees[12].

* Complex input–output relationships in neurons are a result of many factors. These include non-linearities at three processing levels: in the D/A (digital to analog) conversion from all-or-none action potentials in input axons to graded postsynaptic potentials, in the integration of these graded potentials, and in the A/D conversion for output. Sources of non-linearity include an effect of postsynaptic voltage on D/A conversion when NMDA receptors are activated, the participation of current shunting and voltage-dependent membrane channels in the integration of postsynaptic potentials, and the presence of a threshold for action potential generation.

As in other types of cerebral cortex, a large number of classes of non-pyramidal cell can be distinguished on the basis of location, morphology, connections and neurotransmitters. However, in contrast to the neocortex, these different types tend to be lamina- and position-specific – a feature that greatly facilitates experimental analysis and modeling[14,18]. As in other types of cerebral cortex, a large percentage of non-pyramidal cells in the piriform cortex appear to use GABA as their neurotransmitter and therefore probably mediate an inhibitory effect[18,19].

*Afferent fiber systems.* Afferent fibers from the olfactory bulb, which carry incoming olfactory information, terminate in the sharply delimited layer Ia (Ref. 13). It is of special significance, as discussed below, that this fiber system is highly distributed in the horizontal dimension (parallel to the cortical surface): small areas in the olfactory bulb project to the entire extent of the piriform cortex and, conversely, small areas in the piriform cortex receive inputs from cells in all parts of the olfactory bulb[20] (Fig. 5). There is a non-uniformity in this projection but any patterns present are broad and overlapping with no indication of a topographically organized, point-to-point mapping.

In addition to the afferent input from the olfactory bulb, the piriform cortex and other olfactory cortical areas that include the entorhinal cortex, receive inputs from the amygdala, hippocampal formation and neocortical areas[4,12]. These inputs could allow a convergence of olfactory information with that derived from other sensory systems as well as limbic (emotional, visceral) and motor systems.

*Association fiber systems.* Within the piriform cortex there are intrinsic association fiber systems that, in common with the afferent input, are precisely ordered in the vertical dimension but highly distributed in the horizontal dimension[5,21] (Fig. 3). These association fibers both originate from, and terminate on pyramidal cells[17,21]. As illustrated in Fig. 3, at least three different intrinsic fiber systems can be distinguished that synapse on different dendritic segments of pyramidal cells[12,22]. Physiological data from intracellular recording[15,16,23–25] and current source-density experiments[26–28] (Fig. 6) suggest that following activation of afferent fibers, four different EPSPs occur in different dendritic segments of pyramidal cells consistent with expectations from the morphological data: a monosynaptic EPSP mediated by afferent fibers in distal apical segments is followed successively by disynaptic EPSPs at the level of basal dendrites in layer III, middle apical segments in superficial layer Ib, and proximal apical segments in deep layer Ib. Recent studies[27] suggest that this sequence may recur during each cycle of the 40–60 Hz oscillation that accompanies odor responses (see below).

*Inhibitory systems.* A variety of inhibitory systems have been demonstrated in the piriform cortex as in other types of cerebral cortex. Afferent fibers directly synapse on inhibitory interneurons which project to pyramidal cells, thereby producing a feedforward inhibition[15]. Outputs of pyramidal cells contact inhibitory interneurons which project back to pyramidal cells producing feedback inhibition[29]. Physiological study has revealed fast and slow synaptically mediated inhibitory processes mediated

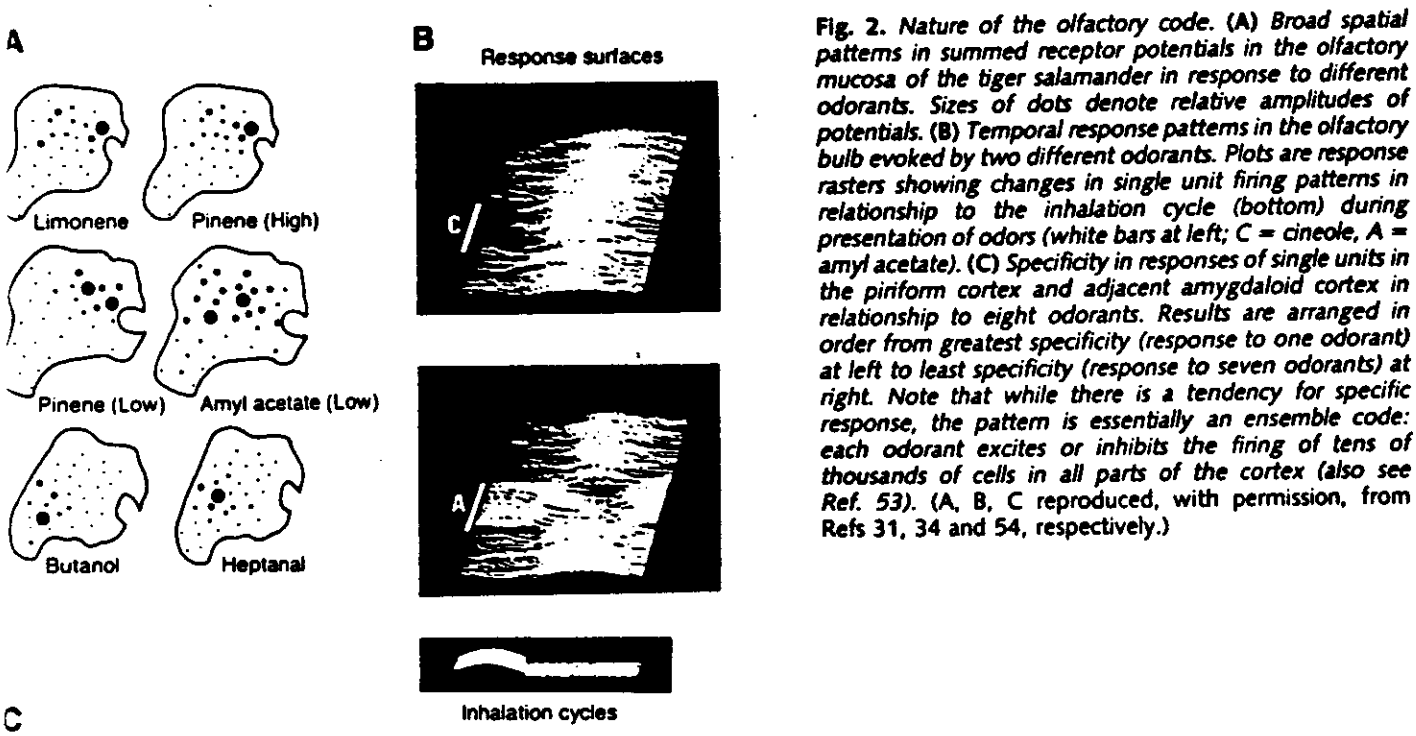


**Fig. 2.** *Nature of the olfactory code.* **(A)** *Broad spatial patterns in summed receptor potentials in the olfactory mucosa of the tiger salamander in response to different odorants. Sizes of dots denote relative amplitudes of potentials.* **(B)** *Temporal response patterns in the olfactory bulb evoked by two different odorants. Plots are response rasters showing changes in single unit firing patterns in relationship to the inhalation cycle (bottom) during presentation of odors (white bars at left; C = cineole, A = amyl acetate).* **(C)** *Specificity in responses of single units in the piriform cortex and adjacent amygdaloid cortex in relationship to eight odorants. Results are arranged in order from greatest specificity (response to one odorant) at left to least specificity (response to seven odorants) at right. Note that while there is a tendency for specific response, the pattern is essentially an ensemble code: each odorant excites or inhibits the firing of tens of thousands of cells in all parts of the cortex (also see Ref. 53).* (A, B, C reproduced, with permission, from Refs 31, 34 and 54, respectively.)

by chloride and potassium[15].

*Efferent systems.* There are direct outputs from the piriform cortex and other olfactory cortical areas to the neocortex, thalamus, hypothalamus, basal ganglia and hippocampal formation[11,12,30] (Fig. 1).

## Olfactory coding and perception

Results from several experimental approaches indicate that the olfactory code includes a highly distributed spatial component[31,32] (Fig. 2A). Studies of summed receptor potentials suggest that this spatial component originates as a consequence of a tendency for receptor cells with similar specificities to be broadly segregated on the receptive surface[31,33]. In addition to the spatial coding, studies at the receptor level and in the olfactory bulb have revealed consistent temporal patterns of activity that could contribute to the olfactory discrimination process[31,34,35] (Fig. 2B). During odor responses high amplitude 40–60 Hz oscillations occur in both the olfactory bulb and cortex[7]. In rodents, rhythmic sniffing that is tied to the θ-frequency[36] evokes envelopes of this oscillatory activity at approximately 200 ms intervals.

An intriguing aspect of the olfactory sense with potential relevance to memory modeling is the strong tendency in man[37] and lower animals[38] for mixtures of odorants to be perceived as single-odor sensations with a poorly developed capacity for dissection into individual components – a feature reminiscent of certain associative memory models where input-triggered activity settles into unitary output patterns (e.g. Ref. 39). It thus resembles the discrimination of colors in the visual system, but stands in marked contrast to visual pattern discrimination where the ability to examine individual stimulus components is well developed.

## Memory modeling

There are several striking parallels between the structure of the piriform cortex and the architecture of certain associative, content-addressable memory models[4]. First, to a large extent the function of artificial associative networks depends upon a spatially distributed input system like that seen in the olfactory bulb projection to the piriform cortex. Second, the discriminative power of many associative networks is greatly enhanced by positive feedback via interconnections between the processing units that receive the distributed input. In the piriform cortex the interconnections between pyramidal cells (associational fiber systems) mediate a distributed positive feedback to dendritic segments that are immediately adjacent to the segments that receive the distributed afferent input[28]. Third, in associative memory models individual inputs are typically weak relative to output threshold, which is also likely to be the case in the olfactory cortex[15]. Finally, many of these artificial networks require activity-dependent changes in excitatory synaptic strengths. While different algor-

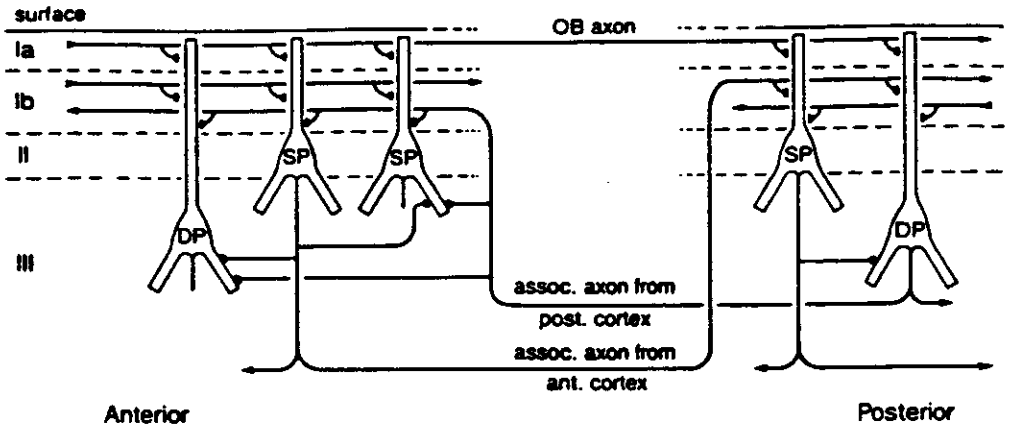


**Fig. 3.** *Summary of excitatory connections of pyramidal cells in the piriform cortex. See Fig. 4 for pyramidal cell morphology. As described in the text, afferent and different intrinsic associational fiber systems synapse in a lamina-specific fashion on different dendritic segments of pyramidal cells. Abbreviations: OB, olfactory bulb (afferent) fibers; SP, superficial pyramidal cells; DP, deep pyramidal cells. Roman numerals denote cortical layers.*

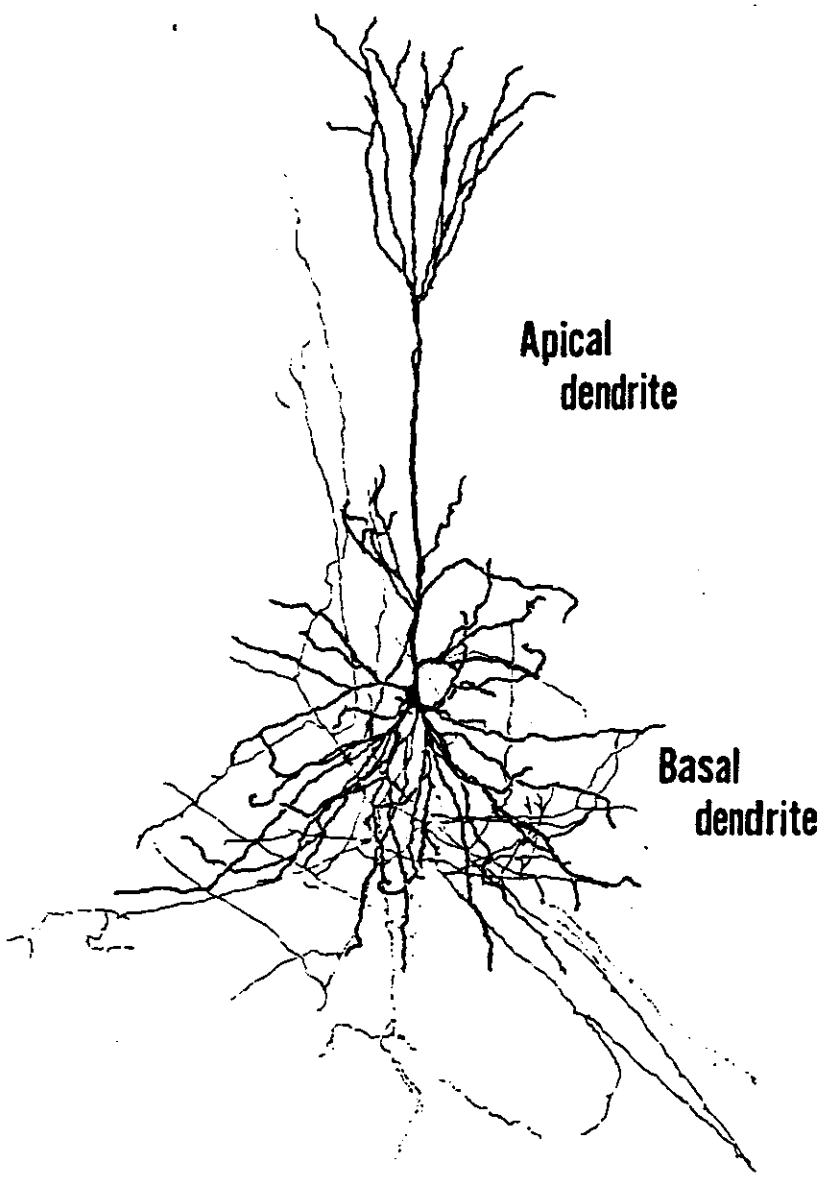


**Fig. 4.** *Pyramidal cell in piriform cortex stained by intracellular dye injection. As in other types of cerebral cortex these cells give rise to an apical dendritic tree that extends toward the cortical surface and a basal dendritic tree that radiates from the cell body. The axon gives rise to many fine collaterals (thin processes interspersed among thicker dendritic processes).* (Figure provided by Guo-Fang Tseng.)

ithms for implementing such changes are employed in different models, many can be thought of as variations of the 'Hebb rule'[40]. These algorithms allow simultaneous activation of multiple inputs, or inputs and outputs, to trigger alterations in the strengths of input connections. While there has been comparatively little study of synaptic plasticity in the piriform cortex, excitatory synapses on to pyramidal cells in the closely related hippocampus display Hebb-like activity-dependent alterations in strength, termed long term potentiation (LTP)[1]. It has recently been demonstrated that interactions between inputs to different portions of the dendritic tree can trigger such alterations[41,42]. If pyramidal cells in the piriform cortex have similar properties, then activation of either afferent or associational fibers with the proper temporal pattern could trigger changes in synaptic strengths. Such changes could also be triggered by coincidence in activation of different dendritic segments by afferent and associational inputs (see Ref. 43 for theoretical implications of this possibility). A recent study[44] has revealed substantial increases in the strengths of excitatory synapses in the piriform cortex when animals are trained to respond to synchronous shock stimuli as if they were odors, but further study will be required to determine whether properties of this process are similar to LTP in hippocampal pyramidal cells.

An important question is whether highly distributed intrinsic connections like those in associative memory models are unique to the olfactory cortex or if they are also present in other types of cerebral cortex – i.e. is there potential for the olfactory cortex to serve as a general model for analysis of associative memory processes? While studies of the intrinsic circuitry in the neocortex have concentrated on the vertical, columnar organization of the receiving areas, recent studies have demonstrated the presence of horizontal intrinsic connections[45] that may be especially well-developed in higher order 'association' areas. Even in area 7 of the cat, however, which appears to have the most extensive intrinsic associational connections yet demonstrated in the neocortex, the horizontal organization is not of a continuous nature as in the olfactory cortex, but is 'fractured' into irregular interconnected patches[46]. Nevertheless, the high degree of convergence and divergence of connections between pyramidal cells that is required for most associative, content-addressable memory schemes does appear to be present.

## Computer simulation models for piriform cortex

Wilson and Bower[47–50] have developed a network simulation for the piriform cortex that replicates basic features of responses to natural and artificial stimuli.

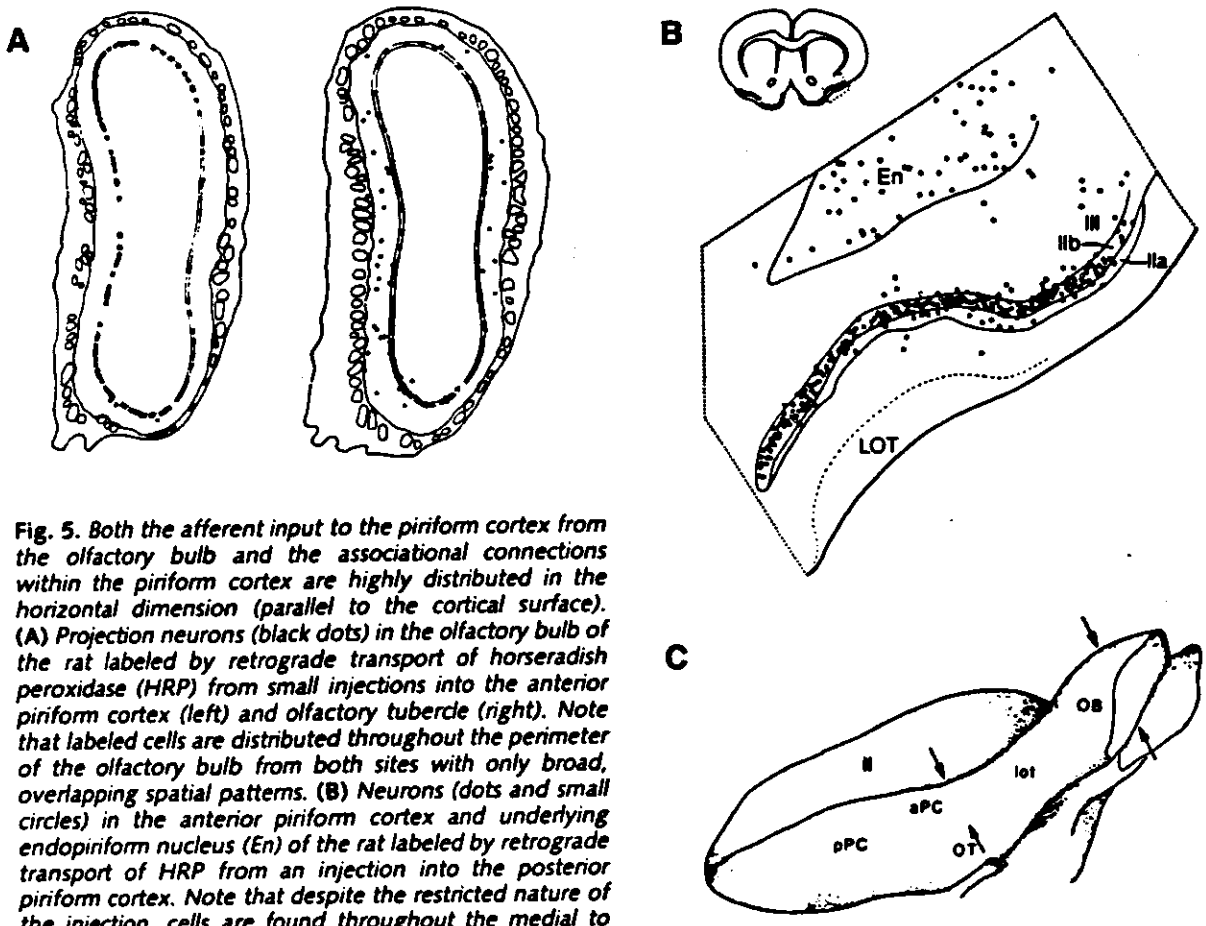


**Fig. 5.** *Both the afferent input to the piriform cortex from the olfactory bulb and the associational connections within the piriform cortex are highly distributed in the horizontal dimension (parallel to the cortical surface).* **(A)** *Projection neurons (black dots) in the olfactory bulb of the rat labeled by retrograde transport of horseradish peroxidase (HRP) from small injections into the anterior piriform cortex (left) and olfactory tubercle (right). Note that labeled cells are distributed throughout the perimeter of the olfactory bulb from both sites with only broad, overlapping spatial patterns.* **(B)** *Neurons (dots and small circles) in the anterior piriform cortex and underlying endopiriform nucleus (En) of the rat labeled by retrograde transport of HRP from an injection into the posterior piriform cortex. Note that despite the restricted nature of the injection, cells are found throughout the medial to lateral extent of layer II and the endopiriform nucleus.* **(C)** *Locations of sections in (A) and (B) (arrows). Abbreviations: aPC, anterior piriform cortex; lot, lateral olfactory tract (afferent fibers to piriform cortex from the olfactory bulb); N, neocortex; OT, olfactory tubercle; pPC, posterior piriform cortex.* (A, B, C reproduced, with permission, from Refs 20, 21 and 55, respectively.)

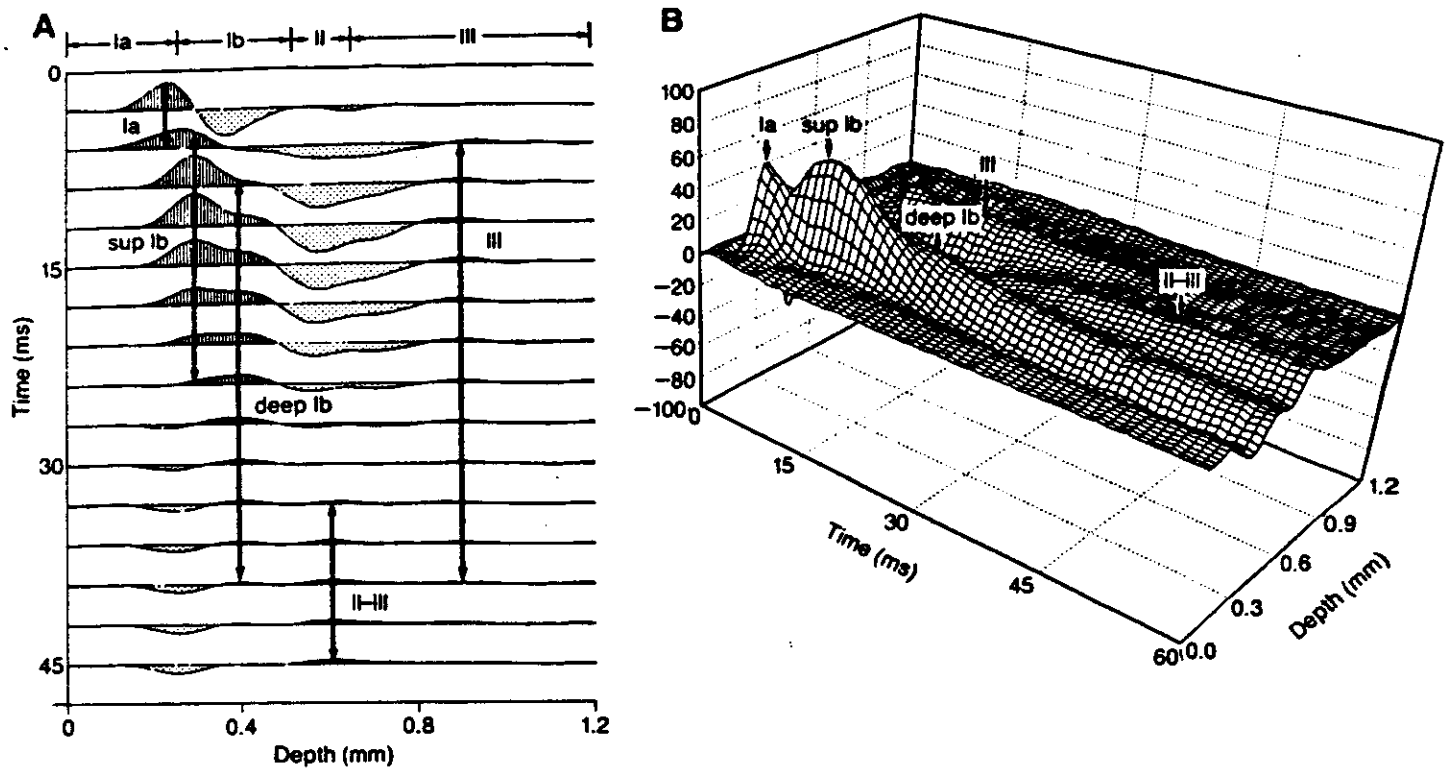


**Fig. 6.** *Synaptic events in the piriform cortex evoked by synchronous activation of afferent fibers as revealed by current source-density analysis.* **(A)** *Raster plot of net membrane currents as a function of depth at a series of times following shock stimulation of afferent fibers from the olfactory bulb. Cortical layers are indicated at the top (compare with the scale on the left in Fig. 3). Net inward currents (sinks) are denoted by vertical hatching; net outward currents (sources) by stippling. Double-headed arrows denote major sinks.* **(B)** *Same data as in (A) represented as a 3-D surface plot. The layer Ia sink [Ia in (A) and (B)] is the inward current that generates the monosynaptic EPSP in distal apical dendritic segments of pyramidal cells. The sinks in the superficial and deep parts of layer Ib [sup Ib and deep Ib in (A) and (B)] and the small sink in layer III [III in (A) and (B)] are believed to be currents that generate the disynaptic EPSPs mediated by different intrinsic associational fiber systems in proximal apical and basal dendritic segments of pyramidal cells (see Fig. 3). The final sink (II–III) is believed to be associated with the fast chloride-mediated IPSP.* (Modified from Ref. 28.)

The ability of a reduced version of this simulated network to carry out pattern recognition and associative functions has been explored[47]. This learning version of the model consists of a 10 × 10 array of simulated input fibers from the olfactory bulb, and 10 × 10 arrays of simulated pyramidal cells and both feedforward and feedback inhibitory neurons. The afferent array projects to the pyramidal cell and feedforward interneuron arrays in a spatially distributed fashion as in the real system. Pyramidal cells project to other pyramidal cells, also in a spatially distributed fashion providing a distributed positive feedback as also demonstrated in the real system. Both the afferent and association systems are randomly distributed with a 0.05 probability of contacting a given neuron in the receiving populations. The simulated synapses of the distributed positive feedback system and both inhibitory systems are modifiable, but synapses of input fibers are not. Synaptic modification is in activity-dependent fashion using a modified Hebb rule. Excitatory and inhibitory inputs to pyramidal cells are integrated in a neuron-like, nonlinear fashion. Outputs from neurons are all-or-none spikes that are triggered at a discrete threshold.

For studies of learning in this model, stimuli consisting of random spatial patterns across ten of the 100 input fibers were presented as 40 Hz bursts to simulate the oscillatory bulb output, and repeated at 200 ms intervals to simulate sniffing at the θ-rhythm. Learning was defined as development of consistent representations in cortical activity for particular input patterns with repeated stimulus presentations. The model has been found to display several types of memory and associative function. First, it has the ability to reconstruct original stimulus patterns from partially degraded inputs. Second, it has the ability to store and retrieve two non-overlapping input patterns without substantial interference, in spite of the fact that interconnections between pyramidal cells result in overlapping response patterns before training. Third, an ability for enhanced differentiation between two partially overlapping stimuli was demonstrated when each was presented during training with non-overlapping 'state' stimuli. This paradigm simulates learning situations where olfactory stimuli are paired with different environmental cues. Because this model was designed to replicate physiological responses, it makes predictions about patterns of activity that should be seen during normal function[49].

A second model for the piriform cortex is being developed by Granger *et al.*[51] to demonstrate the feasibility of a 'sparse combinatorial' approach to classification of olfactory stimuli. This model also consists of a 10 × 10 array of simulated afferent fibers that projects to a 10 × 10 array of simulated layer II pyramidal neurons in a random, distributed fashion. The olfactory code is assumed to be spatial as in the Wilson and Bower model. Alterations in efficacies of the afferent fiber synapses are made according to a modified Hebb rule in local 'unsupervised' fashion,

*Acknowledgements*

*The authors wish to acknowledge the support of grants from the NINCDS and NSF (LBH) and NINCDS, NSF and ONR (JMB).*

although the exact formulation of the algorithm differs from that of Wilson and Bower. Several types of inhibitory process are assumed in the model including a strong local feedback process that imparts a 'winner-takes-all' response mode on sets of 8–12 pyramidal cells. While there are excitatory interconnections between pyramidal cells as in the Wilson and Bower model, in simulations presented thus far, parameters have been adjusted so that these interconnections contribute little to outputs. There is one particularly intriguing feature of this model: its operation requires that each input line contact a relatively small number of simulated pyramidal cells. This is in contrast to most associative networks where performance is enhanced by increasing the degree of connectivity. Another unique feature that underlies operation of this model is a long-lasting 'refractoriness' in inhibitory and excitatory responses of pyramidal cells. The inhibitory refractoriness, which is based on findings for hippocampal pyramidal cells[52], allows responses to inputs that are repeated at the θ-frequency to be strongly facilitated and trigger lasting changes in synaptic efficacy. The excitatory refractoriness suppresses initial strong responses that result from convergence of many input lines so that more selective responses can emerge during continued presentation of input patterns. Test stimuli consist of spatial patterns involving up to 19 of the 100 input lines. Simulations with this model have demonstrated content-addressable memory capabilities that allow categorization of simulated odors (grouping of similar input patterns) as well as increases in the specificity of responses to partially overlapping stimulus patterns with repeated presentations.

## Concluding remarks

While models for the piriform cortex that have been developed thus far consist of relatively small arrays of simulated neurons, and both simplifying assumptions and assumptions concerning unknown parameters are required, they offer encouragement that the theoretical framework provided by associative, content-addressable memory models will be a useful one for study of the nervous system.

## Selected references


1 Landfield, P. W. and Deadwyler, S. A. (1989) *Long-term Potentiation from Biophysics to Behavior* Alan R. Liss
2 Anderson, J. A. and Rosenfeld, E. (1988) *Neurocomputing: Foundations of Research* MIT Press
3 Rumelhart, D. E. and McClelland, J. L. (1986) in *Parallel Distributed Processing: Explorations in the Microstructure of Cognition (Vol. 1: Foundations)* MIT Press
4 Haberly, L. B. (1985) *Chem. Senses* 10, 219–238
5 Luskin, M. B. and Price, J. L. (1983) *J. Comp. Neurol.* 216, 264–291
6 Gray, C. M. and Skinner, J. E. (1988) *Exp. Brain Res.* 69, 378–386
7 Freeman, W. J. (1975) *Mass Action in the Nervous System* Academic Press
8 Baird, B. (1986) in *Evolution, Games, and Learning: Models for Adaptation in Machines and Nature* (Farmer, D., Lapedes, A., Packard, N. and Wendroff, B., eds), pp. 150–176, Physica
9 Skarda, A. and Freeman, W. J. (1987) *Behav. Brain Sci.* 10, 161–194
10 Li, Z. and Hopfield, J. J. *Biol. Cybern.* (in press)
11 Switzer, R. C., de Olmos, J. and Heimer, L. (1985) in *The Rat Nervous System: Forebrain and Midbrain* (Paxinos, G., ed.), pp. 1–36, Academic Press
12 Haberly, L. B. in *Synaptic Organization* (Shepherd, G. M., ed.), Oxford University Press (in press)
13 Price, J. L. (1973) *J. Comp. Neurol.* 150, 87–108
14 Haberly, L. B. (1983) *J. Comp. Neurol.* 213, 163–187
15 Tseng, G-F. and Haberly, L. B. (1988) *J. Neurophysiol.* 59, 1352–1376
16 Tseng, G-F. and Haberly, L. B. *J. Neurophysiol.* (in press)
17 Haberly, L. B. and Behan, M. (1983) *J. Comp. Neurol.* 219, 448–460
18 Haberly, L. B., Hansen, D J., Feig, S. L. and Presto, S. (1987) *J. Comp. Neurol.* 266, 269–290
19 Westenbroek, R. E., Westrum, L. E., Hendrickson, A. E. and Wu, J-Y. (1987) *Dev. Brain Res.* 34, 191–206
20 Haberly, L. B. and Price, J. L. (1977) *Brain Res.* 129, 152–157
21 Haberly, L. B. and Price, J. L. (1978) *J. Comp. Neurol.* 178, 711–740
22 Luskin, M. B. and Price, J. L. (1983) *J. Comp. Neurol.* 216, 292–302
23 Biedenbach, M. A. and Stevens, C. F. (1969) *J. Neurophysiol.* 32, 204–214
24 Haberly, L. B. and Bower, J. M. (1984) *J. Neurophysiol.* 51, 90–112
25 Bower, J. M. and Haberly, L. B. (1986) *Proc. Natl Acad. Sci. USA* 83, 1115–1119
26 Haberly, L. B. and Shepherd, G. M. (1973) *J. Neurophysiol.* 36, 789–802
27 Ketchum, K. L. and Haberly, L. B. (1988) *Soc. Neurosci. Abstr.* 14, 278
28 Rodriguez, R. and Haberly, L. B. (1989) *J. Neurophysiol.* 702–718
29 Satou, M., Mori, K., Tazawa, Y. and Takagi, S. F. (1983) *J. Neurophysiol.* 50, 89–101
30 Price, J. L. (1985) *Chem. Senses* 10, 239–258
31 Kauer, J. S. (1987) in *Neurobiology of Taste and Smell* (Finger, T. E., ed.), pp. 205–231, John Wiley & Sons
32 Sharp, F. R., Kauer, J. S. and Shepherd, G. M. (1975) *Brain Res.* 98, 596–600
33 Edwards, D. A., Mather, R. A. and Dodd, G. H. (1988) *Experientia* 44, 208–226
34 Macrides, F. (1977) in *Chemical Signals in Vertebrates* (Muller-Schwarze, D. and Mozell, M. M., eds), Plenum
35 Chaput, M. A. and Lankheet, M. J. (1987) *Physiol. Behav.* 40, 453–462
36 Macrides, F., Eichenbaum, H. B. and Forbes, W. B. (1982) *J. Neurosci.* 2, 1705–1717
37 Berglund, B. and Lindvall, T. (1982) in *The Nose: Upper Airway Physiology and the Atmospheric Environment* (Proctor, D. F. and Andersen, I., eds), pp. 279–305, Elsevier
38 Staubli, U., Fraser, D., Faraday, R. and Lynch, G. (1987) *Behav. Neurosci.* 101, 757–765
39 Hopfield, J. J. (1982) *Proc. Natl Acad. Sci. USA* 79, 2554–2558
40 Hebb, D. O. (1949) *The Organization of Behavior* John Wiley & Sons
41 Gustafsson, B. and Wigström, H. (1986) *J. Neurosci.* 6, 1575–1582
42 Larson, J. and Lynch, G. (1986) *Science* 232, 985–988
43 Chover, J. (1989) *Synapse* 3, 101–116
44 Roman, F., Staubli, U. and Lynch, G. (1987) *Brain Res.* 418, 221–226
45 Gilbert, C. D. (1985) *Trends Neurosci.* 8, 160–165
46 Callahan, E. C. and Haberly, L. B. (1987) *J. Comp. Neurol.* 258, 125–137
47 Wilson, M. A. and Bower, J. M. (1988) in *Neural Information Processing Systems* (Anderson, D. Z., ed.), pp. 114–126, American Institute of Physics
48 Wilson, M. and Bower, J. M. (1989) in *Methods in Neuronal Modeling: From Synapses to Networks* (Koch, C. and Segev, I., eds), pp. 291–334, MIT Press
49 Bower, J. M. in *An Introduction to Neural and Electronic Networks* (Zornetzer, S., Davis, J. and Yau, C., eds), Academic Press (in press)
50 Nelson, M., Furmanski, W. and Bower, J. M. (1989) in *Methods in Neuronal Modeling: From Synapses to Networks* (Koch, C. and Segev, I., eds), pp. 397–438, MIT Press
51 Granger, R., Ambros-Ingerson, J. and Lynch, G. (1988) *J. Cognitive Neurosci.* 1, 61–87
52 Larson, J. and Lynch, G. (1988) *Brain Res.* 441, 111–118
53 Cattarelli, M., Astic, L. and Kauer, J. S. (1988) *Brain Res.* 442, 180–184
54 Takagi, S. F. (1986) *Prog. Neurobiol.* 27, 195–250
55 Schneider, S. P. and Scott, J. W. (1983) *J. Neurosci.* 50, 358–378

Biol. Cybern. 61, 379–392 (1989)

Biological Cybernetics


# Modeling the Olfactory Bulb and its Neural Oscillatory Processings

Z. Li[1] and J. J. Hopfield[2]

[1] Division of Physics, Mathematics and Astronomy, and [2] Division of Biology, and Division of Chemistry and Chemical Engineering, AT & T Bell Laboratories, California Institute of Technology, Pasadena, Ca 91125, USA

**Abstract.** The olfactory bulb of mammals aids in the discrimination of odors. A mathematical model based on the bulbar anatomy and electrophysiology is described. Simulations of the highly non-linear model produce a 35–60 Hz modulated activity which is coherent across the bulb. The decision states (for the odor information) in this system can be thought of as stable cycles, rather than point stable states typical of simpler neuro-computing models. Analysis shows that a group of coupled non-linear oscillators are responsible for the oscillatory activities. The output oscillation pattern of the bulb is determined by the odor input. The model provides a framework in which to understand the transform between odor input and the bulbar output to olfactory cortex. There is significant correspondence between the model behavior and observed electrophysiology.

## 1 Introduction

The olfactory system is a phylogenetically primitive part of the cerebral cortex (Shepherd 1979). In lower vertebrates, the olfactory system is the largest part of the telencephalon. This system also has a simple cortical intrinsic structure, which in modified form is used in other parts of the brain (Shepherd 1979). The olfactory system deals with a relatively simple computational problem compared to vision or audition, since molecules of the distal object to be detected are bound to and crudely recognized by receptor proteins. Having phylogenetic importance and computational simplicity, the olfactory system is an ideal candidate to yield insight on the principles of sensory information processing.

The olfactory system includes the receptor cells within the nasal cavity, the olfactory bulb, and the olfactory cortex which receives the inputs from the olfactory bulb (Fig. 1). Odorant molecules selectively increase the firing rates of the spontaneously active receptor cells (Sicard and Holley 1984), whose axons carry the odor information to the olfactory bulb. The olfactory bulb also receives inputs from the olfactory cortex and the "diagonal band" (Shepherd 1979) at the base of the brain. Both the bulb and the prepiriform cortex to which it sends its efferents exhibit similar 35–90 Hz rhythmic population activity as seen in EEG recordings, modulated by breathing.

The anatomy and physiology of the olfactory bulb are well studied. Efforts have been made to model its information processing function (Freeman 1979b, c; Freeman and Schneider 1982; Freeman and Skarda 1985; Baird 1986; Skarda and Freeman 1987), which is still unclear (Scott 1986). The position of the bulb in the olfactory pathway makes it a likely location of information processing to increase the identifiability of odors. The linkage of the bulbar and cortical oscillatory activity with the sniff cycles suggests that the oscillation plays an important role in the olfactory information processing (Freeman and Skarda 1985; Baird 1986; Skarda and Freeman 1987). We will examine the way in which the bulbar oscillation pattern originates, and how this pattern, which can be thought of as the decision state about odor information, depends on the input odor.

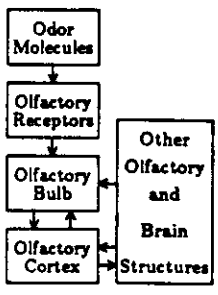


**Fig. 1.** Olfactory system and its environment

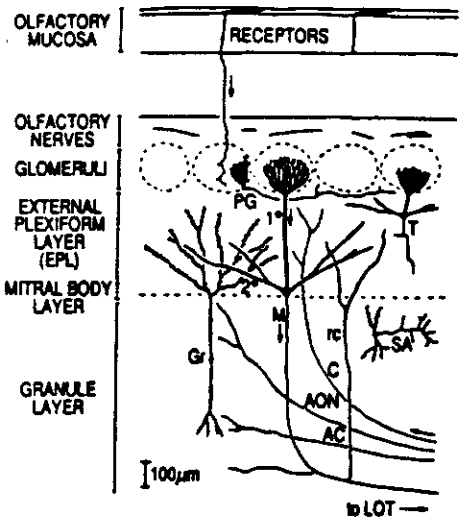


Fig. 2. Neuronal elements of the mammalian olfactory bulb. Inputs: olfactory nerves (above) from the receptors; central fibers (C, AON and AC) from the higher centers. Neurons: mitral cell (M), with primary (1°) and secondary dendrites (2°) and recurrent axon collaterals (rc); tufted cell (T), a smaller version of mitral cells; granule cell (Gr); inhibitory cell (PG) in the input layer; deep short axon cells (SA) which are small in number. Outputs: LOT to olfactory cortex. Taken from Shephard (1979)

## 2 Anatomical and Physiological Background

The olfactory bulb has clearly differentiated types of neurons located on different parallel lamina. These lamina lie on a surface which is roughly a segment of a sphere or ellipsoid. Each receptor sends a single unbranched axon to the topmost layer, terminating in one of the spherical regions of neuropil termed glomeruli (Fig. 2; Shepherd 1979). The receptor axons ramify inside it and synapse on the dendrites of the excitatory mitral cells and on dendrites of inhibitory short axon cells. The short axon cells make local dendrodendritic contacts with mitral cells. A few axons from the diagonal band also synapse on the mitral dendrites in this layer (Shepherd 1979).

The main cell types of the bulb are the (excitatory) mitral cells, whose cell bodies lie below the input layer, and the (inhibitory) granule cells lying deep below the layer of mitral cell bodies (Shepherd 1979). Each mitral cell sends an unbranched primary dendrite to one glomerulus. The granule cell upper dendrites receive excitation from the mitral cell secondary dendrites and send inhibition back to them by local dendrodendritic interaction on their dendritic connections. Most of these dendrodendritic connections are reciprocal and extend locally to other cells within a few hundred microns, the space below several glomeruli (Shepherd 1979) in the input layer. The mitral cell axons also send collaterals to the local granule cell lower dendrites. The granule cells do not have a morphological axon. While

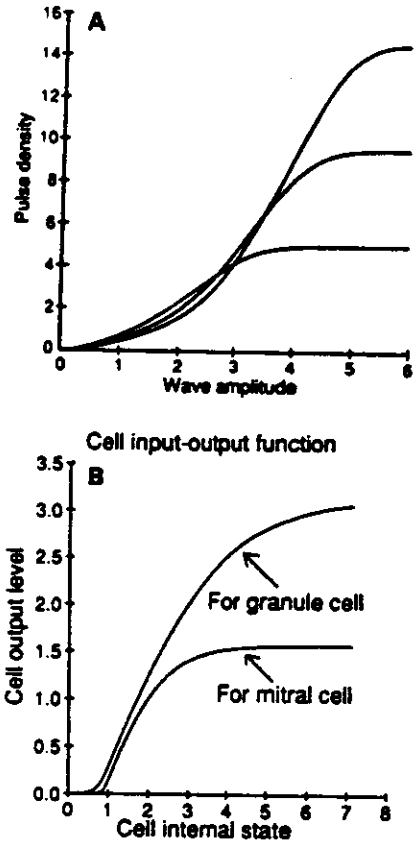


Fig. 3A and B. Cell non-linear input-output functions. A Three examples of experimentally measured functions in a mass of mitral and granule cells, relating the pulse probability of single or small groups of mitral cells to the EEG wave amplitude originated from the granule cells. Taken from Freeman and Skarda (1985). B The model functions for mitral and granule cells respectively

they can produce action potentials (Mori and Kishi 1982), their outputs are dominantly via granule-to-mitral dendrodendritic synapses activated by graded presynaptic depolarization (Shepherd 1979; Jahr and Nicoll 1980). There are also smaller excitatory cells called tufted cells, and inhibitory interneural short axon cells which are very few compared with the interneural granule cells.

Most inputs from higher olfactory centers and other parts of the brain are directed to the dendrites of the granule cells. The outputs of the bulb are carried by the mitral cell axons. There are ~1000 receptor axons and dendrites from 25 mitral cells in each glomerulus, while there are ~200 granule cells for each mitral cell. A rabbit has about 50,000 mitral cells (Shepherd 1979). Both the mitral and granule cells have a non-linear input-output relationship, which can be qualitatively seen in physiological measurement done on a mitral-granule cell mass (Freeman 1975, 1979a; Fig. 3). Both the mitral and granule cells have a membrane time

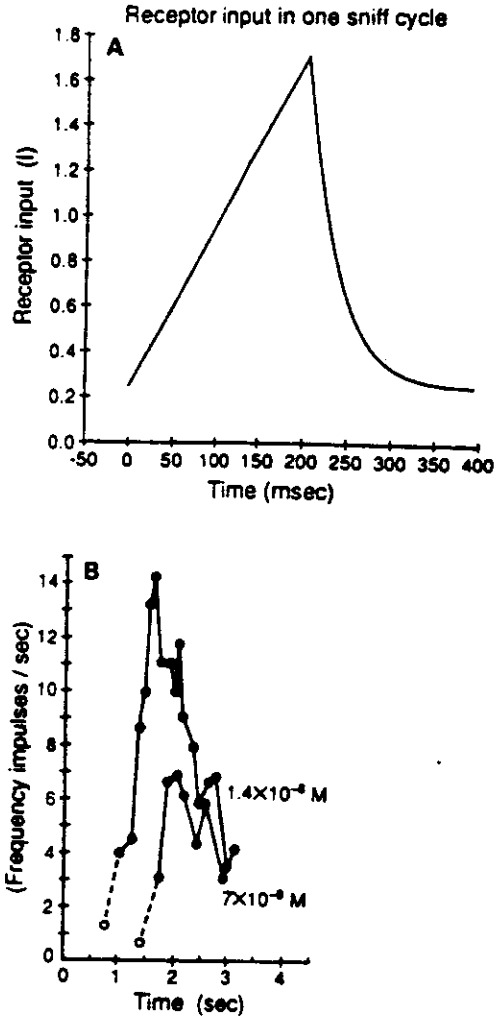


Fig. 4. A Model of receptor cell response time course to odors in a sniff cycle. B Experimentally measured receptor firing frequency with an odor pulse delivered to the nose, two concentration examples of odor plotted, the line below the time axis indicates the odor pulse duration. Taken from Getchell and Shepherd (1978)

constant of 5–10 ms (Freeman and Skarda 1985; Shepherd, Private Communication). Very little is known about the functional strength of synapses in the olfactory bulb.

The receptor cell firing rate increases from the spontaneous background level of 1–3 impulses/s with increasing odor concentration (Getchell and Shepherd 1978), and may reach 10–60 impulses/s. With odor pulses delivered to the mucosa, the receptor firing rate increases approximately linearly in time as long as the pulse is not too long, and then terminates quickly, sometimes as fast as 100 ms, after the odor pulse terminates (Fig. 4). High resolution 2-deoxyglucose autoradiography experiment (Lancet et al. 1982) shows that for an input odor, different and even neighboring glomeruli have different activity levels, while the activity is relatively uniform within a single glomerulus. Little is known about the input from the higher centers to the bulb.

Stimulation with odors, depending on the animal motivation, causes an onset of a high-amplitude bulbar oscillatory activity, which is detected by surface EEG electrodes and returns to a low-amplitude oscillation on the cessation of odor stimulus (Freeman 1978). The oscillation is an intrinsic property of the bulb itself persisting after the central connections to the bulb is cut off (Freeman and Skarda 1985). Central inputs (Freeman 1979a; Freeman and Skarda 1985; Baird 1986) influence oscillation onset; the oscillation exists only in motivated animals, and can be present without an input odor (Freeman 1978). However, the oscillation disappears when the nasal air flow is blocked (Freeman and Schneider 1982). The granule cells are the generators of the surface EEG wave, for the mitral cells produce a closed monopole field which is negligible at bulbar surface (Freeman 1975). The EEG (Freeman 1978; Freeman and Schneider 1982) shows a high amplitude oscillation arising during the inhalation and stopping early in the exhalation. The oscillation bursts have a peak frequency in the range of 35–90 Hz, and ride on a slow background wave phase locked with the respiratory wave. Different parts of the bulb have the same dominant frequency but different amplitudes and phases. A specific odor input will set a specific EEG oscillation pattern across the olfactory bulb.

## 3 Model Organization

For comparisons between experiments and theory of the olfactory bulb, it is essential to model with realism. To do the mathematical analysis and simulation necessary to understand collective and statistical properties, it is necessary to disregard superfluous details. Our model organization is a compromise between these two considerations.

### *3.1 General Model Structure*

Only the mitral and granule cells are included in the bulb model. The glomerular layer structure is neglected, and the receptor input is regarded as effectively directed onto the mitral cells. The tufted cells are considered as mitral cells, and the interneural short axon cells are neglected because they are very few in number compared with the granule cells. Both the receptor and central inputs are included. There are $N$ (excitatory) mitral cells and $M$ (inhibitory) granule cells in the model. Although the mathematical analysis puts no limit on the absolute cell numbers, the following cell

number reductions are used in the computer simulation because of the limited computer capability. The group of mitral cells connecting to the same glomerulus is simplified into one cell by assuming that the activity level changes little locally. Similarly, the ratio $M:N$ is taken to be much less than the 200:1 in the real bulb. Excitation and inhibition are kept in balance by correspondingly increasing the strength of the granule cell (inhibitory) synapses.

### 3.2 *Inputs to the Bulb Model*

The inputs from outside bulb to a mitral cell $i$ is described by the components $I_i$ for $1 \leqq i \leqq N$. This input vector $I$ is a superposition of a true odor signal and a background input, i.e., $I = I_{odor} + I_{background}$. $I_{background}$ is the sum of the receptor background input and the central inputs to the mitral cell dendrites in the input layer. $I_{odor}$ ranges from zero to 10 or 20 times of $I_{background}$, determined by odor pattern $P_{odor}$, with components $P_{odor,i}$ for $1 \leqq i \leqq N$, characterizing the odor concentration and the receptor cells' sensitivity pattern to the odor. Each sniff cycle lasts for 200–500 ms as that of a rabbit. All these inputs are taken to be excitatory. The odor concentration on the mucosa will rise rapidly at the initiation of inhale, and correspondingly drop at initial exhale because of absorption by the lungs. Odorant diffusion through the mucous to the receptors should delay the increase in receptor activities. Thus we model the $I_{odor}$ to increase in time during inhale, as observed in experiment (Getchell and Shepherd 1978). Exhalation is modeled as an exponential return toward the ambient. Then for any mitral cell $i$ exposed to odor,

$$I_{odor,i}(t) = \begin{cases} P_{odor,i} \cdot (t - t^{inhale}) + I_{odor,i}(t^{inhale}), \\ \quad \text{if} \quad t^{inhale} \leqq t \leqq t^{exhale}; \\ I_{odor,i}(t^{exhale}) \cdot e^{-(t - t^{exhale})/\tau_{exhale}}, \\ \quad \text{if} \quad t > t^{exhale}, \end{cases} \tag{3.1}$$

as illustrated in Fig. 4, where $\tau_{exhale} = 33$ ms and $t^{inhale}$ and $t^{enhale}$ are the on-set times for inhale and exhale respectively.

The central input to the granule cells are described by the vector $I_c$ with components $I_{c,j}$ for $1 \leqq j \leqq M$. For now, it is assumed that $I_c$ and $I_{background}$ do not change during a sniff cycle. The scales of $I_{background} = 0.243$ and $I_c = 0.1$ are set such that when $I_{odor} = 0$, most of the mitral and granule cells have their cell internal state just below maximum slope points on their input-output function curves (Freeman 1979a). So there will be weak incoherent oscillatory activity when there is no odor input, as often observed (Freeman and Schneider 1982).

### 3.3 *The Model Cell Property*

Each cell is modeled as one unit since typical (dendro-dendritic) interactions take place locally on the dendrites with electrotonic length less than one (Shepherd 1979). The internal state level of a neuron is described by a single variable resembling the cell membrane potential. Those of the mitral cells and granule cells are respectively $X = \{x_1, x_2, \ldots, x_N\}$ and $Y = \{y_1, y_2, \ldots, y_M\}$. The cell output is described as a continuous function of the cell's internal state, and can be thought of as proportional to the cell firing frequency. They are $G_x(X) = \{g_x(x_1), g_x(x_2), \ldots, g_x(x_N)\}$ and $G_y(Y) = \{g_y(y_1), g_y(y_2), \ldots, g_y(y_M)\}$ for the mitral and granule cells respectively, where $g_x$ and $g_y$ are the neurons' output functions which have the following properties modeled after a real cell:

*1)* $g_x(g_y) \geqq 0$, $g'_x(g'_y) \geqq 0$, i.e., the output firing rate is non-negative and non-decreasing with increasing cell membrane potential.

*2)* $g_x$ and $g_y$ are non-linear, the strongest non-linear region occurs around the firing threshold region of the cell, and the outputs also saturate at high internal state level.

Figure 3 shows the form of input-output relation used for mitral and granule cells. The complicated mathematical form was chosen for convenience, and is inessential to the behavior as long as the shapes are qualitatively preserved.

The function formulae are:

$$g_x(x) = \begin{cases} S'_x + S'_x \cdot \tanh\left(\dfrac{x - th}{S'_x}\right), & \text{if} \quad x < th; \quad S'_x = 0.14, \\ S'_x + S_x \cdot \tanh\left(\dfrac{x - th}{S_x}\right), & \text{if} \quad x \geqq th. \quad S_x = 1.4. \end{cases}$$

$$g_y(y) = \begin{cases} S'_y + S'_y \cdot \tanh\left(\dfrac{y - th}{S'_y}\right), & \text{if} \quad y < th; \quad S'_y = 0.29, \\ S'_y + S_y \cdot \tanh\left(\dfrac{y - th}{S_y}\right), & \text{if} \quad y \geqq th; \quad S_y = 2.9, \end{cases}$$

where $th = 1$. The granule cells were modeled with a larger linear range, reflecting the fact that granule cells do not have axons, and thus have a less strong non-linear threshold effect. The non-linear and threshold functions are essential for the bulbar oscillation dynamics (Freeman 1979a; Freeman and Skarda 1985; Baird 1986) to be studied.

### 3.4 *The Synaptic Connections and System Dynamics*

The geometry of bulbar structure, namely with cells sitting on two dimensional sheets shaped like a seg-

ment of a sphere, is simplified as cells sitting on a one dimensional ring. Each cell is specified by an index, e.g. $i^{th}$ mitral cell, and $j^{th}$ granule cell for all $i, j$ which resemble the spatial location of the cells. The $i^{th}$ mitral cell is the neighbor of $i \pm 1^{th}$ mitral cells and $\frac{i \cdot M^{th}}{N}$ granule cell. The $1^{st}$ and the $N^{th}$ ($M^{th}$) mitral (granule) cells are next to each other. This 1 – d simplification is helpful for understanding but is not essential for the model (see discussion).

The synaptic strength in the model is postsynaptic input: presynaptic output. An $N \times M$ matrix $H_0$ and $M \times N$ matrix $W_0$ are used respectively to describe the synaptic connection from granule cells to mitral cells and vice versa. For instance, $H_{0,ij}$ is the connection strength from the $j^{th}$ granule cell to $i^{th}$ mitral cell. Since the synaptic connection in the bulb is local, $H_{0,ij} \neq 0$ only if $j^{th}$ granule cell and $i^{th}$ mitral cell are near each other, i.e., $j \approx \frac{i \cdot M}{N}$ or $j \approx \frac{i \cdot M}{N} + M$ because of the ring structure. This implies that $H_0$ will be a near diagonal matrix with most non-zero elements near the diagonal line. Here diagonal elements mean those $H_{0,ij}$ with $j = \frac{i \cdot M}{N}$, because $H_0$ need not be a square matrix. $W_0$ has a similar matrix structure. The matrices used in the computer simulations are (for $N = M = 10$):

$$H_0 = \begin{pmatrix} 0.3 & 0.9 & 0 & 0 & 0 & 0 & 0 & 0 & 0 & 0.7 \\ 0.9 & 0.4 & 1.0 & 0 & 0 & 0 & 0 & 0 & 0 & 0 \\ 0 & 0.8 & 0.3 & 0.8 & 0 & 0 & 0 & 0 & 0 & 0 \\ 0 & 0 & 0.7 & 0.5 & 0.9 & 0 & 0 & 0 & 0 & 0 \\ 0 & 0 & 0 & 0.8 & 0.3 & 0.8 & 0 & 0 & 0 & 0 \\ 0 & 0 & 0 & 0 & 0.7 & 0.3 & 0.9 & 0 & 0 & 0 \\ 0 & 0 & 0 & 0 & 0 & 0.7 & 0.4 & 0.9 & 0 & 0 \\ 0 & 0 & 0 & 0 & 0 & 0 & 0.5 & 0.5 & 0.7 & 0 \\ 0 & 0 & 0 & 0 & 0 & 0 & 0 & 0.9 & 0.3 & 0.9 \\ 0.9 & 0 & 0 & 0 & 0 & 0 & 0 & 0 & 0.8 & 0.3 \end{pmatrix},$$

$$W_0 = \begin{pmatrix} 0.3 & 0.7 & 0 & 0 & 0 & 0 & 0 & 0 & 0.5 & 0.3 \\ 0.3 & 0.2 & 0.5 & 0 & 0 & 0 & 0 & 0 & 0 & 0.7 \\ 0 & 0.1 & 0.3 & 0.5 & 0 & 0 & 0 & 0 & 0 & 0 \\ 0 & 0.5 & 0.2 & 0.2 & 0.5 & 0 & 0 & 0 & 0 & 0 \\ 0.5 & 0 & 0 & 0.5 & 0.1 & 0.9 & 0 & 0 & 0 & 0 \\ 0 & 0 & 0 & 0 & 0.3 & 0.3 & 0.5 & 0.4 & 0 & 0 \\ 0 & 0 & 0 & 0.6 & 0 & 0.2 & 0.3 & 0.5 & 0 & 0 \\ 0 & 0 & 0 & 0 & 0 & 0 & 0.5 & 0.3 & 0.5 & 0 \\ 0 & 0 & 0 & 0 & 0 & 0.2 & 0 & 0.2 & 0.3 & 0.7 \\ 0.7 & 0 & 0 & 0 & 0 & 0 & 0 & 0.2 & 0.3 & 0.5 \end{pmatrix}. \quad (3.2)$$

Most of the non-zero elements are near the diagonal line and corners, reflecting the assumed ring geometry. Non-zero elements in $W_0$ occur further from the diagonal line than those in $H_0$, reflecting the longer range mitral-to-granule than granule-to-mitral connections.

The bulb model system has equation of motion:

$$\begin{aligned} \dot{X} &= -H_0 G_y(Y) - \alpha_x X + I, \\ \dot{Y} &= W_0 G_x(X) - \alpha_y Y + I_c, \end{aligned} \quad (3.3)$$

where $\alpha_x = 1/\tau_x$, $\alpha_y = 1/\tau_y$, and $\tau_x = \tau_y = 7$ ms are the time constants of the mitral and granule cells respectively. The minus sign in front of the matrix $H_0$ represents the inhibitory nature of the granule cells. In simulation, weak random noise with a 9 ms correlation time is added to $I$ and $I_c$ to simulate the fluctuations in the system.

The scales of $H_0$ and $W_0$ are chosen to be about the same, with values such that the oscillation frequency in the stimulated model bulb neural activity is about the same as in the real biological bulb (see Sect. 5.1). The individual elements of $H_0$ and $W_0$ in simulation are chosen such that there will be high amplitude oscillations in the model bulb for certain kinds of odor input $I_{odor}$ (see Sect. 6.1).

## 4 Simulation Result

Computer simulation was done with 10 mitral and granule cells. The simulations start with initial cell internal states close to the background state when no odor inputs are present. Different odor input patterns are represented by the different vectors $P_{odor}$.

Figure 5 shows the simulation result of several sniff cycles of a certain odor input $I_{odor}$. The rise and fall of oscillations with input and the baseline shift wave phase locked with sniff cycles are obvious. The surface EEG wave is calculated using the approximation by Freeman (1980) as a weighted sum of each granule cell output $g_\gamma(y_j)$. Physiologically measured EEG waves are shown for comparison.

The activities of individual cells in a sniff cycle across the whole bulb constitute an activity pattern for the particular odor input $I_{odor}$ (Fig. 6). All the cells oscillate coherently with the same frequency as physiologically observed (Freeman 1978; Freeman and Schneider 1982). The mitral cell output pattern is the only output of the bulb. Physiological multi-channel measurement of surface EEG waves (Freeman 1978), though originating in the granule cell activities, also displays a similar information pattern in multi-dimensions. For comparison, both the simulated and measured (band-pass filtered) EEG patterns are included in the figure.

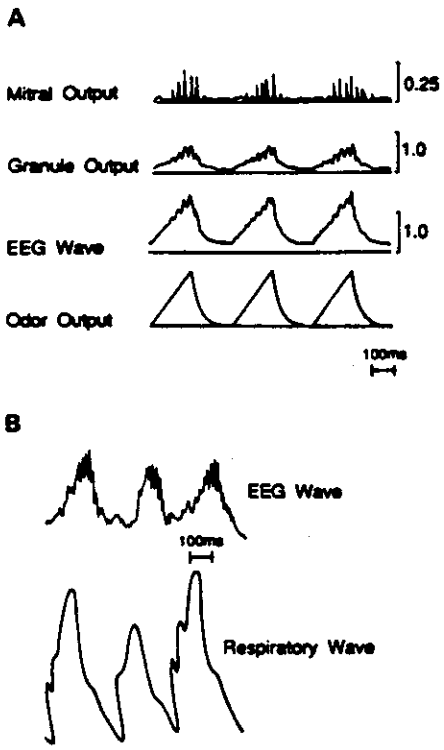


Fig. 5. A Simulation result of bulbar response in several sniff cycles. B Experimentally measured EEG waves with odor inputs, taken from Freeman and Schneider (1982). Both the simulated and measured EEG waves are surface negative waves

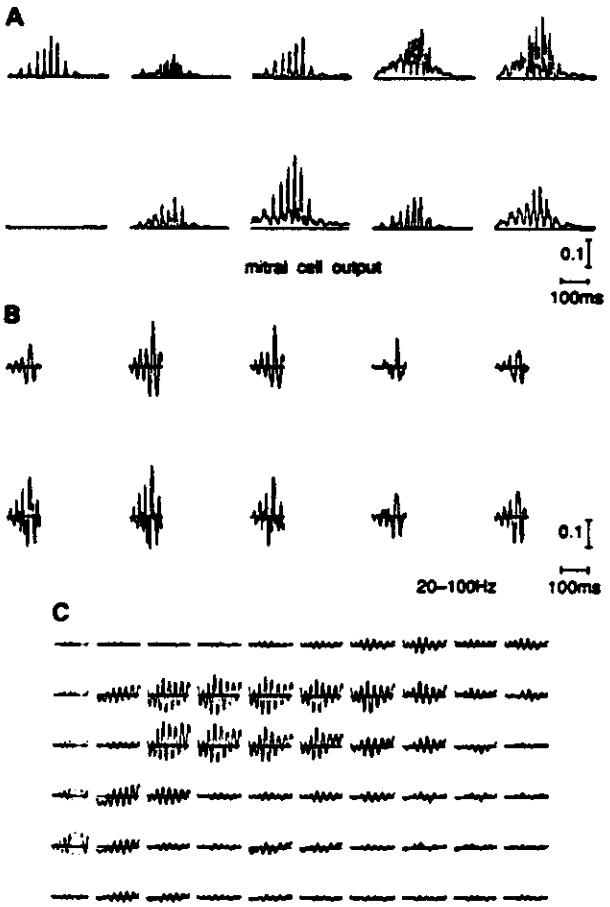


Fig. 6. A Simulated mitral cell output pattern in one sniff cycle with one odor input example. B Segment of a simulated surface EEG wave pattern during the oscillatory bursts with the same odor input as in A. C Multi-channel recorded bulbar surface EEG wave pattern during 100 ms of bursts, taken from Freeman (1978). Both signals in B and C are band-pass filtered

These simulation results show that the model bulb can capture the major known effects of the real bulb. Furthermore, the model shows the capability of a pattern classifier. For a sniff cycle lasting $t_s = 370$ ms in simulation with fixed inhale and exhale time, some input patterns $P_{odor}$ induce oscillation, while others do not, and different $P_{odor}$ induce different oscillation patterns (Fig. 7). Zero odor input $P_{odor} = 0$ induces little activity above background, which is the case observed when the nasal airflow is blocked (Freeman and Schneider 1982). What patterns drive the bulb well is as yet arbitrary in our model, for there is no relation between the particular connections and the odors which are used.

Some measures have been defined to describe the difference between different patterns. The mitral output $G_x(X(t))$ were band-pass filtered above 20 Hz to obtain the oscillatory signal $S_h(t)$, and low-pass below 20 Hz for baseline shift $S_l(t)$. The oscillation period $T$ is the time lag $\geqq 5$ ms which gives the largest autocorrelation for $S_h(t)$. Similarly, oscillation phase differences of the different mitral cells are calculated by cross-correlating the different components of $S_h(t)$ after the higher frequency components ($f > 1.3/T$) are removed. The phase differences are measured with respect to the first cell. The oscillation amplitude of $i^{th}$ cell is the root-mean-square of $S_{h,i}(t)$ averaged in time. The results show that for each response, cells with substantial oscillation amplitudes have frequencies within 1 Hz of each other. Define

$O_{osci}$: an $N$-dimensional complex vector describing the dominant frequency oscillation amplitudes and phases averaged over the sniff cycle;

$O_{mean}$: an $N$-dimensional real vector describing the baseline activities above the background level $(S_l(t) - S_l(t)|_{P_{odor}=0})$ averaged over the sniff cycle;

$\bar{O}_{mean}$ and $\bar{O}_{osci}$: scalars describing the root-mean-square average of the components of $O_{mean}$ and $O_{osci}$ respectively.

We can use these quantities to define the similarity or difference between response patterns. For two

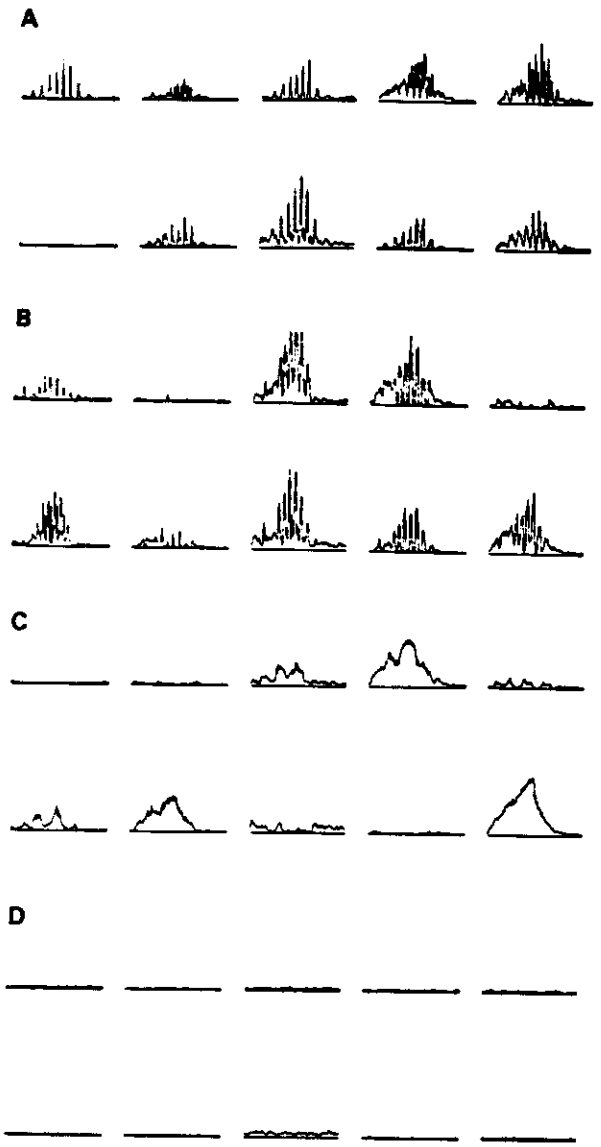


Fig. 7A–D. Mitral output response patterns for different inputs $I_{odor}$ of one sniff cycle lasting 370 ms. A, B Oscillatory responses for two different inputs. C Non-oscillatory response for an input. D Response for no odor inputs

response patterns $a$ and $b$ denoted by superindices, possible distance measures are:

$$d_1 = 1 - \frac{\langle O^a_{mean} O^b_{mean} \rangle}{|O^a_{mean}|\,|O^b_{mean}|},$$

$$d_2 = 1 - \frac{|\langle O^a_{osci} O^b_{osci} \rangle|}{|O^a_{osci}|\,|O^b_{osci}|},$$

$$d_3 = \frac{\bar{O}^a_{mean} - \bar{O}^b_{mean}}{\bar{O}^a_{mean} + \bar{O}^b_{mean}},$$

$$d_4 = \frac{\bar{O}^a_{osci} - \bar{O}^b_{osci}}{\bar{O}^a_{osci} + \bar{O}^b_{osci}}, \qquad (4.1)$$

**Table 1.** Differences between two patterns. Data in each group is the average of three pairs of patterns. Group one: The two patterns in each pair have different odor inputs. Group two: The two patterns in each pair have the same odor input but different system fluctuations

| | $d_1$ | $d_2$ | $\lvert d_3 \rvert$ | $\lvert d_4 \rvert$ | $d_1^{in}$ | $\lvert d_3^{in} \rvert$ |
|---|---|---|---|---|---|---|
| Group one | 0.3217 | 0.4243 | 0.1403 | 0.2840 | 0.0257 | 0.1657 |
| Group two | 0.0007 | 0.0560 | 0.0050 | 0.0413 | 0 | 0 |

where $\langle\ \rangle$ and $|\ |$ denote the dot product and absolute value respectively. $d_1$ and $d_2$ give differences in the response pattern forms, while $d_3$ and $d_4$ give differences in the response amplitudes.

For comparison, $d_1^{in}$, which is indicative of the difference in form (not amplitude) of the input patterns $P_{odor}$, is calculated by replacing $O_{mean}$ with $P_{odor}$ in (4.1) for $d_1$ (similar calculation is done for $d_3^{in}$ corresponding to $d_3$). Table 1 shows that the bulb amplifies the differences in input vector $P_{odor}$ to give output vectors $O_{osci}$ and $O_{mean}$ (compare $d_1^{in}$ with $d_1$ and $d_2$), while the responses to same odor with different noise samples differ negligibly. The noise amplitudes are not crucial for the structure of the oscillation patterns.

## 5 Mathematical Analysis

### *5.1 Olfactory Bulb as a Group of Coupled Non-Linear Oscillators*

An oscillator with frequency $\omega$ can be described by the differential equations

$$\begin{aligned} \dot{x} &= -\omega y \\ \dot{y} &= \omega x \end{aligned} \quad \text{or} \quad \ddot{x} + \omega^2 x = 0 \qquad (5.1)$$

with solution:

$$x = r_0 \sin(\omega t + \phi) \qquad y = -r_0 \cos(\omega t + \phi),$$

where $r_0$ and $\phi$ are arbitrary real constants. The $x(t)$, $y(t)$ trajectory is a circle. With dissipation, (5.1) becomes

$$\begin{aligned} \dot{x} &= -\omega y - \alpha x \\ \dot{y} &= \omega x - \alpha y \end{aligned} \quad \text{or} \quad \ddot{x} + 2\alpha\dot{x} + (\omega^2 + \alpha^2)x = 0. \qquad (5.2)$$

The solution becomes

$$x = r_0 e^{-\alpha t} \sin(\omega t + \phi),$$

where $\alpha$ is the dissipation constant. If a mitral cell and a granule cell are connected to each other, with inputs $i(t)$ and $i_c(t)$ respectively, then

$$\begin{aligned} \dot{x} &= -h \cdot g_y(y) - \alpha_x x + i(t), \\ \dot{y} &= w \cdot g_x(x) - \alpha_y y + i_c(t). \end{aligned} \qquad (5.3)$$

This is the scalar version of (3.3) with each upper case letter representing a vector or matrix replaced by a lower case letter representing a scalar. It is assumed that $i(t)$ has a much slower time course than $x$ or $y$, because the frequency of sniffs is considerably lower than the characteristic neural oscillation frequency, and that $i_c$, input from higher centers, will be kept fixed. We can then use the adiabatic approximation, and define the equilibrium point $(x_0, y_0)$ as

$$\begin{aligned} \dot{x}_0 &\approx 0 = -h \cdot g_y(y_0) - \alpha_x x_0 + i, \\ \dot{y} &\approx 0 = w \cdot g_x(x_0) - \alpha_y y_0 + i_c. \end{aligned} \tag{5.4}$$

Define $x' \equiv x - x_0$, $y' \equiv y - y_0$. Then

$$\begin{aligned} \dot{x}' &= -h(g_y(y) - g_y(y_0)) - \alpha_x x', \\ \dot{y}' &= w(g_x(x) - g_x(x_0)) - \alpha_y y'. \end{aligned}$$

This is already similar to (5.2). If we omitted the dissipation, $\alpha_x = \alpha_y = 0$, then, when $x'$ and $y'$ are small, they oscillate along the solution orbit

$$R \equiv \int_{x_0}^{x_0 + x'} w(g_x(s) - g_x(x_0))\,ds + \int_{y_0}^{y_0 + y'} h(g_y(s) - g_y(y_0))\,ds = \text{constant}$$

which is a closed curve in the original $(x, y)$ space surrounding the point $(x_0, y_0)$. This means $(x, y)$ will oscillate around the point $(x_0, y_0)$. The oscillation becomes strictly sinusoidal if $g$'s are linear functions. When the dissipation is included, the orbit in $(x, y)$ space will spiral into the point $(x_0, y_0)$:

$$dR/dt = -\alpha_x w(g_x(x) - g_x(x_0))(x - x_0) - \alpha_y h(g_y(y) - g_y(y_0))(y - y_0).$$

Therefore, a connected pair of mitral and granule cells behaves as a damped non-linear oscillator, whose oscillation center $(x_0, y_0)$ is determined by the external inputs $i$ and $i_c$. If the oscillation amplitude is small, then the system can be approximated by a damped sinusoidal oscillator via linearization around the point $(x_0, y_0)$:

$$\begin{aligned} \dot{x} &= -h \cdot g_y'(y_0) y - \alpha_x x, \\ \dot{y} &= w \cdot g_x'(x_0) x - \alpha_y y, \end{aligned} \tag{5.5}$$

where $(x, y)$ are now the deviation from $(x_0, y_0)$. The solution is

$$x = r_0 e^{-\alpha t} \sin(\omega t + \phi),$$

where $\alpha = (\alpha_x + \alpha_y)/2$ and $\omega = \sqrt{hwg_x'(x_0)g_y'(y_0) + (\alpha_x - \alpha_y)^2/4}$. If $\alpha_x = \alpha_y$, which is about right in the bulb, then $\alpha = \alpha_x = \alpha_y$, $\omega = \sqrt{hwg_x'(x_0)g_y'(y_0)}$. Using the bulbar cell time constant and the oscillation frequency from the previous section, $\alpha \approx 0.3\omega$. The scale of synaptic connections strength was chosen so that the model bulb oscillation frequency agrees with the biological data (Sect. 3.4). The effect of the input controlled equilibrium point $(x_0, y_0)$ on the frequency implies that the oscillation frequency is modulated by the receptor and central input in the real system. The equilibrium point $(x_0, y_0)$ is always stable, i.e., the non-linear oscillation is always damped, and no sustained oscillation will exist unless driven by an external oscillating input.

$N$ such mitral-granule pairs without interconnections between the pairs, represent a group of $N$ independent damped non-linear oscillators. If the cells in one oscillator also connect to cells in the neighboring oscillators, then these oscillators are no longer independent. This is exactly the situation in the olfactory bulb. A granule cell receiving inputs from a certain mitral cell gives outputs to other mitral cells as well. Similarly, a mitral cell has outputs also to granule cells which do not give outputs to this mitral cell. The locality of synaptic connections in the bulb implies that the oscillator coupling is also local. (That there are many more granule cells than mitral cells only means that there is more than one granule cell in each oscillator.) This situation can be quantitatively treated by including many neurons in the mathematical analysis.

Proceeding as in the single oscillator case,

$$\begin{aligned} \dot{X} &= -H_0 G_y(Y) - \alpha_x X + I(t), \\ \dot{Y} &= W_0 G_x(X) - \alpha_y Y + I_c(t), \end{aligned} \tag{5.6}$$

[cf. (5.3)]. Use the adiabatic approximation and define the equilibrium point $(X_0, Y_0)$ as

$$\begin{aligned} \dot{X}_0 &\approx 0 = -H_0 G_y(Y_0) - \alpha_x X_0 + I, \\ \dot{Y}_0 &\approx 0 = W_0 G_x(X_0) - \alpha_y Y_0 + I_c, \end{aligned} \tag{5.7}$$

linearize around $(X_0, Y_0)$,

$$\begin{aligned} \dot{X} &= -H_0 G_y'(Y_0) Y - \alpha_x X, \\ \dot{Y} &= W_0 G_x'(X_0) X - \alpha_y Y, \end{aligned} \tag{5.8}$$

where $(X, Y)$ are now deviations from $(X_0, Y_0)$ and $G_x'(X_0)$ and $G_y'(Y_0)$ are diagonal matrices with elements: $[G_x'(X_0)]_{ii} = g_x'(x_{i,0})$, $[G_y'(Y_0)]_{jj} = g_y'(y_{j,0})$, for all $i, j$. Define $H \equiv H_0 G_y'(Y_0)$, $W \equiv W_0 G_x'(X_0)$, so

$$\begin{aligned} \dot{X} &= -HY - \alpha_x X, \\ \dot{Y} &= WX - \alpha_y Y. \end{aligned} \tag{5.9}$$

Eliminating $Y$,

$$\ddot{X} + (\alpha_x + \alpha_y)\dot{X} + (A + \alpha_x \alpha_y) X = 0, \tag{5.10}$$

where $A \equiv HW = H_0 G_y'(Y_0) W_0 G_x'(X_0)$. This is the equation for the system of $N$ coupled oscillators [cf. (5.2)]. The second term $(\alpha_x + \alpha_y)\dot{X}$ describes the dissipation, while the third term $(A + \alpha_x \alpha_y)X$ includes also

the indirect couplings between different mitral cells via the granule cells. The $i^{th}$ oscillator (mitral cell) follows the equation

$$\ddot{x}_i+(\alpha_x+\alpha_y)\dot{x}_i+(A_{ii}+\alpha_x\alpha_y)x_i+\sum_{j\neq i}A_{ij}x_j=0. \quad (5.11)$$

The first three terms are like a single ($i^{th}$) oscillator [cf. (5.2)], while the last term describes the coupling to other oscillators. These oscillator couplings are local because the matrix $A$ is near diagonal, which follows from the definition of $A$ and the fact that both $H_0$ and $W_0$ are near diagonal. The elements of matrix $A$ are non-negative by the definition. The coupling from $j^{th}$ oscillator to $i^{th}$ oscillator goes through the connection path from $j^{th}$ mitral cell to $i^{th}$ mitral cell via all those intermediate granule cells. In particular, $A_{ii}$ originates from the connection path from $i^{th}$ mitral cell back to itself via the intermediate granule cells. In our simulated example, the $H_0$ and $W_0$ used implies that each cell connects to about three neighboring cells, so from above argument each oscillator couples to about 5 neighboring oscillators.

The set of mitral and granule cells in the blub can thus be viewed as a group of locally coupled non-linear damped oscillators. The system can be approximated by linear oscillators if the oscillation amplitude is small enough. Non-linear effect will occur when the amplitude is large, and the oscillation wave form will then become non-sinusoidal.

This model of the olfactory bulb can be generalized to other masses of interacting excitatory and inhibitory cells such as those in olfactory cortex, neocortex and hippocampus (Shepherd 1979) etc. where there may as well be connections between the excitatory cells and between the inhibitory cells, as is claimed by some for the olfactory bulb (Nicoll 1971; Freeman 1975, 1979b, c). Suppose that $B_0$ and $C_0$ are excitatory-to-excitatory and inhibitory-to-inhibitory connection matrices respectively, then (5.6) becomes:

$$\begin{aligned}\dot{X}&=-H_0G_y(Y)-\alpha_xX+B_0G_x(X)+I(t),\\ \dot{Y}&=W_0G_x(X)-\alpha_yY-C_0G_y(Y)+I_c(t).\end{aligned} \quad (5.12)$$

Consequently (5.10) becomes

$$\ddot{X}+(\alpha_x-B+\alpha_y+C)\dot{X}+(A+(\alpha_x-B)(\alpha_y+C))X=0, \quad (5.13)$$

where $B\equiv B_0G_x'(X_0)$ and $C\equiv HC_0G_y'(Y_0)H^{-1}$ ($H^{-1}$ is the pseudo-inverse of $H$). If we replace $\alpha_x$ by $\alpha_x-B$, and $\alpha_y$ by $\alpha_y+C$, then (5.10) becomes (5.13). This means that if coupling $B$ and $C$ is local (i.e., almost diagonal), having excitatory connections $B_0$ is like reducing dissipation for oscillators, while having the inhibitory connections is like adding some oscillator dissipation. Strong enough local excitatory-to-excitatory connections $B_0$ can reduce the oscillator dissipations so much that the net can oscillate even without much odor input $I_{odor}$ as is simulated by Freeman (1979b, c). This is however not necessarily true if the connections $B_0$ are non-local (as in the olfactory cortex, Haberly 1985), since a negative dissipation introduced by a local excitatory-to-excitatory connection can become positive non-locally when the two oscillators coupled by $B$ are oscillating with opposite phases.

### 5.2 *Oscillation Pattern Analysis*

If $X_k$ is one of the eigenvectors of $A$ with eigenvalue $\lambda_k$, (5.10) has $N$ independent modes

$$\begin{aligned}X&\propto X_k e^{i\omega_k t}\\ &\equiv X_k \exp\left(-\frac{(\alpha_x+\alpha_y)}{2}t\pm i\sqrt{\lambda_k+\frac{(\alpha_x-\alpha_y)^2}{4}}\,t\right)\end{aligned} \quad (5.15)$$

for $k=1,2,\ldots,N$, where $\omega_k$ is the complex frequency of the oscillation mode. We will denote $X_k$ as the $k^{th}$ oscillation mode of the system. For simplicity, we set $\alpha_x=\alpha_y=\alpha$, then

$$X\propto X_k e^{-\alpha t\pm i\sqrt{\lambda_k}t} \quad (5.16)$$

for all $k$. Each mode has frequency $\mathrm{Re}\sqrt{\lambda_k}$, where Re means the real part of a complex number. The relative phases and amplitudes of the individual oscillators in $k^{th}$ mode are described by the individual components of complex vector $X_k$. If $\mathrm{Re}(-\alpha\pm i\sqrt{\lambda_k})>0$ is satisfied for some $k$, then the amplitude of the $k^{th}$ mode will increase with time, i.e., it is a growing oscillation.

Starting from an initial condition of arbitrary small amplitudes in linear analysis, the mode with the fastest growing amplitude will dominate the output. When there is a single dominating mode, the whole bulb will oscillate in the same frequency as observed physiologically (Freeman 1978; Freeman and Schneider 1982) as well as in the simulation. When the non-linear effect is considered, the strongest modes will suppress the others, and the final activity output will be a single "mode" in a non-linear regime.

The collective oscillation mode is a result of coupling. Each oscillator gets external driving "forces" from the neighboring oscillators. When they influence each other in harmony, a global oscillation mode results. The amplitude of an oscillator will increase when its driving "force" is larger than its damping "force". An oscillation mode with growing amplitude emerges when each oscillator with substantial amplitude in the mode has enough driving "force" through coupling with other oscillators. Recall that a single oscillator in our analysis is always damped, which means that the equilibrium point $(x_0, y_0)$ is always stable. Because of coupling between the oscillators, the

equilibrium point $(X_0, Y_0)$ of a *group* of oscillators *is no longer always stable* with the possibility of growing oscillation modes.

In order that some mode $X_k$ can be both a growing and oscillatory mode, $\lambda_k$ must be complex. For this, a necessary (but not sufficient) condition is that matrix $A$ is non-Hermitian. It follows that systems of less than three oscillators will not have growing modes, since if $A$ is real and is of dimension 1 or 2, it will only have real eigenvalues.

For illustration, for the symmetric matrix

$$A=\begin{pmatrix} a & b & 0 & 0 & & \dots & & 0 & b \\ b & a & b & 0 & & \dots & & 0 & 0 \\ 0 & b & a & b & 0 & 0 & \dots & 0 & 0 \\ \vdots & \vdots & & & & \dots & \ddots & & \vdots \\ b & 0 & & & \dots & & 0 & b & a \end{pmatrix}. \qquad (5.17)$$

The $N$ oscillation modes will be

$$\begin{pmatrix} \sin(k1) \\ \sin(k2) \\ \vdots \\ \sin(ki) \\ \vdots \\ \sin(kN) \end{pmatrix} e^{-\alpha t \pm i\sqrt{\lambda_k}t} \quad \begin{pmatrix} \cos(k1) \\ \cos(k2) \\ \vdots \\ \cos(ki) \\ \vdots \\ \cos(kN) \end{pmatrix} e^{-\alpha t \pm i\sqrt{\lambda_k}t}, \qquad (5.18)$$

where $k=\dfrac{2\pi K}{N}$, $K$ is an integer, $0\leqq K<\dfrac{N}{2}$, $\lambda_k=a+2b\cos(k)$. For $b<a/2$, $\lambda_k>0$, all the modes will be damped oscillations with similar frequencies close to $\omega=\sqrt{a}$. Notice that in each mode, all the oscillators have the same oscillation phase, but with different amplitudes. If we have a non-symmetric matrix

$$A=\begin{pmatrix} a & b & c & 0 & & \dots & & 0 & 0 \\ 0 & a & b & c & & \dots & & 0 & 0 \\ 0 & 0 & a & b & c & 0 & \dots & 0 & 0 \\ \vdots & \vdots & & & & \dots & \ddots & & \vdots \\ c & 0 & & & \dots & & 0 & a & b \\ b & c & & & \dots & & 0 & 0 & a \end{pmatrix}, \qquad (5.19)$$

then the oscillation modes will be

$$\begin{pmatrix} e^{i\beta} \\ e^{2i\beta} \\ \vdots \\ e^{im\beta} \\ \vdots \\ e^{iN\beta} \end{pmatrix} e^{-\alpha t \pm i\sqrt{\lambda_\beta}t} \qquad \begin{aligned} &\beta=2\pi K/N, \\ &K \text{ is an integer}, \\ &0\leqq K<N, \\ &\lambda_\beta=a+be^{i\beta}+ce^{2i\beta}. \end{aligned} \qquad (5.20)$$

Notice that in this case $\lambda_\beta$'s are non-real complex numbers. It is possible to have growing modes if for some $\beta$, $\mathrm{Re}(-\alpha\pm i\sqrt{\lambda_\beta})>0$. Also notice that the individual oscillators in most modes have different oscillation phases.

### 5.3 *Explanation of Olfactory Bulb Activities*

One prediction of this model is that the local mitral cells' oscillation phase leads that of the local granule cells by a quarter cycle, as is clear already from the single oscillator analysis. This is confirmed in experiments (Freeman 1975) in which the local mitral cell unit activity was compared with the granule cell generated surface EEG waves for phase difference. [Note that the orientation of the granule cell dipole field gives the surface EEG wave an opposite sign to that of granule cell activities (Freeman 1975). Therefore the sign of the EEG oscillation is to be reversed before comparing it with the local mitral cell oscillation for phase difference.]

A second property of the model is that for any particular stimulus, oscillatory activity should have the same dominant frequency everywhere on the bulb. This is also true in experiments (Freeman 1978; Freeman and Schneider 1982). Furthermore, the range of oscillation frequencies possible should be narrow. The observed range covers 35–90 Hz. A damped oscillator will not have high amplitude response unless the frequency of the external driving force is close to the oscillator resonant frequency. Therefore, an oscillation mode will not be non-damping unless its frequency, which is the frequency of the driving force for the oscillators in the system, is close to the oscillator resonant frequencies.

A third feature of the model is the non-zero phase gradient field across the bulb, as suggested by the examples in Sect. (5.2), which is also present in the physiologically observable oscillations. In order that the $i^{th}$ damping oscillator with frequency $\omega$ sustains its oscillation amplitude, the external driving force $F_i\equiv -A_{ij}x_j$ should be relatively in phase with the velocity $\dot{x}_i$ of the oscillator, so that the "energy" inflow from external force is no less than the dissipation. If all the coupling oscillators $x_j$ are in phase with $x_i$, such "energy" transfer can not occur since $F_i$ is perpendicular to $\dot{x}_i$. An excited oscillator in a growing mode requires coupling to neighbors oscillating with phases different from its own. Only those oscillations with non-zero phase gradient field can be stable or grow. This will not be necessarily true if the excitatory-to-excitatory connections or other synaptic connection types are present, since the nature of oscillator coupling will be different [see (5.13)].

The fourth consequence of the model is that the oscillation activity will rise during the inhale and fall at exhale, and that the oscillatory wave rides on a slow wave of background baseline shift phase locked with

the sniff cycles. The oscillation equations

$$\ddot{X}+2\alpha\dot{X}+(A+\alpha^2)X=0 \tag{5.21}$$

have solutions which depend on the matrix $A=H_0G'_y(Y_0)\,W_0G'_x(X_0)$, which in turn depends on the operation point $(X_0, Y_0)$. From (5.7), $(X_0, Y_0)$ depends on the receptor input $I$ as follows:

$$\begin{aligned} dX_0 &\approx(\alpha^2+HW)^{-1}(\alpha dI+d\dot{I}),\\ dY_0 &\approx(\alpha^2+WH)^{-1}(WdI-\alpha H^{-1}d\dot{I}). \end{aligned} \tag{5.22}$$

It turns out that the $d\dot{I}$ terms are negligible except at the initial inhale and exhale instant. Thus the oscillation center $(X_0, Y_0)$ or the baseline shift wave rises and falls with $I$, or is phase locked with the sniff cycles. Furthermore, the oscillation Eq. (5.21) will have growing oscillation mode only if $\mathrm{Re}(-\alpha\pm i\sqrt{\lambda_k})>0$ for some $k$, which means that the eigenvalue $\lambda_k$ of $A$ is large enough. This requires the gain $G'_x(X_0)G'_y(Y_0)$ be high enough to make $A=H_0G'_y(Y_0)W_0G'_x(X_0)$ large. Before inhaling, $(X_0, Y_0)$ is low on the input-output curve and the gain is too small. During the inhale, the increasing receptor input $I$ raises $(X_0, Y_0)$ towards higher gain points. When at some point $\mathrm{Re}(-\alpha\pm i\sqrt{\lambda_k})>0$ is satisfied for some mode $k$, the oscillation mode will emerge from noise. During the exhale, the receptor input decreases and the process reverses its direction, thus the oscillation decays away.

## 6 Computations in the Olfactory Bulb

### *6.1 Information Transmission and Extraction in the Olfactory Bulb*

Different odors $I$ give different mean firing rates of the bulb output response. More importantly, since the operation point $(X_0, Y_0)$ also determines the oscillation solutions of (5.21) through matrix $A=H_0G'_y(Y_0)W_0G'_x(X_0)$, different receptor inputs $I$ also give different oscillation pattern outputs indirectly through $(X_0, Y_0)$.

A surge of odor input due to inhalation raises $(X_0, Y_0)$ to a higher gain point $(G'_x(X_0), G'_y(Y_0))$. When there is no or little odor input $I_{\text{odor}}$, the point $(X_0, Y_0)$ is still stable and no high amplitude oscillation burst occurs because oscillation modes are damped. Increasing $I_{\text{odor}}$ not only raises the mean activity level, but also slowly changes the oscillation modes by structurally changing the oscillation Eq. (5.21) through matrix $A$. If $(X_0, Y_0)$ is raised to such an extent that one of the modes can grow with time, the equilibrium point $(X_0, Y_0)$ becomes unstable and this mode emerges with oscillatory bursts. In these cases, different oscillation modes that emerge are indicative of the different odor input patterns which are controlling the system parameters $(X_0, Y_0)$. When $(X_0, Y_0)$ is very low, all modes are damped, and only small amplitude oscillations occur, driven by noise and the weak time variation of the odor input.

The stability change (bifurcation) of the equilibrium point $(X_0, Y_0)$ for the oscillation Eq. (5.21) has been suggested by others (Freeman and Skarda 1985; Baird 1986; Skarda and Freeman 1987) for olfactory processing. Baird (1986) has showed how single or double Hopf bifurcation in one or two oscillators can make stable (non-damping) cycles occur. Baird used excitatory-to-excitatory connections in the mitral cells to ensure the possibility of the stable cycles, which are otherwise impossible in systems with less than three coupled oscillators. Our model shows the multiple ($N$ oscillators) Hopf bifurcations with or without requiring excitatory-to-excitatory connections which are weak or absent in the olfactory bulb (Nicoll 1971; Shepherd 1979).

Our larger system shows the relation between the odor input and the oscillation mode in terms of the eigenvectors and eigenvalues of matrix $A$. The oscillation modes which emerge from the bulbar activity with odor input can be thought of as the decision states reached for odor information. The bulb output classifies the odor inputs by two stages. First, it fails to oscillate appreciably for weak odors (or some particular stronger odors). The absence of oscillation can be interpreted by higher processing centers as the absence of an odor (Skarda and Freeman 1987). Second, when the odor produces an oscillation, the particular pattern of mitral cell activity is specific to an input pattern and its minor variants, i.e., the pattern of oscillation classifies odors. This is chiefly apparent when the responses of individual mitral cells are studied, and tends to disappear in the EEG average.

High gain alone does not ensure the existence of non-damping modes. A symmetric $A$ will not result in growing modes, as argued in Sect. 5.2. Two examples will illustrate how the bulb selectively responds (or doesn't respond) to certain input patterns. The matrix $A$ in (5.17) might for example have the components

$$H_0=\begin{pmatrix} h & h' & 0 & 0 & & \cdots & & 0 & h'\\ h' & h & h' & 0 & & \cdots & & 0 & 0\\ 0 & h' & h & h' & 0 & 0 & \cdots & 0 & 0\\ \vdots & \vdots & & & & \cdots & \ddots & & \vdots\\ h' & 0 & & & \cdots & & 0 & h' & h \end{pmatrix}$$

$$W_0=\begin{pmatrix} w & 0 & 0 & 0 & & \cdots & & 0 & 0\\ 0 & w & 0 & 0 & & \cdots & & 0 & 0\\ 0 & 0 & w & 0 & 0 & 0 & \cdots & 0 & 0\\ \vdots & \vdots & & & & \cdots & \ddots & & \vdots\\ 0 & 0 & & & \cdots & & 0 & 0 & w \end{pmatrix}$$

i.e., each mitral cell gives output to its nearest granule cell neighbor only, while each granule cell connects to three nearest mitral cells. The connections are symmetric and uniform. If the receptor input $I$ and central input $I_c$ are also uniform across the bulb, then the matrix $A = H_0 G_y'(Y_0) W_0 G_x'(X_0)$ will be symmetric, and there will be no growing oscillatory response in the bulb output. Such a bulb however, can respond to some non-uniform inputs $I$, which induce a non-uniform $(X_0, Y_0)$ and, if $g_x$ and $g_y$ are non-linear, a non-symmetric matrix $A$. A decision state oscillatory output may be reached if the input $I$ is sufficiently non-uniform, (i.e., the odor selectively excites different mitral cells.)

On the other hand, if

$$H_0 = \begin{pmatrix} h & h' & 0 & 0 & & \dots & & 0 & 0 \\ 0 & h & h' & 0 & & \dots & & 0 & 0 \\ 0 & 0 & h & h' & 0 & 0 & \dots & 0 & 0 \\ \vdots & \vdots & & & & \dots & \ddots & & \vdots \\ h' & 0 & & & \dots & & 0 & 0 & h \end{pmatrix}$$

$$W_0 = \begin{pmatrix} w & w' & 0 & 0 & & \dots & & 0 & 0 \\ 0 & w & w' & 0 & & \dots & & 0 & 0 \\ 0 & 0 & w & w' & 0 & 0 & \dots & 0 & 0 \\ \vdots & \vdots & & & & \dots & \ddots & & \vdots \\ w' & 0 & & & \dots & & 0 & 0 & w \end{pmatrix}$$

the synaptic connection is uniform but non-symmetric across the bulb. If everything else stays the same as in the previous example, matrix $A$ will have the form in (5.19) with uniform receptor input $I$. A bulb with this connection structure can be responsive to a uniform receptor input pattern $I$ if it is strong enough. These two examples demonstrate that the pattern of the synaptic connections in the bulb determines the input patterns to which the bulb selectively responds.

In the real olfactory bulb, the dendrodendritic connections between the mitral and granule cells are mostly reciprocal, suggesting that $W_0 \approx H_0^T$ (the transpose of $H_0$) if we ignore other connections and presume roughly equal connection strengths. This implies a near symmetric matrix $A$ for uniform inputs if the synaptic connection structure is approximately uniform across the bulb. But mitral cells also send axon collaterals to the granule cells, suggesting $W_0 \approx H_0^T$ *+extra connections*, which have less reason to be thought symmetric.

### *6.2 Performance Optimization in the Olfactory Bulb*

An active mammalian olfactory system samples the inputs by sniffs, each lasting 200 ms to 1 s in rabbits. The olfactory system should make itself ready for the next sniff which may contain different odor information from the previous sniff. If $(X, Y)$ is the initial deviation of the system from the equilibrium point $(X_0, Y_0)$, then the degree to which the $k^{th}$ oscillation mode gets excited is proportional to $\langle XX_k \rangle$. $X = 0$ corresponds to no excitation of any modes, while a random $X$ corresponds to equal chances of excitation for all the modes. Terminating the oscillation during the exhale leaves only random noise and minimum information contamination in the system and helps the bulb to reach an unbiased decision on the odor information for the next sniff. Furthermore, exhaling also changes the operation point $(X_0, Y_0)$ back to the original value before the inhale (Sect. 5.3), making the system ready for the next sniff.

The initial operation point $(X_0, Y_0)$ before a sniff input should be controlled by the motivation level of the animal. If $(X_0, Y_0)$ is very low initially, a strong input $I_{odor}$ is needed to raise the bias $(X_0, Y_0)$ high enough for an oscillation burst output. Less strong input $I_{odor}$ would be required for an initially higher bias. Since the initial bias $(X_0, Y_0)$ is determined by $I_{background}$ and the central input $I_c$ by (5.7), it seems likely that the motivation level of the animal will be controlled through inputs from higher centers. Our simulation value for $I_{background}$ and $I_c$ are set such that the $(X_0, Y_0)$ with $I_{odor} = 0$ is just below the maximum gain point on the non-linear input-output curves (Sect. 3.2). This corresponds to a motivated state; a small amount of odor input can raise the gain to maximum values. Physiologically, the bulbar oscillatory bursts are observed to occur only in motivated animals (Freeman 1978; Freeman and Schneider 1982). And the experimentally measured gain (defined as the change in the mitral firing rate with respect to the change in EEG amplitude) for bulb neural mass is shown to be higher in the motivated states (Freeman 1979a), which can be achieved by raising $I_{background}$ through central inputs. Experiments even show the existence of oscillations without odor input with nasal breathing in motivated animals (Freeman and Schneider 1982).

The central input $I_c$ is also likely to participate in other olfactory functions as odor masking or sensitivity enhancing for particular odors (see also Freeman and Schneider 1982). These issues will be studied in a further paper.

## 7 Discussion

Our model of the olfactory bulb is a simplification of the known anatomy and physiology. The net of the mitral and granule cells simulates a group of coupled non-linear oscillators which are the sources of the rhythmic activities in the bulb. The coupling makes the

oscillation coherent across the whole bulb surface with a single frequency for each sniff but different amplitudes and phases for different mitral cells. The model suggests, in agreement with Freeman and coworkers, that stability change bifurcation is used for the bulbar oscillator system to decide primitively on the relevance of the receptor input information. Different non-damping oscillation modes emerging from the bifurcation are used to distinguish the different odors which are the driving source for the bifurcations. These oscillation modes are approximately thought of as the decision states of the system for the odor information. The coupling between the oscillators implies that information from different parts of the bulb is combined to produce a coherent output oscillation mode, and thus a unitary decision. A succeeding paper will use this basic model to study the ability to discriminate odors and to use input from higher centers to suppress or enhance sensitivity to particular target or masking odors.

Our model bulb encodes the non-oscillatory input into oscillatory "AC" output. Since the oscillation is intrinsic to the bulb, the model amplifies the weak odor input by transforming it to the oscillatory output. Consequently, whether or not an oscillatory mode exists indicates whether an odor is present. With the extra information represented in the oscillation phases of the cells, the bulb emphasizes the differences between different input patterns (Sect. 4). Both the analysis and simulation show that the bulb is selectively sensitive, i.e., non-uniformly sensitive, to different receptor input patterns. This selectivity as well as the motivation level of the animal could also be modulated from higher centers (Sect. 6.2). The information encoding scheme suggests that to extract information from the oscillation amplitudes and phases, we should look at the mitral cells rather than the EEG waves in which the detailed amplitude and phase information tend to be averaged out. Within this model, the information is carried by the detailed pattern of activity of the individual mitral cells; the spatial EEG pattern is an information epiphenomenon. This model does not exclude the possibility that the information be coded in the non-oscillatory slow wave $X_0$, since as is shown in (5.22), $X_0$ is determined by the odor input.

The chief behaviors do not depend on the number of cells in the model. The frequencies of the oscillation modes are close to the resonant frequency of a single oscillator in the system, and thus independent of the size of the model. However, since the number of the possible oscillation modes is the same as the mitral cell numbers, the simulated model with a small cell number has few oscillation modes, i.e., the simulated model has less decision states or smaller memory capacity than the real bulb. Therefore the simulated bulb does not

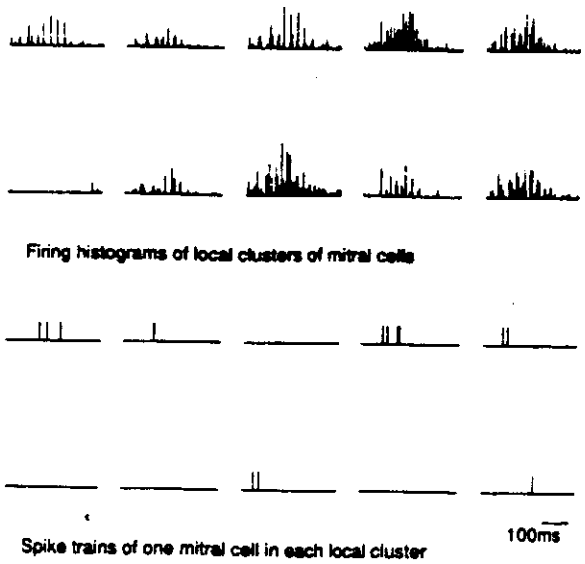


**Fig. 8.** Simulated bulbar mitral cell response pattern corresponding to Fig. 6A. Each cell is modeled to have discrete action potential firings of maximum rate about 300/s. Each cluster has about 310 mitral cells, and thus a maximum firing rate 93,000/s

respond oscillatorily to most randomly selected input patterns $P_{odor}$.

Most of the analysis is done for the model bulb without excitatory-to-excitatory and inhibitory-to-inhibitory connections. When those extra connection types are included, the system (5.13) is still a group of coupled non-linear oscillators. This more complicated system is more difficult to analyze, but the solutions will still be oscillation modes which depend on the inputs.

Our model uses a continuous input-output function, instead of discrete spikes that real neurons generate, to describe the neuron outputs. Since the continuous output value is meant to simulate the average of the firing rate of the neurons, unaveraged discrete spike output should chiefly introduce more fluctuations in the system. If the biological system had approximately equivalent close by neurons, then a continuous output would be a good approximation to the group average. Simulation was also done on a model in which each cell in the original model is replaced by a group of cells which generate action potentials rather than continuous valued outputs (Fig. 8). Oscillatory behavior is obvious in the summed spike trains of groups of local cells. But the spike train of a single cell appear very noisy and sparse with barely recognized oscillatory behavior. In the physiological experiment, each mitral cell fires on the average about once in 100 ms (Freeman and Skarda 1985), making it hard to recognize an oscillation with a period of 25 ms in the spike train of a single cell. On the other hand, the

EEG wave is clearly oscillatory since it is from the averaged activities of many local granule cells.

Our simulation has been done on a one-dimensional ring of mitral and granule cells, while the real bulb has cells sitting on two-dimensional segments of a sphere. The dimension of the cell arrangement is not crucial in the model. One simulation was done on a two-dimensional surface of the cells to mimic the real bulb, and the basic oscillation phenomena were very similar to those of the one dimensional rings.

*Acknowledgements.* This research was supported by ONR contract N00014-87-K-0377.

## References

Baird B (1986) Nonlinear dynamics of pattern formation and pattern recognition in rabbit olfactory bulb. Physica 22D:150–175

Bressler S (1987) Relation of olfactory bulb and cortex. I. Spatial variation of bulbo-cortical interdependence. Brain Res 409:285–293

Freeman WJ (1975) Mass action in the nervous system. Academic Press, New York

Freeman WJ (1978) Spatial properties of an EEG event in the olfactory bulb and cortex. Electroencephalogr Clin Neurophysiol 44:586–605

Freeman WJ (1979a) Nonlinear Gain mediating cortical stimulus-response relations. Biol Cybern 33:237–247

Freeman WJ (1979b) Nonlinear dynamics of paleocortex manifested in the olfactory EEG. Biol Cybern 35:21–37

Freeman WJ (1979c) EEG analysis gives model of neuronal template-matching mechanism for sensory search with olfactory bulb. Biol Cybern 35:221–234

Freeman WJ (1980) Use of spatial deconvolution to compensate for distortion of EEG by volume conduction. IEEE Trans Biomed Eng 27:421–429

Freeman WJ, Schneider WS (1982) Changes in spatial patterns of rabbit olfactory EEG with conditioning to odors. Psychophysiology 19:44–56

Freeman WJ, Skarda CA (1985) Spatial EEG patterns, nonlinear dynamics and perception: the Neo-Sherringtonian view. Brain Res Rev 10:147–175

Getchell TV, Shepherd GM (1978) Responses of olfactory receptor cells to step pulses of odour at different concentrations in the salamender. J Physiol 282:521–540

Haberly LB (1985) Neuronal circuitry in olfactory cortex: anatomy and functional implications. Chem Sens 10:219–238

Jahr CE, Nicoll RA (1980) Dendrodendritic inhibition: demonstration with intracellular recording. Science 207:1473–1475

Lancet D (1986) Vertebrate olfactory reception. Ann Rev Neurosci 9:329–355

Lancet D, Greet CA, Kauer JS, Shepherd GM (1982) Mapping of odor-related neuronal activity in the olfactory bulb by high-resolution 2-deoxyglucose autoradiography. Proc Natl Acad Sci USA 79:670–674

Mori K, Kishi K (1982) The morphology and physiology of the granule cells in the rabbit olfactory bulb revealed by intracellular recording and HRP injection. Brain Res 247:129–133

Nicoll RA (1971) Recurrent excitation of secondary olfactory neurons: a possible mechanism for signal amplication. Science 171:824–825

Scott JW (1986) The olfactory bulb and central pathways. Experientia 42:223–232

Shepherd GM (1979) The synaptic organization of the brain. Oxford University Press, New York

Sicard G, Holley A (1984) Receptor cell responses to odorants: similarities and differences among odorants. Brain Res 292:283–296

Skarda CA, Freeman WJ (1987) How brains make chaos in order to make sense of the world. Behav Brain Sci 10:161–195

Received: November 28, 1988

Accepted in revised form: May 3, 1989

Dr. Zhaoping Li
Division of Physics, Mathematics and Astronomy
California Institute of Technology
Pasadena, CA 91125
USA